FIELD OF VIEW EFFECTS ON REFLEXIVE MOTOR RESPONSE IN FLIGHT SIMULATION

by

JAVIER M COVELLI
B.S. Ocean Engineering, U.S. Naval Academy, 1983
M.S. Electrical Engineering, U.S. Naval Postgraduate School, 1992
M.S. Industrial Engineering, University of Central Florida, 2001

A dissertation submitted in partial fulfillment of the requirements
for the degree of Doctor of Philosophy
in the Department of Industrial Engineering and Management Systems
in the College of Engineering and Computer Science
at the University of Central Florida
Orlando, Florida

Spring Term
2008

Major Professors:
Jannick P. Rolland
J. Peter Kincaid

ABSTRACT

Virtual Reality (VR) and Augmented Reality (AR) Head Mounted Display (HMD) or Head Worn Display (HWD) technology represents low-cost, wide Field of Regard (FOR), deployable systems when compared to traditional simulation facilities. However, given current technological limitations, HWD flight simulator implementations provide a limited effective Field of View (eFOV) far narrower than the normal human 200º horizontal and 135º vertical FOV. Developing a HWD with such a wide FOV is expensive but can increase the aviator's visual stimulus, perception, sense of presence and overall training effectiveness. This research and experimentation test this proposition by manipulating the eFOV of experienced pilots in a flight simulator while measuring their reflexive motor response and task performance. Reflexive motor responses are categorized as information, importance and effort behaviors. Performance metrics taken include runway alignment error (RAE) and vertical track error (VTE). Results indicated a significant and systematic change in visual scan pattern, head movement and flight control performance as the eFOV was sequentially decreased. As FOV decreased, the average visual scan pattern changed to focus less on out-the-window (OTW) and more on the instruments inside the cockpit. The head range of movement significantly increased below 80º horizontal x 54º vertical eFOV as well as significantly decreasing runway alignment and vertical track performance, which occurred below 120° horizontal x 81° vertical eFOV.

This dissertation is dedicated to my wife, Lisa, and to my children, Anthony and Danny. Last, but not least, I dedicate this to my mother and father, Elsa and Nicolas, who encouraged me to never stop learning at a young age.

ACKNOWLEDGMENTS

There are a number of people without whom this dissertation might not have been written, and to whom I am greatly indebted. I would like to extend many thanks to my advisors and committee members for their guidance and help on staying focused. First, I would like to personally thank my co-advisors, Dr. Jannick Rolland and Dr. Peter Kincaid, for their time, valuable insight, encouragement and generous support. I extend deep thanks to Dr. Rolland and the Optical Diagnostics and Applications Laboratory (ODALab) for their help in the field of optics and with the loan of their head tracking system, made possible in part by the National Science Foundation grant II/HCI 03-07189. I offer a special thanks to Dr. Kincaid and the Institute for Simulation and Training (IST) for their generous grant, making the purchase and use of the Arrington Research EyeTracker possible. I would like to thank Dr. Michael Proctor for his timely feedback and golden nuggets of valuable information. I would like to thank Dr. Denise Nicholson for her advice and needed help in my literature review. Finally I would like to thank Dr. Peter Hancock, who graciously agreed to share his limited time and critical experience in human factors by serving on my dissertation committee.

I would like to also thank Patrick Corr, Senior VP of Bristow Group Inc., Jens Jehnes, Chief Flight Instructor, and Ben Kao of Bristow Academy for the use of their flight simulator and their extremely professional flight instructor staff that graciously volunteered for all the experiments. I would like to thank my family for their support and encouragement. Last, but not least, I would like to thank my best friend, my lovely wife Lisa, for putting up with the long hours and hectic schedule caused by my attempt to juggle family life, working full-time and of course the long road towards this degree.

TABLE OF CONTENTS

LIST OF FIGURES

LIST OF TABLES

LIST OF ACRONYMS

ANOVA	Analysis of Variance
AOI	Area Of Interest
AR	Augmented Reality
ARI	Army Research Institute
ARL	Aviation Research Lab
AV	Augmented Virtuality
CDTI	Cockpit Display of Traffic Information
ChrAVE	Chromakeyed Augmented Virtual Environment
COR	Conjugate-Optical Retroreflector
CRT	Cathode Ray Tube
DFA	Dwell Frequency per Area of Interest
ECATT-MR	Embedded Combined Arms Team Training and Mission Rehearsal
eFOV	effective Field Of View
FAA	Federal Aviation Administration
FCS	Future Combat System
FNPT	Flight Navigation Procedure Trainer
FOR	Field of Regard
FOV	Field of View
FPD	Flat Panel Display
FTE	Flight Technical Error
HCI	Human Computer Interaction
HMD	Head-Mounted Display
HMPD	Head-Mounted Projection Display
HUD	Heads Up Display
HWD	Head Worn Display
IERW	Initial Entry Rotary Wing
IFR	Instrument Flight Rating
IP	Instrument Pannel
IST	Institute for Simulation and Training
LCD	Liquid Crystal Display
LOFT	Line Oriented Flight Training
MDD	Mean Dwell Duration
MFD	Multi-Function Display
MOVES	Modeling, Virtual Environments, and Simulation
MR	Mixed Reality
MSE	Mean Square Error
NASA	National Aeronautics and Space Administration
ND	Navigation Display
NPS	Naval Postgraduate School
ODALab	Optical Diagnostics and Applications Lab
OFT	Operational Flight Trainer
OKCR	Opto-kinetic Cervical Reflex
OTW	Out the Window
OTW-L	Out the Window - Left

OTW-LC	Out the Window - Left of Center
OTW-LL	Out the Window - Lower Left
OTW-LR	Out the Window - Lower Right
OTW-R	Out the Window - Right
OTW-RC	Out the Window - Right of Center
OW	Outer World
PDT	Percentage Dwell Time
PFD	Primary Flight Display
PQ	Presence Questionnaire
RAE	Runway Alignment Error
RMSE	Root Mean Square Error
ROI	Region of Interest
SA	Situation Awareness
SAGAT	Situation Awareness Global Assessment Technique
SVIS	Synthetic Vision Information System
TER	Transfer Effectiveness Ratio
TOT	Transfer of Training
UCF	University of Central Florida
VE	Virtual Environment
VEHELO	Virtual Environment Helicopter
VFR	Visual Flight Rules
VMC	Visual Meteorological Conditions
VOR	Vesibulo-Ocular Reflex
VR	Virtual Reality
VTE	Vertical Track Error

CHAPTER ONE: INTRODUCTION

The training of a pilot is presently a relatively prolonged and evidently expensive business. The cost of producing an effective and licensed commercial helicopter pilot, for example, continues to increase in terms of both resource expenditure and time to completion (Bristow Academy, 2007). Not only must one train such pilots but their skills must be maintained through periodic refresher and reinforcement training as well as programs such as Line Oriented Flight Training (LOFT) (LOFT, 2005). When a military unit deploys, reaching and maintaining a certain level of proficiency is required. It is common knowledge in the aviation community that a decrease in training leads to a decrease in proficiency, which contributes to an increase in accident rate and decrease in combat effectiveness (Shappell & Wiegmann, 2000). One of the major methods that aviation has consistently relied upon to resolve this conundrum is the use of simulation (Flexman & Stark, 1987). In an effort to cut costs and improve pilot proficiency, the military has been implementing a policy to decrease actual flight hours and increase flight training reliance on simulators (French, 2003).

Conventional flight simulators consist of an emulated cockpit and the associated instruments and controls. Added to this physical assemblage is a visual display ranging in sophistication from a simple flat computer monitor to the 360° Field of Regard (FOR) dome screens with bulky projectors and digital image blending techniques. Field of View (FOV) here is defined as the momentary subtending visual angle of the scene at the pilot's eye. The FOR refers to the overall FOV of the simulated scene one can perceive via head movements. Thus, the FOV at any one moment is a subset of the overall possible field of regard, which itself is typically measured in degrees and is contingent upon the capacities of the immediate image

generation system. Mobile simulation systems most often use simple cathode ray tube (CRT) or liquid crystal display (LCD) monitors. In contrast, static facilities such as high fidelity simulator domes provide a significantly greater degree of immersion (Ames, 2005), but naturally at the expense of far less deployment flexibility. Limited effective fields of view (eFOVs) provided by a single computer may suffice for cockpit familiarization but they are largely impractical with respect to providing realistic out-the-window situation awareness for advanced pilot training (Proctor, Panko & Donovan, 2004). Desktop computer simulations are also impractical for providing realistic crew coordination training for aircrews (Stewart, Dohme & Nullmeyer, 2002). This simple display FOR is much smaller than a normal human's FOV of about 200º horizontal (h) and 135º vertical (v) (Arthur, 2000). Unfortunately, it is neither practical nor feasible to deploy a conventional dome system to mobile aviation units in order to sustain either initial or refresher pilot training proficiency. This constraint is especially true for training in cockpits with side-by-side seating, for which the display system is inherently large. Operational Flight Trainers (OFTs) are the most practical way to keep proficient, but they are impractical when needed in tight spaces or with limited budgets.

Head-worn display (HWD) technologies have been touted as possible alternatives and are often associated with fully immersive virtual reality simulations (Cakmakci & Rolland, 2006; Rolland, & Hua, 2005). Augmented reality (AR) head-worn display technologies are thus being considered as novel alternatives to provide operational cockpit heads up display (HUD) and also embedded training in a low-cost, wide FOR system (Rodriguez, Foglia, & Rolland, 2003). However, there are inherent differences in characteristics among different HWDs and between forms of AR displays and conventional displays (Rolland & Hua, 2005; Pausch, Crea, & Conway, 1992). For example, the eFOV in most HWDs are less than 60º h x 45º v (assuming a

4:3 format), which is far narrower than the human's normal FOV of approximately 200º h x 135º v (Arthur, 2000). A pilot will normally use peripheral vision during a flight but developing a head-worn display with a wide 200º h x 135º v FOV is not only challenging to design but, at present, would prove very expensive to fabricate (Sisodia et al., 2007). Much of the effectiveness of simulator training is conceived to be contingent upon the fidelity of these systems, and this reduced eFOV can reduce the pilot's visual stimulus, perception, sense of presence and training effectiveness (Azuma, Baillot, Behringer, Feiner, Julier & MacIntyre, 2001; Fidopiastis, Fuhrman, Meyer, & Rolland, 2005).

Attempts to measure presence were historically conducted with questionnaires (Witmer & Singer, 1998; Biocca, Harms & Burgoon, 2003). Although more convenient, the validity of measuring the continuous experience of presence with post experience questionnaires has been challenged (Slater, 2004). Generally, the use of continuous indicators of behavioral or physiological response is considered more sensitive and valid. The major argument is that after-the-event questionnaire-based measures cannot in principle rule out the possibility that the reported "presence" was called into being simply by its having been asked about. To prove this, Slater made up an arbitrary concept ("colorfulness of the experience"), constructed a questionnaire to "measure" this phenomenon, and showed how results were obtained that mirror results with presence questionnaires. A fundamentally different view offered by Zahoric & Jenison (1998), and Flach & Holden (1998) is that presence is "tantamount to successfully supported action in the environment." What is important in this approach is action (i.e. how things are done) and the affordances offered in the virtual environment (VE), rather than just appearances. In other words, the sense of "being there" is grounded on the ability to "do" there.

A scientific basis for "presence" as it is usually understood in virtual environments research cannot be established solely on the basis of post-experience presence questionnaires alone.

Augmented Reality Overview

Mixed Reality (MR) is a technique that merges real-world and virtual-world scenes to produce a new environment where physical and synthetic images merge both worlds in a single interactive environment. Paul Milgram defines a reality-virtuality continuum where MR displays are defined to include the real environment and the virtual environment with various categories in between (Milgram & Kishino, 1994). Augmented Virtuality (AV) lies closer to the Virtual Reality (VR) end of the spectrum, where one injects a real image into a surrounding virtual environment. An example would be digital terrain texture mapping from aerial photography. AR lies on the opposite end of the spectrum, where one can superimpose virtual objects on a real environment. An innovative new approach to provide a deployable flight simulator is to use VR, or more specifically AR for a flight simulator display system that can be used in a small space with a low-cost, deployable simulator—or even with an embedded training system on the actual aircraft. Embedded training mode in modern fly-by-wire aircraft is possible if designed into the system, similar to the Army's Future Combat System (FCS) Embedded Combined Arms Team Training and Mission Rehearsal (ECATT-MR) concept (Marshal, Ragusa, Grayson & Green, 2004).

An optical see-through approach pioneered by the Modeling, Virtual Environments, and Simulation (MOVES) Institute of the Naval Postgraduate School (NPS) in Monterey, CA was to use chromakey technology to mix a video see-through (i.e. camera) real image with a

corresponding head-oriented virtual image on a standard Head Mounted Display (HMD) (Darken, Sullivan & Lennerton, 2003).

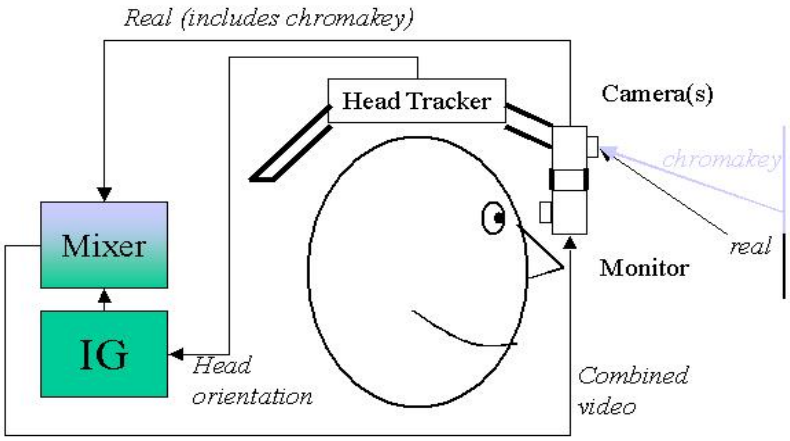

Figure 1: Using a Video See-through HMD for Simulator Display

This configuration depicted in Figure 1 is classified as a video see-through display, using a head-mounted video camera (or set of cameras for stereoscopic vision) to merge the real environment image as normally seen by the eye with a computer generated virtual image (Azuma, Baillot, Behringer, Feiner, Julier & MacIntyre, 2001). The system head-tracker allows image generation (IG) to be tailored for the user and thus, separate display systems can be used to present simulated imagery from different view points (e.g. to individual pilots in a mult-piloted aircraft simulator). Another advantage, when used with one set of camera and monitor for each eye, is the ability to provide binocular imagery to the user (Arrington & Geri, 2000). It is important to note that the mixing process for this approach requires special hardware and software and, with frequent head movements, can add considerable latencies in generating the final AR image to the pilot's HMD.

In a dynamic flight simulation environment, any display process induced latency must be minimized to provide a realistic out of the cockpit or Outer World (OW) simulated environment.

An optical display system has more recently been developed that could provide highly detailed, wide-field imagery using relatively simple, light-weight, and inexpensive optical components (Arrington & Geri, 2000). Conjugate-Optical Reflector (COR) display systems provide the same binocular and multiple viewpoint advantages of video see-through systems, without the associated IG latencies due to the mixing process.

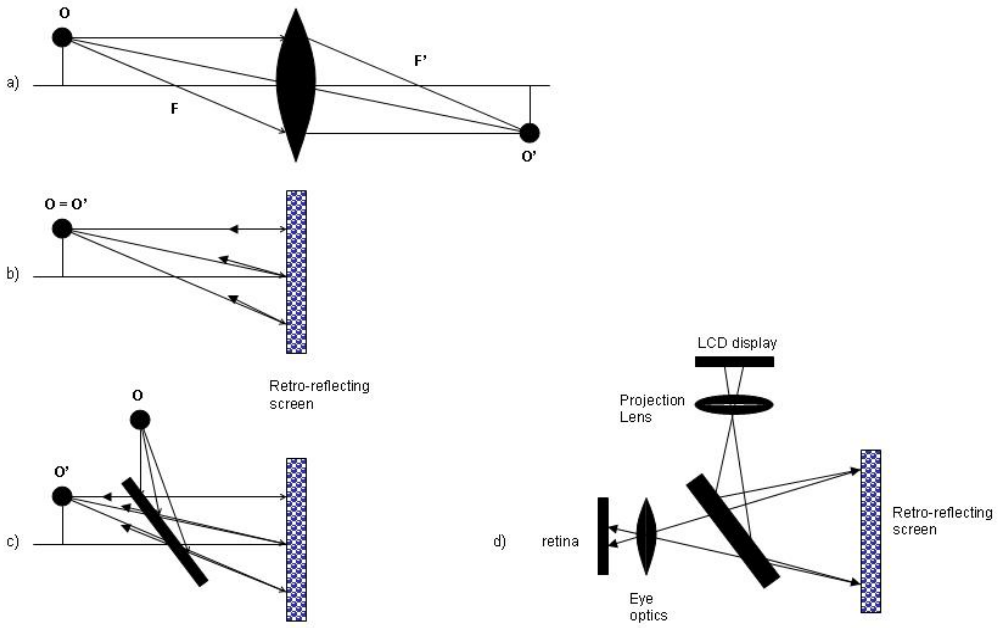

Figure 2: Conjugate Optical Display System [Adapted from Arrington & Geri, 2000]

In Figure 2 a) the upper ray from object, O, is parallel to the lens axis and will pass through one focal point, F', after being refracted by the lens. The lower ray passes through the other focal point, F, and exits the lens parallel after being refracted. The point of intersection of these two rays determines the location and size of image, O'. The object, O, and its image, O', are located at conjugate (i.e. interchangeable) planes about the lens. In Figure 2 b) a retro-reflecting surface has replaced the lens and the result is that O' is now co-located with O. In

Figure 2 c) a plate-glass beam-splitter has been introduce to re-separate O and O' and this is the basis for a COR display system as shown in Figure 2 d) (Arrington & Geri, 2000).

A recent AR COR display implementation at the University of Central Florida (UCF) involves a lightweight, stereoscopic HWD projecting a computer-generated scene of the simulated environment onto a retro-reflective screen fabric placed strategically in the environment (Rodriquez, Foglia & Rolland 2003).

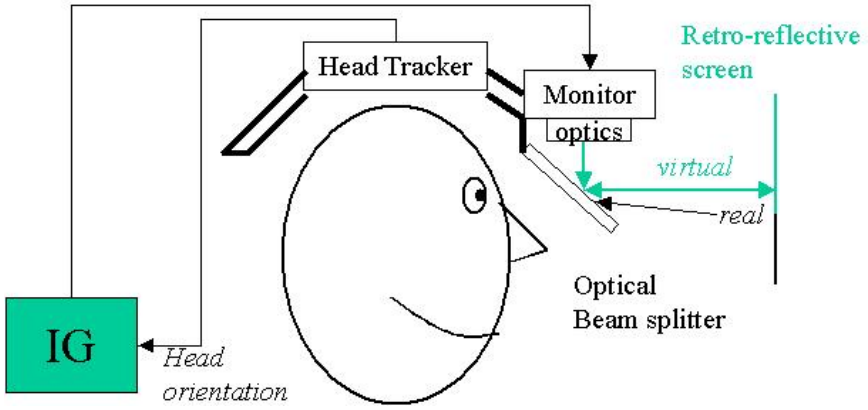

Figure 3: Using an Optical See-through HWD for Simulator Display

A flight simulator with this HWD configuration depicted in Figure 3 eliminates the need for a separate mixing process since the virtual image is only seen on the retro-reflective material strategically placed on the cockpit canopy for the OW and the real image inside the cockpit is seen normally by the naked eye. The HWD visualization system provides simple functional stereopsis (stereoscopic vision), and a small footprint if one laminates the cockpit simulator canopy or windows with the retro-reflective screen material. This is a huge advantage when used for aircraft simulators with side-by-side seat configurations (e.g. S-3B, E-2D, SH-60, CV-22, AH-60, C-130) that normally require large, bulky and expensive projection display systems. The HWD optical see-through visualization system provides a realistic simulation experience

(Covelli, Martins & Rolland, 2005). Both approaches are suitable for cockpits with tandem or side-by-side seat configurations, and are an inexpensive alternative with several advantages over conventional simulator display systems.

Research Summary

To successfully utilize a VR or AR display device in a simulator, the user must have the same or an even higher mental immersion experience, situation awareness and presence as compared with the simulator experience of unrestricted FOV in a conventional wide FOR simulator.

This research describes an experimental approach used to manipulate the eFOV of experienced pilots in a flight simulator while measuring their reflexive motor response and task performance. Reflexive motor responses are categorized as information, importance and effort behaviors. Performance metrics taken include runway alignment error (RAE) and vertical track error (VTE).

It was hypothesized that depending on the task, limiting the pilot eFOV will impose additional workload and stress due to the limited peripheral image data. To be more specific, as the pilot's eFOV is artificially reduced, eye scan patterns will change, head movement range (in degrees) and head rate of movement (in degrees/second) will increase to compensate for the reduced peripheral visual data.

It was further hypothesized that a threshold exists, while decreasing the eFOV, at which the pilot can no longer compensate sufficiently to maintain an adequate cognitive mental image that leads a measurable decrease in task performance. Somewhere between the onset of measured eye and head movement pattern changes and the measured decrease in task

performance, negative training becomes a concern. These FOV effects will provide insight into AR or VR HWD device FOV design for this type of flight simulation application.

Dissertation Outline

This document is comprised of five chapters. The first chapter provides an introduction to the topic and a review of the use of lightweight, stereoscopic HMDs and Head-Mounted Projection Displays (HMPDs) using AR technology as a new type of display system for an inexpensive and deployable simulator. Chapter 2 provides a literature review of current human factors research regarding simulator display effects, and head and eye movement patterns as they relate to normal mental image processing and task accomplishment. Chapter 3 provides the experimental methods involving measurement and modeling of normal head and eye movement patterns of experienced pilots while accomplishing specific tasks in a wide FOR conventional flight simulator with a 170° horizontal x 75° vertical wrap-around, rear projected display system. It outlines measurements taken using head and eye tracking equipment, and expected results of pilot head and eye movements between different Areas of Interest (AOIs) inside and outside the cockpit. Chapter 4 provides the experimental results with regard to task performance and FOV effects. Chapter 5 provides a summary of findings, experiment limitations, lessons learned and potential areas for future research.

CHAPTER TWO: LITERATURE REVIEW

Technical Background

Immersion and Presence

A distinction is made between immersion and presence by many researchers (e.g., Slater & Wilbur, 1997; Draper et al., 1998). Immersion is a description of overall fidelity in relation to physical reality provided by the display and interaction systems (Witmer & Singer, 1998). The fidelity parameters (e.g. display contrast, cockpit instrument panel) can be objectively measured and compared. Schloerb (1995) has proposed an alternative psychometric approach, based on the idea of just noticeable differences between virtual and real worlds, but to his knowledge this has never been followed up "probably because there are no VEs available that approach real-world experiences," except maybe a high fidelity flight simulator. Presence is the subjective experience of being in one place or environment, even when one is physically situated in another. Attempts to measure presence were historically conducted with questionnaires (Witmer & Singer, 1998); (Biocca, Harms & Burgoon, 2003). Perhaps the most recent explication of presence is found in the International Society for Presence Research. (2000) where "Presence (a shortened version of the term "telepresence") is a psychological state or subjective perception in which even though part or all of an individual's current experience is generated by and/or filtered through human-made technology, part or all of the individual's perception fails to accurately acknowledge the role of the technology in the experience."

Subjective Measures of Presence

Subjective measures of presence include such psychological measuring devices as rating scales or equivalence classes, the method of paired comparisons, and cross-modality matching (Stanney & Salvendy, 1998). Witmer and Singer (1998) developed a presence questionnaire (PQ) that measures presence along three subscales: involvement/control, naturalness, and interface quality. Rating scales require the experiment designer (i.e. user) and participant to understand what is meant by presence. For rating scales it is possible that different users may apply these scales differently or the participants may interpret aspects of presence differently, opening the possibility of bias from one experiment to the next. The method of paired comparison eliminates errors due to subjective interpretation and estimation by asking the participant to differentiate between a real scene and a virtual scene, which doesn't require an explanation of presence. The user systematically degrades the perception of the real scene until the participant can no longer differentiate it from the virtual scene. The amount of degradation entered serves as a measure of the degree of presence. Some individuals are more sensitive to degradations in different parameters of a scene. This requires a very difficult and complex scene degradation process to ensure all aspects of a scene are covered. Stanney and Salvendy (1998) believe cross-modality matching could be applied for the scaling of presence. An example of cross-modality matching would be asking the participant to make a light as bright as the strength of presence experienced in the VE. However, this method still requires the user to explain what is meant by presence to the participant, allowing participant induced bias to influence the results.

Validity of Presence Questionnaires

A fundamentally different view (Zahoric & Jenison, 1998; Flach & Holden, 1998) is that presence is ". . . tantamount to successfully supported action in the environment." What is important in this approach is action (how things are done) and the affordances offered in the virtual environment, rather than just appearances, and that the sense of "being there" is grounded on the ability to "do" there. A scientific basis for "presence" as it's usually understood in virtual environments research cannot be established on the basis of post-experience presence questionnaires alone. The major argument is that after-the-event questionnaire-based measures cannot in principle rule out the possibility that the reported "presence" was called into being simply by its having been asked about. To prove this, they make up an arbitrary concept ("colorfulness of the experience"), construct a questionnaire to "measure" this phenomenon, and show how results are obtained that mirror results with presence questionnaires.

Objective Measures of Presence

Objective measures of presence include neurophysiological responses and reflexive motor acts (Stanney & Salendy, 1998). Physiometric measures to events in a VE include posture, muscular tension, cardiovascular behavior, and ocular responses (Barfield & Weghorst, 1993). Other possible measures proposed by Barfield and Weghorst (1993) involve examining virtual world task performance and natural world task performance. The relationship between sense of presence and task performance has yet to be fully understood and is likely to be highly task dependent (Stanney & Salvendy, 1998). Researchers also believe that presence implies situation awareness or that observers perceive their self-orientation and self-location with respect

to an environment (Prothero, Parker, Furness, & Wells, 1995) and that this orientation/position illusion (i.e. presence) is also related to motion illusion (i.e. vection) in the VE. In a research paper (Prothero et al., 1995) introduced the "presence rest frame hypothesis" which states we maintain a subjective coordinate frame with respect to which we determine positions, orientations and motions. Disturbances to this rest frame can result in either change to vection or presence. They proposed an objective nulling measure for presence based on conflicting virtual (visual) and real (inertial) yaw sinusoidal oscillation cues. The proposed experiment examines if it is possible to induce yaw or rotation vection using available VE equipment, and to adjust for phase differences between the human visual and inertial systems (objective nulling measure).

Variables that Influence Presence

Variables that influence presence include ease of interaction, user control response, pictoral realism, length of exposure, social interactions, and system factors (Stanney & Salvendy, 1998). Ways to ease interaction involve design of degree of abstractness of objects, as well as the ground plane (e.g. terrain) and other spatial landmark objects. User control of their VE involves immediacy of the system response and appropriateness of user-initiated actions along with naturalness of the mode of control. Pictoral realism is based on continuity, consistency, feeling of depth and meaningfulness of the perceptual stimuli presented to the user. Extended exposure to a VE is thought to enhance other factors thought to be related to presence, including practice, familiarity and the level of sensorial adaptation. However, adverse effects such as cybersickness intensify during prolonged VE exposure, so the overall effect of length of exposure is still unknown. Social factors involve interactions with entities in the VE. System

factors involve number of sensory modalities stimulated by the VE, the use of head tracking and stereoscopic cues, small display system response or latency and naturalness of display medium (e.g. screen based projections vs. head mounted displays).

Simulators and Display FOV Effects

HWD FOV Effects

The HWD FOV is an important parameter that has an effect on spatial awareness, navigation, visual search tasks and also simulator sickness (Arthur, 2000). Simulator sickness involves symptoms similar to those of motion sickness but less severe, and originates from elements of visual display and visuo-vestibular interaction atypical of conditions that induce motion sickness (Kennedy, Lane, Berbaum & Lilienthal, 1993). The Army Research Institute (ARI) has categorized the main factors affecting simulator sickness (Kolasinski, 1995). Simulator display system design factors affecting simulator sickness include calibration, color, contrast, FOV, flicker, inter-pupillary distance, motion, position tracking error, refresh rate, resolution, scene content, transport delay, update rate and viewing region. Simulator tasks that can cause simulation sickness include altitude, global visual flow, degree of control, duration, head movements (Pseudo-Coriolis stimulation), luminance, linear or rotation accelerations, sitting and standing movements, unusual maneuvers, near and far vision application, and vection; also known as self-motion illusion.

When an HMD is used in an environment involving acceleration and/or vibration, involuntary head movements elicit reflexive eye movements called Vesibulo-Ocular Reflex

(VOR) effect (Winterbottom, Patterson, & Pierce, 2006). VOR compensates for the involuntary head movements so that fixation is maintained on a given object and the image is stabilized on the retina. For example, if an individual's head vibrates upward, the position of a given object would move downward relative to the eye, and the retinal image would slip upward. The VOR would then elicit a compensatory downward eye movement to maintain fixation on the object during the head movement. When an HMD is worn, the VOR eye movements can confuse vision because during the involuntary head movement produced by vibration, the retinal image moves with the head in an unnatural manner. Therefore HMD visual performance declines with head vibration and it has been suggested that VOR mismatch can cause simulator sickness.

Finally, factors regarding the type of individual in the simulator include age, gender, experience or adaptation and spatial abilities. Pausch, Crea and Conway (1992) conducted VR simulator sickness research and found the main factors include HMD FOV, scene complexity, display system lag (117 ms or more), refresh rate and flicker (30 Hz or less), gender and age (females and younger individuals are more susceptible to simulator sickness). The overall conclusion was simulator sickness is a combination of perceptual adaptation and motion sickness.

Wells and Venturino (1990) measured performance and head movement when using an HMD with an adjustable FOV between 20°-120° horizontal and 20°-60° vertical. The participants had to search for and fire at a set of targets and threats in a narrow, normal and widespread VE. The objective was to find the optimum HMD FOV specification for a third person shooter game. They found the participants were hitting fewer targets and were threatened longer durations with smaller FOVs. The more complex tasks (9 targets widespread) required a FOV greater than 60°x60°. The participants moved their head less but with faster bursts with the

larger FOVs and performed better. There was an apparent inverse relation between head velocity and error at replacing the targets, possibly related to memory. It also appeared performance was limited by how well subjects integrated information about target locations or how well they developed a cognitive target image. It is hypothesized that head velocity may have been mediated by how sure subjects were about target locations. This hypothesis is supported by an apparent (but not statistically significant) inverse relation between head velocity and error at recalling target locations. Gallimore, Patterson, Brannon, and Nalepka (2000) studied the opto-kinetic cervical reflex (OKCR) or head tilt (roll axis) pilot behavior that establishes a horizon retinal image. They concluded that during Visual Meteorological Condition (VMC) maneuvers, pilots exhibited significant OKCR, similar in solo and formation flight tasks, but reduced OKCR during low level navigation tasks, indicating a difference in visual cues between tasks. Additionally, under three FOV conditions (40°, 60°, and 100° circular) they concluded FOV did not significantly affect the OKCR.

Presence and FOV

Presence, performance and FOV are intricately related as demonstrated by Arthur (2000), in which he used a tiled wide-FOV (up to 176°) Kaiser HMD to measure navigation and target detection performance in VR. The primary research was to measure task completion time and VR sickness with varying FOVs. The generic tasks included search (navigation and target detection), walking, distance judgment and spatial memory. A secondary research topic was measuring a sense of presence affected by FOV and head movement patterns with varying FOVs. Results indicated that performance degradation (navigation and target detection) began at

112° FOV and quickly progressed at 48° FOV. The effect of reducing the FOV was inconclusive with regard to cybersickness but it had a negative effect on the task performance and also decreased the user's sense of presence, as measured by a presence questionnaire.

Measuring Pilot Situation Awareness and Performance

Endsley (2000) defines Situation Awareness (SA) as the "perception of elements in VE, comprehension of their meaning, and projection of their status in near future," which leads to a decision and ultimately a performance of action. An *International Journal of Aviation Psychology* paper examined the validity of real-time probes as measures of SA vs. SA Global Assessment Technique (SAGAT). Real-time probes are verbal queries (derived from an SA requirements analysis; delivered over headsets during simulation) posed to the operator concurrent with operations. SAGAT provides an objective measure of SA (Endsley, 1988, 1995b); however, this method is designed to be used in a simulation environment and is more difficult to use in many real-time operational environments (Jones & Endsley, 2004). SAGAT has been shown to have predictive validity, with SAGAT scores indicative of pilot performance in a combat simulation (Endsley, 1990a). Real-time probes are developed from an extensive SA requirements analysis that delineates the operator's goals and the associated SA requirements. The probes are designed to specifically query an aspect of SA needed for task performance. Unlike SAGAT (in which operations are suspended and operators are presented with a series of questions), the operator is periodically presented a single verbal query and is required to verbally respond. Results from these experiments are mixed. A weak but significant correlation was found between real-time probes (both accuracy and latency measures) and SAGAT queries,

indicating that real-time probes were measuring some facet of SA. However, correlations with workload were also found, and this correlation needs to be investigated further. More research is needed to assess the utility of real-time probes as a metric of SA.

A similar paper evaluated a Synthetic Vision Information System (SVIS) against conventional glass cockpit primary flight displays (PFDs) and multifunction displays (MFDs), which included Navigation Display (ND), to assess whether or not SVIS could improve pilot flight technical error (FTE) performance, situation awareness (SA), and workload. A fixed-base laboratory flight simulator (three forward projection units for a total FOV of 140° circular) was used by 12 pilot evaluators to fly fairly difficult simulated approaches into the Eagle County, Colorado, airport. Questionnaires were used in various phases of the flights to estimate workload, SA, and user preference. SA was collected using the SAGAT (Endsley, 1995; Endsley & Bolstad, 1994) and workload estimates were obtained using the National Aeronautics and Space Administration (NASA) Task Loading Index technique. Eye movement data was collected using a modified IScan ETL 500 system, and analyzed to find a link analysis (an analysis of eye movement transitions between areas of interest on the displays), scan length, fixation frequencies, location of fixations, and duration of fixations. Ten static AOIs were defined on the SVIS PFD and ND. Those were the airspeed indicator, bank indicator, center of tunnel, vertical speed indicator, altitude tape, and altitude indicator window on the PFD, as well as the track indicator and aircraft position on the ND. Additionally, the entire PFD and ND area were defined as two higher level AOIs. The boundaries of the AOIs were set about 15% larger than the actual areas to allow for slight inaccuracies in the eye tracking system. A link analysis (% transitions between AOIs) was performed for all the AOIs (Schnell & Merchant, 2001). FTEs that were assessed included the vertical track error (amount that the aircraft is off path vertically), the

cross-track error (amount that the aircraft is off track laterally), the flight path angle error (extent to which the vertical flight path angle is in error), the track angle error (extent to which the lateral track angle is in error), and the speed deviation error (deviation from commanded speed). Results indicated that the SVIS is superior to the conventional displays (i.e. reduced workload and FTEs) for the majority of the measures that were obtained in the experiments.

Visual System Effect on Measured Transfer Effectiveness Ratio

The quality of the display system, which includes the eFOV and FOR, affects presence and overall training effectiveness. Hays, Jacobs, Prince and Salas (1992) conducted fixed-wing research which demonstrated that potential cost and transfer of training (TOT) benefits could be derived from simulation-augmented primary flight training. However the authors did not find this to be the case for rotary-wing aircrew TOT research. Currently, the U.S. Army does not use simulation in the primary (contact) phase of initial entry rotary-wing (IERW) training. Research performed by the Army Research Institute (Stewart, Dohme, & Nullmeyer, 2002) showed that a combination of synthetic flight simulation and criterion-based training during the primary phase of IERW had the potential for saving training time and costs in the aircraft. This research was performed using a low-cost simulator based upon the UH-1 helicopter.

Measured transfer effectiveness ratio (TER) is equal to the number of control group (no simulator training group) iterations to criterion in aircraft minus the number of experimental group (simulator pre-training group) iterations to criterion in aircraft, all divided by the number of experimental group iterations to criterion in simulator. In other words, TER is the ratio of savings in aircraft maneuver iterations to the number of iterations performed criterion in the

simulator by experimental students (or training cost). In the 4 quasi-experiments reported, positive TERs were observed for most flight maneuvers pre-trained in the simulator; student pilots in the simulator group required fewer iterations than control participants to reach proficiency on most flight maneuvers in the UH-1 training aircraft. As the visual display and flight modeling systems were upgraded, greater TERs were observed, and differences among groups tended to become significant.

Head and Eye Patterns using Cockpit Display of Traffic Information

Eye scan pattern metrics have been used to analyze the effectiveness of AR display devices. Wickens, Xu, Hellenberg, Carbonari and Marsh (2000) conducted a study funded by Aviation Research Lab (ARL) Institute of Aviation for the Federal Aviation Administration (FAA) Civil Aeromedical Institute, which looked at effectiveness of the Cockpit Display of Traffic Information (CDTI) device for free-flight scenario avoidance of traffic. The study questioned FAA guidance (Aeronautical Information Manual, 2000) for pilots to conduct outside world (OW) visual scan 75% of the time, which was based on no known data that measured fixations in visual flight simulation. They defined "dwell" as time in an Area of Interest (AOI) before leaving, "fixation" as an endpoint when the eye enters an AOI, and "transition" as movement from one fixation point to another. The pilot workload was partitioned in two components: visual (distributed between CDTI and OW) and cognitive (planning and executing avoidance maneuvers). The focus of the report was on visual workload, specifically the critical aspect of pilot head down time; not on OW. The objective of the experiment was to provide data regarding change in visual scanning patterns imposed by a task of self-separation. Baseline (i.e.

VMC with tower assistance and no CDTI) and change in baseline (i.e. free-flight avoidance using CDTI) scanning data collected was the Percentage Dwell Time (PDT) which equaled the Mean Dwell Duration (MDD) times the number of fixations in a given AOI. The three factors in pilot information acquisition model included Information content (i.e. characteristic sampling frequency), Importance (related to the number of samples to minimize defects), and Information access effort (distance head/eye must move); there is more effort in vertical eye movement based on Wickens, Xu, Hellenburg, Carbonair and Marsh (2000). It was hypothesized that in VMC flight simulation, expert pilots make more fixations for shorter dwells (Bellenkes et al., 1997; Fox, Fadden, Knorad, Marsh, Merwin, Sochacki, Sohn, Tham, Wickens, Lintern, Kramer, & Doane, 1995). Also, the effort based effect predicted the eyes will tend to remain head down longer to increase easier lateral scanning and longer dwells OW to take advantage of the distant screen. The resulting PDT indicated pilots looked 55-60% of the time at the instrument panel (IP) and 20-25% of the time on OW (contrary to FAA guidance). Also, the CDTI use decreased OW use. The pattern of first order transitions suggest IP (6.5 sec dwells) is the "home base" from all scans. However, they didn't measure IP subcomponent transition & dwell times. Also, pilots tended to fly Instrument Flight Rating (IFR) in VMC conditions, even when provided traffic avoidance commands. The IP importance is consistent with the "aviate-navigate-communicate" pilot mantra, so dwells shortened in conflict maneuvers. One effort based effect confirmed the eye was mainly head down to accommodate easier lateral CDTI-IP scanning, but not OW dwell increase effect.

Eye Movement and Mental Image

Eye scan metrics have been used to analyze mental images formed from visual stimulus. Johanson, Holsanova and Holquist (2005) published a paper showing evidence that eye movements reflect the positions of objects during the description of a previously seen picture, while listening to a spoken description, and during the retelling of a previously heard spoken description. The effect is equally strong in retelling from memory irrespective of whether the original elicitation was spoken or visual. This is directly applicable to pilot eye scan patterns for traffic avoidance based on a heard controller warning. (Johansson, Hlsanova & Holqvist, 2005).

Test subjects were presented with a picture for 30 seconds that was later orally described while they faced a white board. Then a pre-recorded verbal description that lasted 126 seconds later retold the description while they looked at the white board. Eye movements were recorded while test subjects recalled objects that were either previously observed in a complex picture or presented in a verbal description. In both cases, the subjects spontaneously looked at regions on a blank board that reflected the spatial locations of the objects they recalled. Results provide evidence that the eyes are connected with the cognitive processes that occur during imagery. Eye movements occur because of visual indexes in the external world, or because they are a product of procedures or neural re-enactments that make us experience mental images. (Johansson, Holsanova & Holqvist, 2005). Results from the experiment indicate a central fixation resulted in a decreased ability to recall a pattern. Also, eye movements reflect an internal mental image that is constructed in a "visual buffer" (e.g. Kosslyn, 1994). They used a Wilcoxon Signed-Ranks test for significance between number of correct eye movements and expected number of correct movements by chance. The results of retelling what could be seen in picture (experiment 1) and

retelling of verbal description (experiment 2) were almost identical. The eye movements in all three cases (description of previously seen picture, listening to spoken description, retelling of previously heard spoken description) indicate the spatial locations of objects from the picture and the description, respectively.

FOV Effect on Visual Cue Detection in Noisy Environments

FOV and display context has an effect on measured eye scan patterns. Nikolic, Orr and Sarter (2004) examined how display context affects the effectiveness of abrupt onset signals. Sixteen Ohio State University student participants performed an externally paced visual task seated in front of 2 side-by-side 21" monitors. There was a Tetris puzzle-completion task on a left monitor, and a peripheral target detection task on a right monitor (approximately 35-45º offset) while trying to detect abrupt-onset stimuli (monochrome, white or color solid green box), which were presented against 5 different display backgrounds and at 2 different eccentricities (35º & 45º). The display background varied in terms of its dynamics and its color similarity to the target. Results indicated that color similarity, the movement of background elements, and increasing target eccentricity resulted in reduced detection performance. The lowest target detection rate was observed in the color-dynamic condition. This illustrates the importance of considering display context and need to adapt findings from laboratory research when designing interfaces for complex environments (i.e. prevent pilots from missing changes in status of their automated systems).

Recent research indicates that flashing an element to notify a user (e.g. pilot) of important events in a data-rich event-driven domain (e.g. aviation) is not very successful (Sarter & Woods,

1997, 2001; Pashler, Jonston & Ruthruff, 2001). The likelihood of detection depends on a match between a person's active attention control settings and properties of appearing signal, also known as contingent orienting (Folk, Remington & Johnston, 1992; Pasher et al., 2001). Although cues can be detected at peripheral eccentricities up to 50º FOV (Rinalducci & Rose, 1986), other studies have shown tunneling effect of functional FOV during demanding tasks (Chan & Courtney, 1993; Rinalducci, Lassiter, MacArthur, Piersal & Mitchell, 1989; Williams, 1985).

Eccentricity results are FOV effect related since they indicate resulting effects (i.e. fewer targets detected) are more pronounced in the color-dynamic condition, independent of Tetris speed (i.e. workload), which suggests that it is not the result of attention narrowing caused by increased task difficulty. A possible explanation may be that increasing the distance between user focus areas and the location of target onset, the number of dynamically changing objects between the two points increased, thus amplifying the masking effect (Martin-Emerson & Kramer, 1995; Schons & Wickens, 1993).

Eye Movement Models

Various eye scan pattern models have been formulated to analyze visual system effectiveness. The Encyclopedia of Biomaterials and Biomedical Engineering provides a history on how eye movement was measured from the 19th century to today and the importance of studying eye movement for Human Computer Interaction (HCI). Virtually all animals with developed visual systems actively control their gaze using eye or head movements (Land, 1995). Saccades (large ballistic scanning movements) typically occur 3-4 times every second (Bridgeman, 1992) taking

30-50 msec in between movement (McConkie & Rayner, 1975). Evolution appears to have selected a solution to process vast amounts of visual information by inspecting small portions of the visual world in rapid sequence (Treue, 2001). Consequently the human eye monitors a visual field of about 200º, but receives detailed information from only 2º (Levi, Lkein, & Aitsebaomo, 1985). This region is the fovea and is jerked around at speeds of up to 500° per second, during which its sensitivity drops to near blindness levels (Martin, 1974; Thiele, Henning, Kubischik, & Hoffmann, 2002). During the 200-300 msec the fovea is at rest, over 30,000 densely packed photoreceptors provide high acuity color vision. It is believed that saccades can provide insight into cognitive processes such as mental imagery and decision making. Eye movements of individuals can also reveal differences in aptitude and expertise. Some form of short-term memory for saccade pattern is used to scan a scene for information (Leek, Reppa, & Tipper, 2003; Henderson & Hollingworth, 1999) but it is not clearly understood (Henderson & Hollingworth, 2003). Conversely, memory processes also recruit eye movements (Spievey & Geng, 2001) observed in subjects as young as six months of age (Richardson & Kirkham, 2004). Therefore, anticipatory behavior should be more evident in experienced pilots (e.g. quick glance to clear a turn during flight).

Tsinhoni and Liu (2003) published an article that introduced two modeling studies of eye movement. First, random menu search was modeled using a queuing network approach and second, a reinforcement learning algorithm was used to generate a simulation of various eye movement patterns. Q-Learning, one of the reinforcement learning methods, was adopted to generate different patterns in eye movement. Approach to modeling eye movement was to consider each eye movement as a Markov decision process and then to find an underlying policy using reinforcement learning method (which action should be taken in a certain state to

maximize discounted long term reward). Simulated results compared against Yarbus (1967) experiment: subject was shown a picture and then asked seven different questions about the picture (e.g. give the ages of the people, what has the family been doing?). The subject's eye movement was recorded for each question and the results showed that the subject moved his/her eyes over the picture very differently depending on the questions. (Tsimhoni & Liu, 2003). The paper suggests using the queuing network model, which has been successfully applied in other task domains (e.g., response time, driver performance). Yarbus experiment patterns of eye movement compared close to queuing network under the same (questions asked) conditions. Markov decision process is described by four attributes: S is the state space, A is the action space, T(s, a, s') is the transition function that indicates the probability of arriving in state s' when action a is taken in state s, and the reward function is R(s, a, x). The solution to a Markov Decision Process can be expressed as a policy π, which gives the action to take for a given state, regardless of prior history. The standard family of algorithms to calculate the policy requires storage for two arrays indexed by state: value V, which contains real values, and policy π, which contains actions and will contain the solution at the end of the algorithm. In summary, Q-learning is a reinforcement learning technique that works by learning an action-value function that gives the expected utility of taking a given action in a given state and following a fixed policy thereafter.

Jones and Endsley (2004) published a paper that evaluated the SVIS against conventional glass cockpit PFDs and MFDs, which includes a ND, to assess whether or not SVIS can improve pilot FTE performance, SA, and workload. They used a fixed-base laboratory flight simulator with three forward projection units at a total FOV of 140° and 12 pilot evaluators. The pilots flew fairly difficult simulated approaches into the Eagle County, Colorado, airport.

Questionnaires were used in various phases of the flights to estimate workload, SA, and user preference. SA was collected using the SAGAT (Endsley, 1995; Endsley & Bolstad, 1994) and workload estimates were obtained using the NASA Task Loading Index technique. Eye movement data was collected using a modified IScan ETL 500 system, and analyzed to find a link analysis (an analysis of eye movement transitions between areas of interest on the displays), scan length, fixation frequencies, location of fixations, and duration of fixations. (Schnell, Kwon, Merchant, & Etherington, 2004). It was hypothesized the SVIS displays can reduce workload and FTEs and increase SA. They also wanted to ensure the SVIS displays would not disrupt the pilot's scan patterns. Ten static AOIs were defined on the SVIS PFD and ND. Those were the airspeed indicator, bank indicator, center of tunnel, vertical speed indicator, altitude tape, and altitude indicator window on the PFD, as well as the track indicator and aircraft position on the ND. Additionally, the entire PFD and ND area were defined as two higher-level AOIs. The boundaries of the AOIs were set about 15% larger than the actual areas to allow for slight inaccuracies in the eye tracking system. Three conditions: PFD & ND, SVIS PDF & ND, PFD & exoview 3D display. A link analysis (% transitions between AOIs) was performed for all the AOIs (Schnell & Merchant, 2001). FTEs that were assessed included the vertical track error (amount that the aircraft is off path vertically), the cross-track error (amount that the aircraft is off track laterally), the flight path angle error (extent to which the vertical flight path angle is in error), the track angle error (extent to which the lateral track angle is in error), and the speed deviation error (deviation from commanded speed). The results indicated that the SVIS is superior to the conventional displays (i.e. reduced workload and FTEs) for the majority of the measures that were obtained in the experiments.

Head Movement Models

For HMD use, accurate head tracking is a critical aspect of maintaining a natural view during voluntary head movements, and to maintain clear vision during involuntary head movements due to acceleration and/or vibration (Winterbottom, Patterson, & Pierce, 2006). Temporal delays or lags in the computation of head position, or in the update of the displayed imagery, can impair human performance and create disorientation, nausea and discomfort cause, in part, by a sensory conflict between proprioception and vision. According to the *Encyclopedia Britannica*, proprioception is the perception by an animal of stimuli relating to its own position, posture, equilibrium, or internal condition. In other words, when wearing an HMD and making voluntary and involuntary head and eye movements, corresponding unnatural HMD visual stimuli will cause proprioception conflicts. Despite general agreement concerning negative effects of temporal delays or lags, there is little agreement on the critical delay or lag beyond which impairment can be expected. Winterbottom et al. (2006) suggest we understand the visual events occurring when a head movement occurs and imagery is updated within a short duration, such that visual perception is undisturbed. They introduce the concept of head-movement suppression, similar in concept to saccadic suppression (Martin, 1974), to make visual perception stable and uninterrupted while rapidly moving images are sweeping across the retina during a head movement. For the update of imagery to go unnoticed, its delay would need to be shorter than the duration of head-movement suppression. Additional head-suppression research is needed to understand and possibly control for the effects of a perceptual mismatch between vision and proprioception when head-movements are performed with an HMD.

HMD head tracker position accuracy and sampling frequency of at least 120 Hz (Winterbottom et al., 2006) is important. Degree of accuracy varies with application (e.g. 10 mrad for launching air-to-air missiles, 2 mrad for weapon aiming).

FOV effects on Visual Pathways

Winterbottom, Patterson and Pierce (2006) researched perceptual issues relevant to the use of HMDs for flight simulation and training applications. They concluded that a large FOV would produce a greater sense of immersion as well as provide the stimulus conditions necessary for adequate visual functioning. This is based on the fact that the visual system is anatomically subdivided into two different visual pathways: the parvocellular and magnocellular pathways depicted in Figure 4. The central retina parvocellular pathway connects to areas in the visual cortex that make up the ventral cortical stream where spatial pattern information is analyzed. The ventral stream is thought to be involved in the functional analysis of spatial pattern information for the purpose of identifying objects. The central and peripheral retina magnocellular pathway connects to areas in the visual cortex that make up the dorsal cortical stream where optic flow information for heading control and biological motion is analyzed, integrating vision with action. The dorsal stream is thought to be involved in the functional analysis of motion information for the purpose of determining spatial relations and controlling heading during motion.

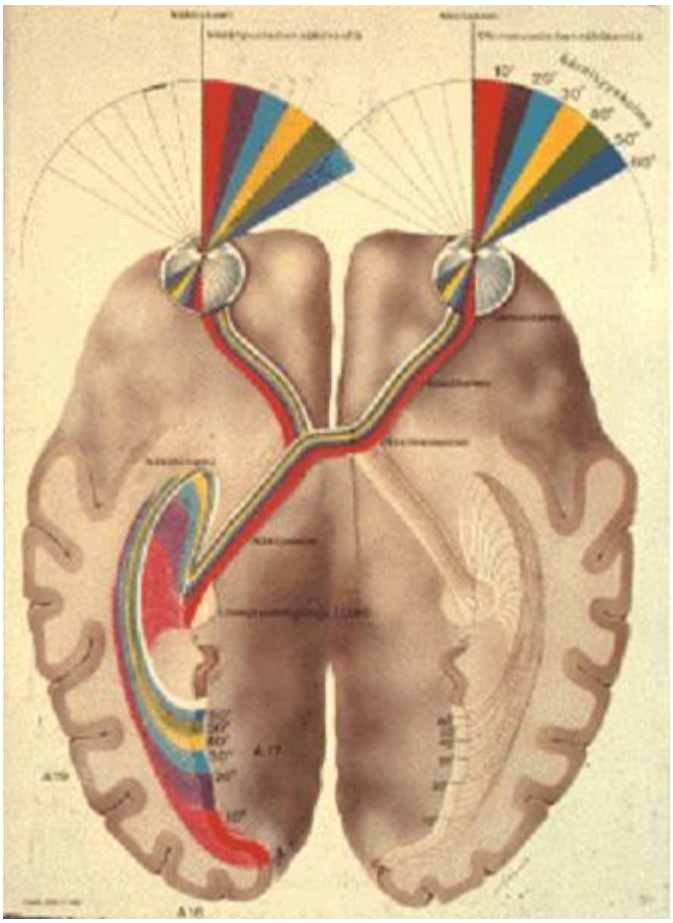

Figure 4: Visual Pathways [Hyvärinen, 2007]

Restricting the FOV would restrict the dorsal stream, which can lead to impaired ability to control heading or process spatial orientation. Winterbottom et al. also suggest restricting the FOV can compromise the sense of immersion, citing other research, which suggest a FOV of at least 50° (circular) is needed for some sense of immersion in a roll vection application. Also reported was heading control in a flight simulator led to impaired performance in narrow (e.g. 25°) FOV relative to larger (e.g. 55°) FOV. Surely the required size of FOV for a HMD would depend upon the application under consideration.

If we consider situation awareness to be an overlapping construct with presence (Prothero et al, 1995) and the visual stimulus to provide the perception of data and the elements in the environment (Endsley, 2000), then we can infer the reduction of FOV will also have an effect on perception, comprehension and projection (i.e. situation awareness), which in turn will affect decisions and task performance for a pilot navigating in a virtual world. However, task performance analysis is not always a good implicit measurement of situation awareness (Reber, 1995). As an example of reduced FOV, one pilot might have more flight experience than another, allowing them to need less visual stimulus to comprehend and project and make better decisions leading to better task performance. In other words, their situation awareness would be better simply by having more knowledge. By averaging task performance of a group of pilots with similar experience, one can obtain a more accurate measure of situation awareness FOV effects (Arthur, 2000).

CHAPTER THREE: EXPERIMENTAL METHOD

In the case of this research involving flight simulation, the dependent variables relate to behavior and performance measures for basic pilot tasks in a helicopter simulator. The independent variable is the pilot's eFOV, which will vary by a fraction of 100% for each consecutive test run. As the eFOV is reduced, a measurable difference in the dependent behavior (i.e. head and eye movement pattern) is likely, and a measurable difference in performance is expected. Normal image processing occurs at different instantaneous FOVs where head/eye movement patterns change and performance is measurably reduced. These FOV effects will provide insight into AR display device FOV design for this type of flight simulation application.

Experimental Participants

Through cooperation with a local Florida flight simulation and training facility we solicited a group of experienced Bell 206 certified instructor pilots who volunteered to participate in the present experiment. A total of seven pilots, six males and one female, varying in age from 21 to 35, who each had a minimum of 300 hours in the Bell 206, were eventually included in the sample we were able to secure. None had any self-described sources of debilitation, which would have interfered with their presently required performance.

Equipment and Materials

A local training facility provided a Bell 206 flight simulator for this experiment. It was a Aero Simulators Flight Navigation Procedure Trainer (FNPT) II. The FNPT II has a 170° horizontal x 75° vertical wrap-around field of regard, rear-projected display. The entire

helicopter simulator depicted in Figure 5 is supplied in a self-contained 18 foot trailer classroom, complete with instructor station. All pilot volunteers used in the experiment were intimately familiar with the FNPT II operation and the airport visual scene used.

Figure 5: Aero Simulators FNPT II

The UCF Optical Diagnostics and Applications Lab (ODALab) provided an InterSense IS-1200 VisTracker for head orientation tracking. The Institute for Simulation and Training (IST) provided an Arrington Research ViewPoint EyeTracker® system and EyeFrame Hardware demonstration unit for this research (Arrington and Geri, 2000). They are depicted on a pilot participant in Figure 6.

Figure 6: Pilot Wearing Head and Eye Tracking System; No Mask

The eFOV masks were created and custom fit to attach to the EyeTracker goggles as demonstrated by the pilot participants in Figure 7.

Figure 7: Pilot Wearing Head and Eye Tracking System; With Mask

Experimental Design

In the present study, our pilots were tested in the flight simulator with varying FOVs. The development of an optimized eFOV for a stereoscopic augmented reality-based display system to perform such tasks requires an understanding of FOV effects. These effects are related to the function of different visual pathways in the brain such as (a) the dorsal stream whose function relates primarily to spatial orientation, heading control, sense of immersion and visual-motor tasks requiring a wide FOV and (b) the ventral stream whose function relates more to targeting, object recognition, and visual-motor tasks requiring a narrower FOV (see Winterbottom, Patterson & Pierce, 2006). We hypothesized that, depending on the task, limiting a pilot's eFOV would impose an additional workload due to the limited peripheral image data. As a pilot's eFOV is artificially reduced, measurable changes in pilot eye scan behavior would presumably change, as would head movement range (in degrees), which we hypothesized would increase, and head rate of movement (in degrees/second), which we expected to increase to compensate for the reduced peripheral visual information assimilation capacity.

A question for investigation is what level of change in natural eye and head movements are permitted in a task, in order for the user to still perform according to what is considered an acceptable level. We thus postulated that a threshold exists at which decreasing the eFOV below this threshold means a pilot can no longer compensate sufficiently to maintain an adequate image of the overall environment, thus leading to a measurable decrease in response proficiency. Somewhere between the onset of measured eye and head movement changes and the measured decrease in task performance, negative transfer becomes a concern. Such FOV effects can provide insight into an augmented reality or virtual reality head-worn display FOV design for this type of flight simulation application. To evaluate these respective propositions, a single

group, within-participant repeated measures design was employed. This is a common approach when only a few high level experts are available as participants. The primary independent variable was the pilot's eFOV, which was varied across each consecutive test run according to a previously imposed random order. The primary dependent variables were head and eye movements and resultant flight profile changes.

Experiment Procedure

All testing was conducted during the evening hours when the commercial simulator was available. The pilot volunteers were briefed on the procedures and the functioning of the head/eye tracking system. Each volunteer was asked to read and sign an informed consent form before any experimentation began. All simulation test runs began with a pilot initialized at the base leg of a visual flight rule pattern at 600 ft. and 85 kts. This condition is depicted in Figure 8 for a bird's-eye view perspective. The pilot wore a helmet with the IS-1200 VisTracker camera and the Arrington Research ViewPoint EyeTracker system and goggles with the appropriate masking to achieve the randomly selected eFOV. The pilot maneuvered to make a coordinated turn to line up with the runway, while descending to land at the runway intersection. Time to land, flight path over the ground and descent path were recorded in each run. Each pilot completed a total of five such runs.

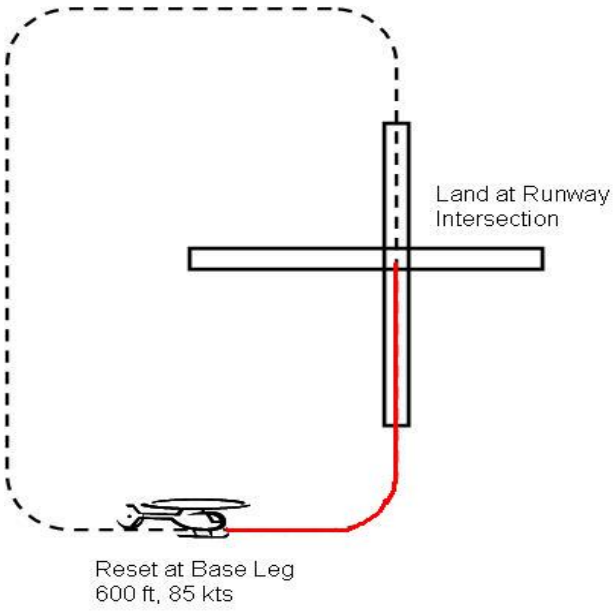

Figure 8: Simulation VFR Pattern

Random selections from a Latin Square were used to determine the sequence of test runs in order to address the potential problem of asymmetric transfer effects (Lowry, 2007; Poulton, 1973). Consequently, before each run, each participant was assigned to one specific sequence of eFOV conditions. The independent variable was the pilot's eFOV as a percentage of maximum unobstructed standard human 200º horizontal (h) x 135º vertical (v) FOV, which is defined here as the 100% baseline value. The five possible FOVs for testing were 160° h x 108° v (80%), 120° h x 81° v (60%), 80° h x 54° v (40%), 40° h x 27° v (20%), and 20° h x 13.5° v (10%), where the percentage values are expressed as a function of the defined 100% maximum. Each pilot completed five test runs, taking approximately four minutes for each run, depending upon their individual performance. This short, simulated visual landing task was pre-planned in order to prevent pilot fatigue due to spending more than a half hour in the simulator. Masking portions of the EyeTracker goggles restricted the eFOV to the five respective conditions (80%, 60%, 40%, 20% and 10%). The different horizontal and vertical eFOV openings of the mask were

calculated based on an eye to mask distance of 15 mm. These dimensions ranged from 170.1 mm x 41.3 mm at the maximum extent to a 5.3 mm x 3.6 mm aperture at the minimum extent. The eFOV mask sizes are depicted in Figure 9.

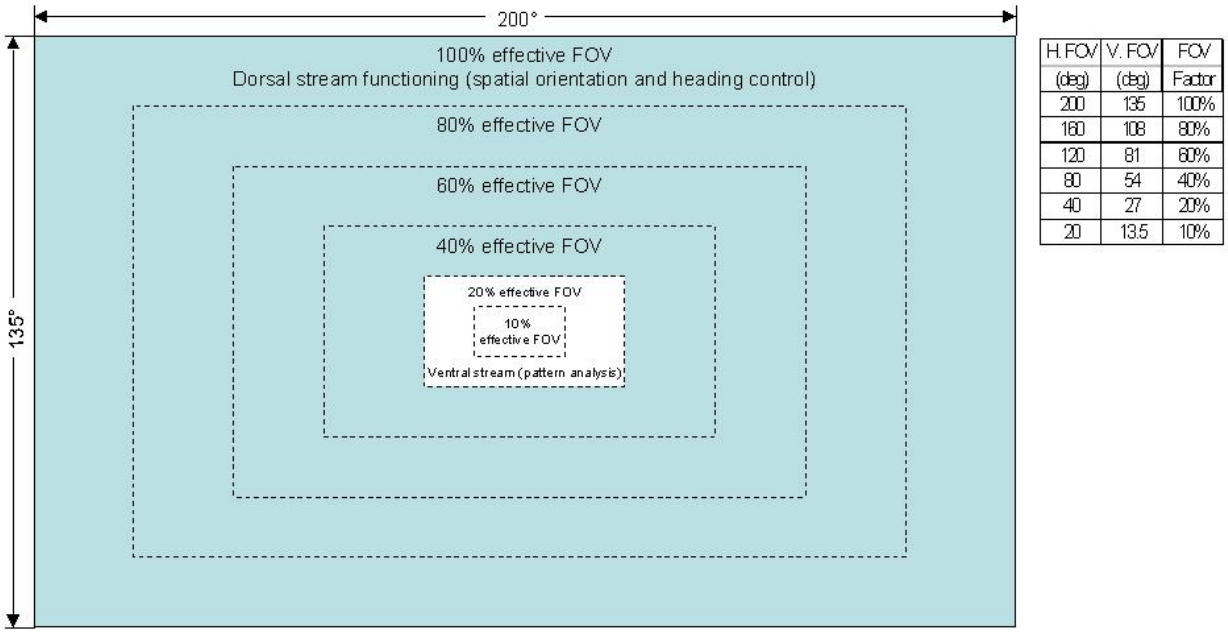

H. FOV (deg)	V. FOV (deg)	FOV Factor
200	135	100%
160	108	80%
120	81	60%
80	54	40%
40	27	20%
20	13.5	10%

Figure 9: The effective FOV (eFOV) Reduction Factors

The order in which a pilot participant used an eFOV reduction factor condition can be selected at random from a possible six-factorial (6!) or 720 possible sequences. Consequently, before the simulation test runs each pilot participant was systematically assigned a counter-balanced sequence of eFOV conditions per run as indicated in Table 1.

Table 1: Latin Square Design

	Sequence					
	eFOV1	eFOV2	eFOV3	eFOV4	eFOV5	eFOV6
Participant 1	80%	20%	100%	60%	40%	10%
Participant 2	40%	100%	60%	20%	10%	80%
Participant 3	60%	10%	40%	100%	20%	80%
:	80%	20%	10%	100%	40%	60%
Participant n	10%	20%	100%	40%	60%	80%

The different horizontal and vertical eFOV openings of the mask were calculated based on an eye to mask distance of 15 mm. The following Table 2 summarizes the mask H x V opening dimensions in millimeters.

Table 2: The effective FOV (eFOV) Mask Openings

H FOV (deg.)	V. FOV (deg.)	Factor	H (mm)	V (mm)
200	135	100%		
160	108	80%	170.1	41.3
120	81	60%	52.0	25.6
80	54	40%	25.2	15.3
40	27	20%	10.9	7.2
20	13.5	10%	5.3	3.6

Recall in the FNPT II simulator, the 100% eFOV is limited to essentially 80% by the 170° h x 75° v simulator FOR. Therefore each pilot completed only a total of five test runs, taking roughly 4 minutes for each run. This short visual flight rule (VFR) base leg to landing simulation run was planned to prevent the pilot from spending more than a half hour in the simulator for all five simulation runs. This minimized fatigue effects on measured performance.

Determining Sample Size

It was anticipated that no more than twelve certified pilot instructors would be available to volunteer given the limited number of instructors at Bristow Academy and their extremely busy schedule. Given this anticipated limitation, a limited sample size was predicted to be at best twelve pilot subjects multiplied by five eFOV conditions providing a maximum of 60 effect observation samples. To ensure this sample size and the predicted sample mean were adequate to represent a larger population mean, the method used to determine adequate sample size was to determine an acceptable margin of error (E), which is the maximum difference between the observed sample mean and population mean based on a normally distributed population.

This formula can be used when one knows (or can predict) the population standard deviation (σ), and want to determine the sample size (n) necessary to establish, with a confidence of $1-\alpha$, the population mean value (μ) to within an acceptable margin of error ($\pm E$) (How to determine sample size).

$$n = \left[\frac{z_{\alpha/2}\sigma}{E} \right]^2$$

where:

$z_{\alpha/2}$ is known as the critical value, the positive z value that is at the vertical boundary for the area of $\alpha/2$ in the right tail of the standard normal distribution.

σ is the population standard deviation.

n is the sample size.

Using horizontal head movement samples in the FNPT II simulator (FOR =170º horizontal) as an example, the smallest 10% eFOV (20º horizontal) should force a subject to move their head horizontally between 0º and a maximum of 75º to their left or to their right

((170º - 20º)/2 restriction to their left or right). Therefore the population mean can deviate 37.5º (75º/2), which is the predicted population standard deviation. For 95% confidence that the sample mean is within 11º of the population mean, the sample size must be 45, which can be satisfied with nine (9) pilot participants if each of the nine pilots are tested under 5 different eFOV conditions, yielding a sample size of 45.

Measurement Procedures

Head and eye movement patterns were categorized based on the three factors that influence where a pilot looks: Information, Effort, and Importance (Wickens, Xu, Hellenberg, Carbonari and Marsh, 2000).

Information Behavior

For *Information* expectancies, the pilot's Areas of Interest (AOIs) is that in which the pilot can gather visual information, as shown in Figure 10. The number of eye fixations, defined as dwells greater than 100 ms per AOI within a 0.5º radius from the AOI boundary (Manor & Gordon, 2003; Guest & Rolland, 1999), was the measure collected to represent Dwell Frequency per AOI. The 0.5º radius corresponds to half of the EyeTracker's angular accuracy. Also, how long the eye fixated in an AOI was a value measured as the Mean Dwell Duration in an AOI (Poole, Ball, & Phillips, 2004). These eye-dwell metrics were collected to provide an indication of pilot scan pattern changes during the simulated visual approach and landing phase as the eFOV was varied.

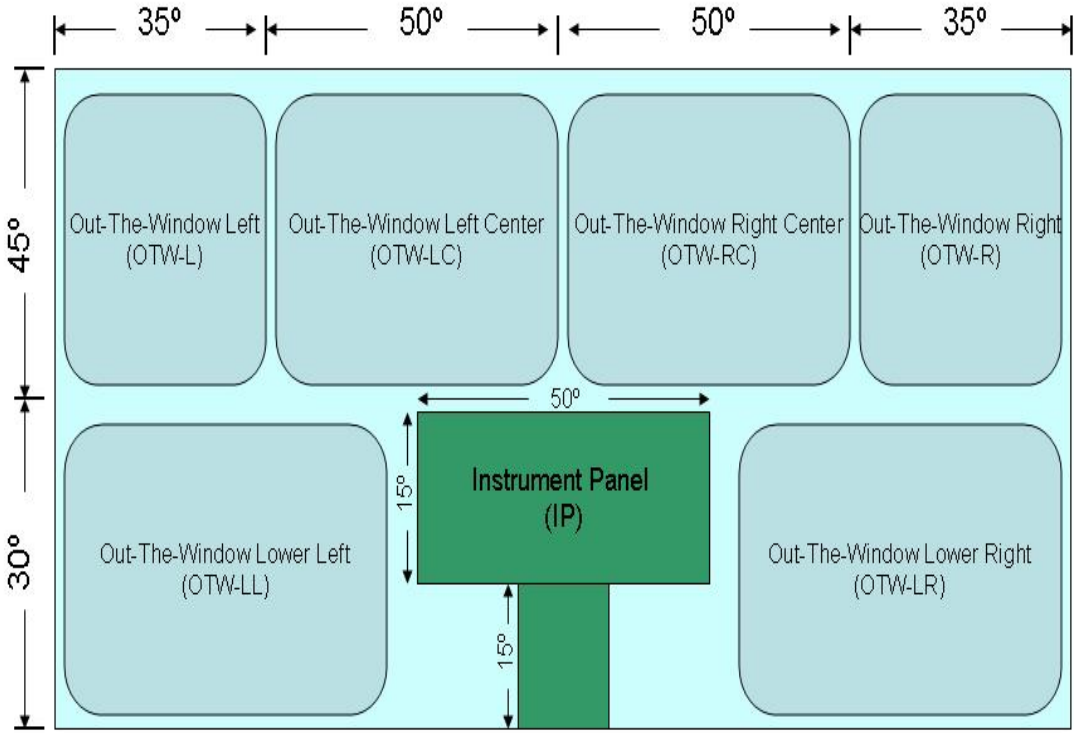

Figure 10: Bell 206 Cockpit AOIs

Inside the cockpit, certain instrument panel gauges are differentially important for communication of information during different phases of the simulated flight. As a result, all transitions to and from the instrument panel were recorded. Likewise, for the Out-the-Window (OTW) views, different AOIs provided the needed information during various phases of the simulated flight. The Out-the-Window view was divided into six large areas of interest, evenly distributed to the left and to the right of the simulator. All pilots were seated in the right seat for the simulation runs.

Effort Behavior

For *Effort* expectancies, the eye and head movements were recorded to understand the pilot's degree of effort exerted in gathering visual data from their environment; the greater the movement range (measured in degrees), the greater the effort (Wickens et. al., 2000). Pitch, roll and yaw head movements were recorded by the head tracking system and converted to vector form and the scalar values were plotted for each pilot for each simulation run. A rotating Cartesian coordinate system depicted in Figure 11 was used for measuring the head and eye rigid body rotations. (Agrawal, 1986).

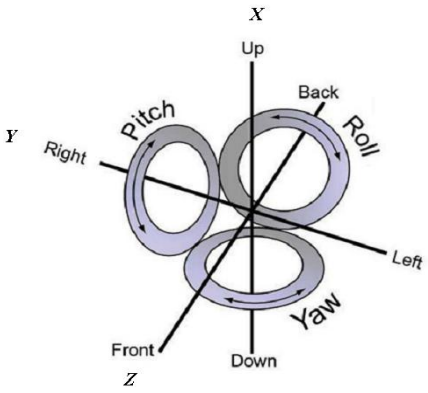

Figure 11: Head and Eye Coordinate System

Importance Behavior

For *Importance*, head movement velocity (in degrees/second) were calculated and plotted for each pilot during each simulation run. Also, each pilot was video-taped to validate head tracking data collected during each simulation run. After all sequence runs for the pilot were

complete, a post-flight debrief documented the overall FOV effects perceived by the pilot. Debrief notes are summarized in Appendix A.

Simulated Flight Performance Proficiency

The FNPT II simulator only provides a recording of aircraft course over ground and vertical movement for each simulation run. The result is a JPEG file (upper right Figure 12) showing a trail of the aircraft's course over ground and its vertical movement. This file allows subsequent performance analysis similar to the one conducted by Keller, Schnell, Lemos, Glaab, and Parrish (2003) for example, where they calculated Runway Alignment Error (RAE) and Vertical Track Error (VTE). Runway Alignment Error is the angle formed between the extended runway centerline and aircraft track as it rolls out of the turn for the straight in approach. Vertical Track Error here is represented by the maximum vertical deviation of the aircraft's actual position from the ideal path or vertical glide-slope. The dark grey glide slope triangle is used during an instrumented approach to the beginning of the runway. It needs to be translated (see semi-transparent grey triangle) to the intersection of runway 36 and runway 27, which was the actual landing area used.

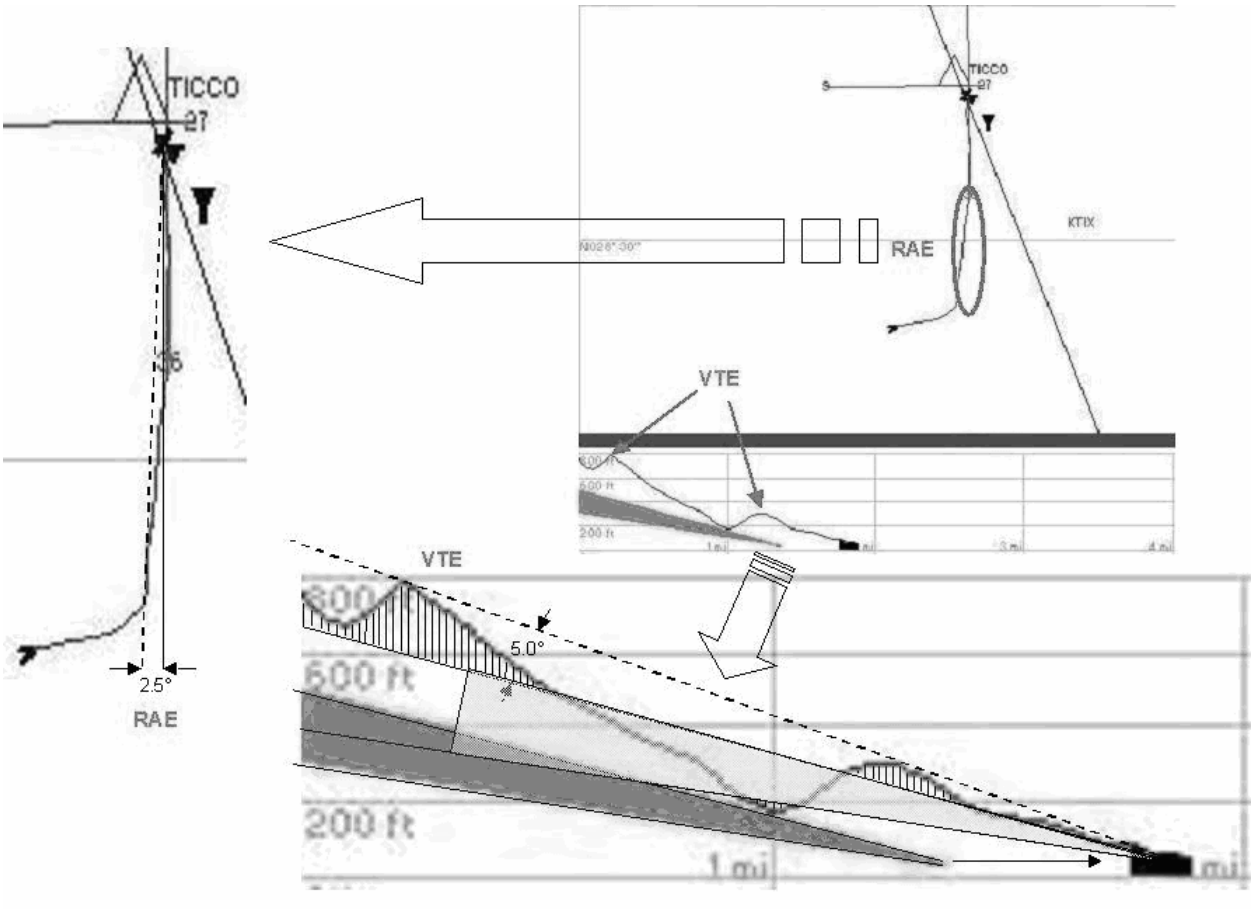

Figure 12: Measuring Runway Alignment and Vertical Track Errors

After measuring the RAE and VTE for each pilot eFOV simulation run, the Mean Square Error (MSE) and Root Mean Square Error (RMSE) was calculated (Kell et al, 2003) and shown in Appendix C.

Expected Results

It was anticipated, based on previous research that the pilot scan would remain the same but head movement would increase and performance would decrease as the pilots eFOV is limited beyond a certain threshold (Arthur, 2000; Wells & Venturino; 1990; Wickens et. al. 2000; Foyle, Kaiser

& Johnson, 1992). For Effort expectancies, DFA and MDD were anticipated to remain relatively constant across AOIs for varying eFOVs. The rationale being the pilot will attempt to continue gathering information from AOIs by increasing head and eye movements as the eFOV decreases. For Importance expectancies, the head movement distances (i.e. range of movement) were expected to increase with decreasing eFOVs.

For Importance expectancies, the head and eye rates of movement (i.e. sinusoid frequencies) were expected to increase with decreasing eFOV. It was also anticipated that flight performance would decrease due to the added stress of having to perform the same tasks with a constrained eFOV. Performance measurements were expected to deteriorate quickly as eFOV is decreased beyond a threshold value.

CHAPTER FOUR: RESULTS

Results and Discussion

The data extracted from the Head and Eye Tracker measurements were based on the previously described factors that influence where a pilot looks: Information, Effort, and Importance. For each simulation run, the simulator recorded aircraft course over ground and elevation. The results described here represent an analysis of these measures and tracking performance as the eFOV was changed for each simulation run.

Information Behavior

Dwell Frequency per AOI (DFA)

The average dwell frequency per AOI by eFOV for all pilots is shown in Table 3. The large values indicate that pilots tend to mainly look outside left of center (OTW-LC) and also outside right of center (OTW-RC), as well as the instrument panel (IP) for flight information, with some glances outside at far left (OTW-L), outside far right (OTW-R) and outside lower right (OTW-LR), when landing the aircraft. Also, as the eFOV is decreased, the data indicates an increasing trend for a greater focus on OTW-L and IP areas of interest.

These measurements are for the base course, turn, and final approach phases combined. After conducting a single factor Analysis of Variance (ANOVA) F-test with an alpha factor of

0.05 across the five eFOV groups, it was discovered only the OTW-L had a statistically significant change when comparing the 80% and the 10% eFOV data points.

Table 3: Average Dwell Frequency per AOI (DFA)

	Average Dwell Frequency per AOI (DFA)						
eFOV	OW-L[1]	OW-LC	OW-RC	OW-R	IP[1]	OW-LL	OW-LR
10%	3.57	13.86	14.43	0.14	20.43	0.00	0.29
20%	3.00	17.57	9.14	0.29	19.71	0.00	0.14
40%	2.71	16.57	7.57	0.14	16.14	0.00	0.43
60%	1.43	18.00	8.00	0.29	15.71	0.00	0.29
80%	1.29	16.57	9.29	0.00	14.57	0.00	0.00
Key OTW-L is Out The Window – Left OTW-LC is Out the Window – Left of Center OTW-RC is Out The Window – Right of Center				OTW-R is Out The Window – Right IP is Instrument Panel OTW-LL is Out The Window – Lower Left OTW-LR is Out The Window – Lower Right			
For Decreasing eFOV, "**1"** indicates an Increasing trend.				For Decreasing eFOV, "2" indicates a Decreasing trend.			

To analyze the FOV effect during each phase of the simulated flight, the Dwell Frequency per AOI data was processed separately for each phase of the simulation run. The results are reported in Table 4, which shows the average dwell frequency per AOI by phase. The data indicates that for a decreasing FOV, there is a decreasing trend for the IP in the base phase, then an increasing trend for OTW-L and OTW-LC and the IP in the turn phase, followed by a decreasing trend for OTW-LC, and an increasing trend for OTW-RC and the IP in the approach phase.

By analyzing each phase separately, changes in scan pattern as measured by Dwell frequency per AOI appear to indicate increased eye movement as the pilot transitions from one phase of the simulated flight to the next. In general, when restricting a pilot's FOV, they tend to make more frequent looks to the horizon in the direction of turn to gather more runway and aircraft relative orientation information, and more frequent looks at the instrument panel to gather more aircraft orientation information (e.g. altitude, airspeed, rate of descent). During the

turn phase the pilot normally needs to gather more spatial orientation information to the runway and heading control information in preparation for the approach phase. When transitioning to the straight in approach phase, they make more frequent looks at the horizon straight ahead of them and at the instrument panel as the eFOV decreased. The only OTW decrease in mean dwell frequency was during the approach phase, when the pilot needed less OTW-LC information.

Table 4: Average Dwell Frequency per AOI (DFA) by Phase

Base	OTW-L	OTW-LC	OTW-RC	OTW-R	IP[2]	OTW-LL	OTW-LR
10%	1.00	3.14	1.14	0.00	2.43	0.00	0.00
20%	1.43	4.29	0.86	0.00	2.71	0.00	0.00
40%	0.71	3.00	0.57	0.00	2.71	0.00	0.00
60%	0.43	3.00	1.43	0.00	2.43	0.00	0.00
80%	0.86	4.57	2.00	0.00	2.86	0.00	0.00
Turn	OTW-L[1]	OTW-LC	OTW-RC	OTW-R	IP[1]	OTW-LL	OTW-LR
10%	2.57	6.71	0.86	0.00	6.14	0.00	0.00
20%	1.57	6.43	1.14	0.00	6.71	0.00	0.00
40%	2.00	6.71	1.00	0.00	4.86	0.00	0.00
60%	1.00	4.71	1.86	0.00	4.14	0.00	0.00
80%	0.43	4.57	1.71	0.00	4.00	0.00	0.00
Apch	OTW-L	OTW-LC	OTW-RC[1]	OTW-R	IP	OTW-LL	OTW-LR
10%	0.00	4.00	12.43	0.14	11.86	0.00	0.29
20%	0.00	6.86	7.14	0.29	10.29	0.00	0.14
40%	0.00	6.86	6.00	0.14	8.57	0.00	0.43
60%	0.00	11.43	5.86	0.29	9.71	0.00	0.43
80%	0.00	7.43	5.57	0.00	7.71	0.00	0.00

Key	
OTW-L is Out The Window – Left	OTW-R is Out The Window – Right
OTW-LC is Out the Window – Left of Center	IP is Instrument Panel
OTW-RC is Out The Window – Right of Center	OTW-LL is Out The Window – Lower Left
	OTW-LR is Out The Window – Lower Right
For Decreasing eFOV, "1" indicates an Increasing trend.	For Decreasing eFOV, "2" indicates a Decreasing trend.

Although mean dwell frequencies per AOI indicated a change in scan pattern due to a changing eFOV, the single factor ANOVA F-test did not indicate a statistically significant change for any of the AOIs In summary, the measured mean dwell frequency changes indicate the pilot's normal scan pattern changed with the decreasing size of eFOV. It was statistically significant in the measured overall dwell frequency changes in OTW-L. We might infer this is

pilot dwell frequency compensation due to decreasing situation awareness (e.g. orientation to runway, altitude, rate of descent, airspeed).

Mean Dwell Duration (MDD)

Values for mean dwell duration are shown in Table 5, which details pilot duration averages for the areas of interest that registered any dwell time, listed by eFOV. The data indicate a decreasing trend for OTW-LC and OTW-RC and an increasing trend for the IP areas of interest as the eFOV is decreased. However a single factor ANOVA F-test did not indicate a statistically significant change for any of the AOIs.

Table 5: Mean Dwell Duration (MDD)

	Mean Dwell Duration (MDD)						
eFOV	OW-L	OW-LC[2]	OW-RC[2]	OW-R	IP[1]	OW-LL	OW-LR[2]
10%	1.25	2.07	3.52	0.27	1.26	0.21	0.37
20%	0.98	2.23	4.14	0.16	1.12	0.00	0.76
40%	1.15	2.95	7.46	0.10	0.97	0.00	1.30
60%	1.32	3.00	7.56	0.15	0.90	0.00	1.27
80%	0.64	3.27	7.27	0.00	1.03	0.00	0.00
Key OTW-L is Out The Window – Left OTW-LC is Out the Window – Left of Center OTW-RC is Out The Window – Right of Center				OTW-R is Out The Window – Right IP is Instrument Panel OTW-LL is Out The Window – Lower Left OTW-LR is Out The Window – Lower Right			
For Decreasing eFOV, ”1” indicates an Increasing trend.				For Decreasing eFOV, ”2” indicates a Decreasing trend.			

The Mean Dwell Duration was also processed for the base, turn, and approach phases, and results are shown in Table 6. As the eFOV decreases, the pilot dwells more OTW-L and less OTW-LC and OTW-RC during the base phase, then dwells less for OTW-LC, but slightly more for the IP during the turn phase, followed by dwelling less for OTW-RC and for OTW-LR during the approach and land phase. This mean dwell duration measurement also indicates a

change in scan pattern with a changing eFOV. In general, when restricting a pilot's FOV, they tend to dwell less OTW in all phases of flight, and dwell slightly longer on their IP during the turn phase. One can infer the pilots were gathering less orientation and navigation information from OTW and more from their instrument panel during the turn as their peripheral vision was reduced. Although mean dwell durations per AOI indicated a change in scan pattern due to a changing eFOV, the single factor ANOVA F-test did not indicate a statistically significant change for any of the AOIs.

After analyzing the Scene Camera video during these phases, with a decreasing eFOV, it appeared the pilots reverted to previously learned instrument flight rule visual scan pattern behavior in setting up for the approach phase, requiring more information from the instrument panel AOI and less from the OTW. Once on the approach phase, the pilots tended to revert back to previously learned visual flight rule visual scan pattern behavior, as indicated by the significant drop in dwell time on their instrument panel.

Table 6: Mean Dwell Duration (MDD) by Phase

Base	OTW-L[1]	OTW-LC[2]	OTW-RC[2]	OTW-R	IP	OTW-LL	OTW-LR
10%	0.83	0.93	0.39	0.00	1.46	0.00	0.00
20%	0.71	1.13	1.03	0.00	1.16	0.00	0.00
40%	0.50	1.42	0.28	0.00	1.18	0.00	0.00
60%	0.24	1.74	1.55	0.00	0.90	0.00	0.00
80%	0.54	1.87	2.06	0.00	1.29	0.00	0.00
Turn	OTW-L	OTW-LC[2]	OTW-RC	OTW-R	IP[1]	OTW-LL	OTW-LR
10%	1.16	1.61	1.02	0.00	1.57	0.00	0.00
20%	0.87	1.99	1.08	0.00	1.16	0.00	0.00
40%	1.10	1.88	1.59	0.00	0.85	0.00	0.00
60%	1.24	3.33	1.56	0.00	0.85	0.00	0.00
80%	0.33	4.06	1.54	0.00	0.88	0.00	0.00
Apch	OTW-L	OTW-LC	OTW-RC[2]	OTW-R	IP	OTW-LL	OTW-LR[2]
10%	0.00	3.30	4.07	0.06	1.08	0.00	0.16
20%	0.00	2.67	5.23	0.16	1.13	0.00	0.76
40%	0.00	3.69	11.14	0.10	0.93	0.00	1.30
60%	0.00	2.46	14.77	0.15	0.87	0.00	2.08
80%	0.00	3.53	19.59	0.00	0.97	0.00	0.00

Key
OTW-L is Out The Window – Left
OTW-LC is Out the Window – Left of Center
OTW-RC is Out The Window – Right of Center
OTW-R is Out The Window – Right
IP is Instrument Panel
OTW-LL is Out The Window – Lower Left
OTW-LR is Out The Window – Lower Right

For Decreasing eFOV, ”1” indicates an Increasing trend.
For Decreasing eFOV, ”2” indicates a Decreasing trend.

Product of Dwell Frequency at AOI (DFA) and Mean Dwell Duration (MDD)

The product of the dwell frequency and mean dwell duration (in seconds) for each pilot and AOI, the sum for all the areas of interest for an eFOV yields an accurate total simulation run time (in seconds). This also provides a good indication of important areas of interest during a particular phase of flight. The average for all the pilots tested is listed in Table 7, which shows this product of dwell frequency and mean dwell duration by phase. For a decreasing eFOV, the data indicates pilot decreasing focus on OTW in all phases and an increasing focus on the instrument panel during turn and landing phase. A single factor ANOVA F-test did indicate a

statistically significant change for OTW-LC in the base phase, OTW-LC and the IP in the turn phase, and OTW-LC in the approach phase.

Table 7: Product of Dwell Frequency and Mean Dwell Duration by Phase

Base	OTW-L	OTW-LC[2]	OTW-RC[2]	OTW-R	IP	OTW-LL	OTW-LR
10%	1.06	3.00	0.98	0.00	3.78	0.00	0.00
20%	1.45	5.03	1.16	0.00	3.01	0.00	0.00
40%	0.72	3.83	0.73	0.00	3.07	0.00	0.00
60%	0.36	4.35	2.59	0.00	2.21	0.00	0.00
80%	0.66	9.14	4.13	0.00	3.59	0.00	0.00
Turn	OTW-L	OTW-LC[2]	OTW-RC[2]	OTW-R	IP[1]	OTW-LL	OTW-LR
10%	3.55	10.70	1.46	0.00	8.59	0.00	0.00
20%	1.56	11.76	1.45	0.00	7.33	0.00	0.00
40%	2.13	11.31	2.07	0.00	4.04	0.00	0.00
60%	2.75	11.72	3.69	0.00	3.78	0.00	0.00
80%	0.33	14.48	2.76	0.00	3.75	0.00	0.00
Apch	OTW-L	OTW-LC[2]	OTW-RC[2]	OTW-R	IP[1]	OTW-LL	OTW-LR[2]
10%	0.00	22.50	43.34	0.06	13.16	0.00	0.16
20%	0.00	28.32	41.60	0.16	11.32	0.00	0.76
40%	0.00	36.58	51.74	0.10	8.06	0.00	2.21
60%	0.00	44.05	36.80	0.15	10.32	0.00	2.08
80%	0.00	33.04	42.04	0.00	7.32	0.00	0.00

Key	
OTW-L is Out The Window – Left	OTW-R is Out The Window – Right
OTW-LC is Out the Window – Left of Center	IP is Instrument Panel
OTW-RC is Out The Window – Right of Center	OTW-LL is Out The Window – Lower Left
	OTW-LR is Out The Window – Lower Right
For Decreasing eFOV, "1" indicates an Increasing trend.	For Decreasing eFOV, "2" indicates a Decreasing trend.

To visualize this numerical data graphically, the values were transformed to circles superimposed on their respective areas of interest, as shown in Figure 13.

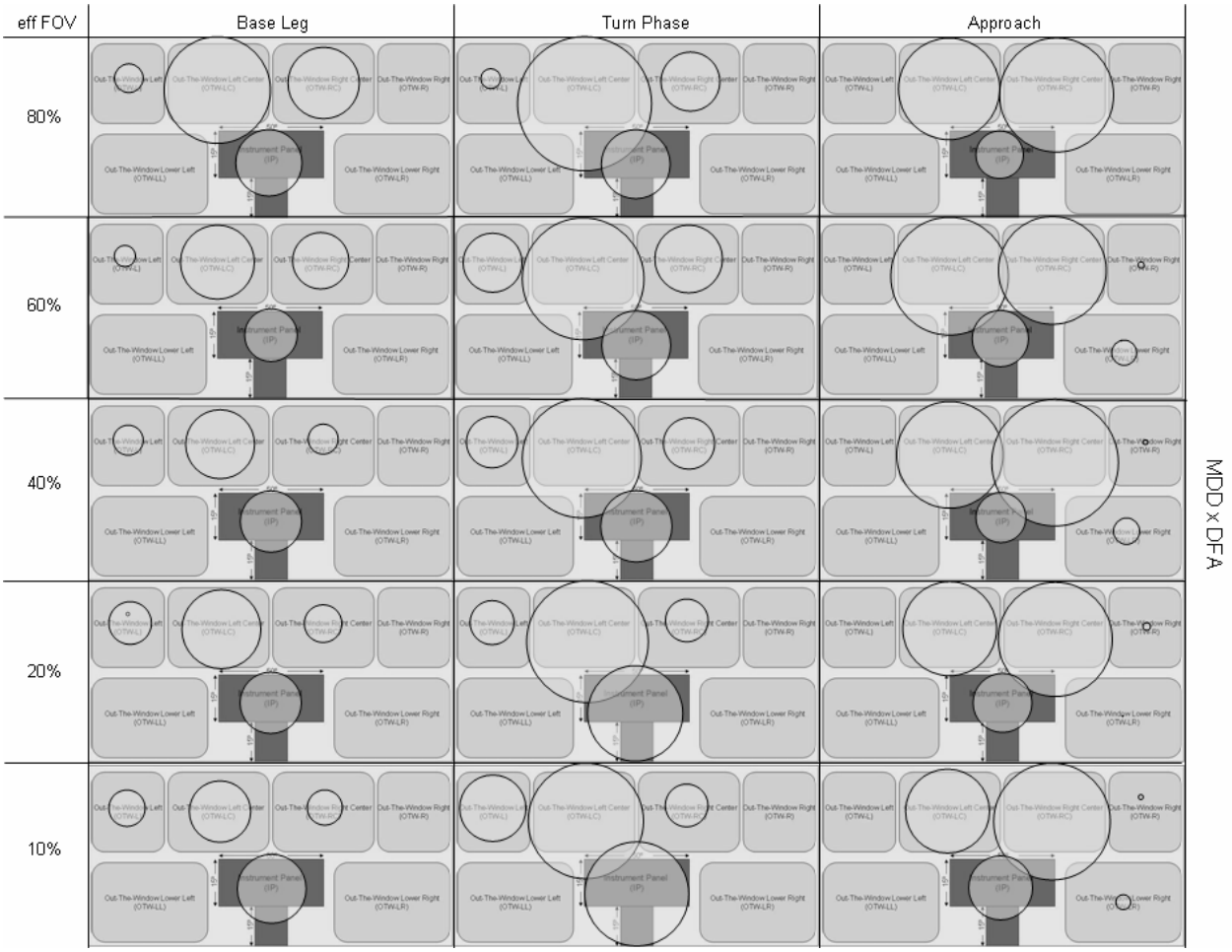

Figure 13: Product of Dwell Frequency and Mean Dwell Duration as the Area in a Circle

Normalized Information Behavior Analysis

The maximum and minimum range values for each pilot in each AOI, across all eFOVs were normalized and averaged for the dwell frequency per AOI. There was no evident trend for the base phase of flight. However for the turn phase, and decreasing eFOV, Table 8 shows a decreasing trend for OTW-L and OTW-R with an increasing trend for the IP and OTW-LC. During the approach phase, there was a decreasing trend for OTW-LC and OTW-R and an increasing trend for OTW-LR. We need to confirm here that the normalized average dwell

frequency trends in Table 8 are similar to the un-normalized average dwell frequency trends in Table 4.

Table 8: Normalized Average Dwell Frequency by Phase

Base	OTW-L	OTW-LC	OTW-RC	OTW-R	IP	OTW-LL	OTW-LR
10%	0.52	0.30	0.43	0.00	0.32	0.00	0.00
20%	0.57	0.64	0.37	0.00	0.50	0.00	0.00
40%	0.26	0.24	0.18	0.00	0.43	0.00	0.00
60%	0.14	0.28	0.41	0.00	0.32	0.00	0.00
80%	0.55	0.57	0.69	0.00	0.40	0.00	0.00
Turn	OTW-L[2]	OTW-LC[1]	OTW-RC	OTW-R[2]	IP[1]	OTW-LL	OTW-LR
10%	0.29	0.73	0.61	0.18	0.24	0.47	0.00
20%	0.24	0.47	0.68	0.46	0.21	0.63	0.00
40%	0.59	0.53	0.77	0.29	0.04	0.44	0.00
60%	0.65	0.38	0.34	0.33	0.14	0.24	0.00
80%	0.79	0.27	0.48	0.52	0.13	0.28	0.00
Apch	OTW-L	OTW-LC[2]	OTW-RC	OTW-R[2]	IP	OTW-LL	OTW-LR[1]
10%	0.00	0.00	0.18	0.14	0.65	0.14	0.54
20%	0.00	0.23	0.07	0.21	0.41	0.29	0.53
40%	0.00	0.42	0.13	0.16	0.47	0.14	0.38
60%	0.00	0.80	0.21	0.29	0.49	0.29	0.36
80%	0.00	0.89	0.14	0.29	0.47	0.00	0.20

Key	
OTW-L is Out The Window – Left	OTW-R is Out The Window – Right
OTW-LC is Out the Window – Left of Center	IP is Instrument Panel
OTW-RC is Out The Window – Right of Center	OTW-LL is Out The Window – Lower Left
	OTW-LR is Out The Window – Lower Right
For Decreasing eFOV, "1' indicates an Increasing trend.	For Decreasing eFOV, "2" indicates a Decreasing trend.

For the normalized mean dwell duration data points, and decreasing eFOV, Table 9 indicates a decreasing trend for OTW-LC in the base phase, decreasing trend for OTW-L and OTW-RC with an increasing trend for the IP and out the window lower left (OTW-LL) during the turn phase, and a decreasing trend for OTW-LC and the IP with an increasing trend for OTW-R for the approach and landing phase. Again, the normalized mean dwell duration trends in Table 9 are similar to the un-normalized mean dwell duration trends in Table 6.

Table 9: Normalized Average Mean Dwell Duration by Phase

Base	OTW-L	OTW-LC[2]	OTW-RC	OTW-R	IP	OTW-LL	OTW-LR
10%	0.60	0.16	0.25	0.00	0.64	0.00	0.00
20%	0.49	0.32	0.24	0.00	0.37	0.00	0.00
40%	0.29	0.48	0.11	0.00	0.57	0.00	0.00
60%	0.10	0.53	0.46	0.00	0.16	0.00	0.00
80%	0.38	0.72	0.51	0.00	0.60	0.00	0.00
Turn	OTW-L[2]	OTW-LC	OTW-RC[2]	OTW-R	IP[1]	OTW-LL[1]	OTW-LR
10%	0.18	0.51	0.20	0.25	0.20	0.62	0.00
20%	0.19	0.56	0.25	0.33	0.14	0.40	0.00
40%	0.48	0.54	0.41	0.22	0.01	0.09	0.00
60%	0.65	0.33	0.51	0.32	0.16	0.09	0.00
80%	0.76	0.39	0.54	0.36	0.11	0.26	0.00
Apch	OTW-L	OTW-LC[2]	OTW-RC	OTW-R[1]	IP[2]	OTW-LL	OTW-LR
10%	0.00	0.14	0.29	0.36	0.33	0.09	0.42
20%	0.00	0.20	0.11	0.29	0.49	0.22	0.61
40%	0.00	0.52	0.13	0.27	0.60	0.14	0.39
60%	0.00	0.62	0.05	0.13	0.62	0.29	0.32
80%	0.00	0.90	0.10	0.35	0.57	0.00	0.36

Key	
OTW-L is Out The Window – Left	OTW-R is Out The Window – Right
OTW-LC is Out the Window – Left of Center	IP is Instrument Panel
OTW-RC is Out The Window – Right of Center	OTW-LL is Out The Window – Lower Left
	OTW-LR is Out The Window – Lower Right
For Decreasing eFOV, ”1” indicates an Increasing trend.	For Decreasing eFOV, ”2” indicates a Decreasing trend.

In summary, with a decreasing FOV, pilots tend to focus more on their instruments for situation awareness and less on the horizon during the turn phase. One can infer pilots revert to previously learned instrument scan patterns with more frequent checks of the horizon as their eFOV is reduced; essentially reverting to a low visibility instrument landing behavior. This could be because they are familiar with instrument scan patterns and feel more comfortable reverting to these scan patterns when their eFOV restricts the information normally provided by the OTW areas of interest to maintain good situation awareness. This change in normal visual scan pattern behavior caused by an artificially restricted FOV is of concern in a training environment because a normal scan pattern is an important skill to learn for safe flight.

Effort Behavior

All pilots tested had a tendency to increase their head movement maximum range in pitch and yaw as the eFOV was decreased. The following Table 10 contains the calculated mean for pilot head pitch and yaw movement range values by eFOV for each phase. The data indicates that the original hypothesis of increased head movement to compensate for limited peripheral data was correct for all phases of the simulation runs. We infer that pilot effort to gather visual data tends to increase with a decreasing eFOV in all phases of the simulation run.

Table 10: Pilot Head Pitch and Yaw Movement Range Mean

eFOV	Pitch (base)	Pitch (turn)	Pitch (apch)
10%	45.40	70.94	34.08
20%	32.44	42.83	19.66
40%	24.32	29.51	19.74
60%	22.62	18.83	19.64
80%	22.21	22.38	14.58
eFOV	Yaw (base)	Yaw (turn)	Yaw (apch)
10%	22.42	35.66	39.95
20%	15.06	19.51	24.15
40%	12.47	12.88	19.28
60%	11.94	7.28	12.98
80%	12.31	8.36	11.77

The effort behaviors were graphed and analyzed for trend using the curve fit feature in Microsoft Excel. The best curve fit appears to be a power decay/growth function.

$y(f) = y_0 * x^{(k)}$

where

y(x) is the head range of movement in degrees

y_0 is the normal head range of movement in degrees based on phase

x is the eFOV

k is the decay/growth factor based on phase

The Pitch, Yaw and Roll graphs with best-fit power functions are listed in Appendix B.

Head pitch and yaw data for each phase is depicted in the following figures, along with standard deviations. In Figure 14 one can clearly see the increasing trend in head pitch with decreasing eFOV. For all phases, significant change occurs below 40% eFOV, with the turn phase showing the greatest FOV effect.

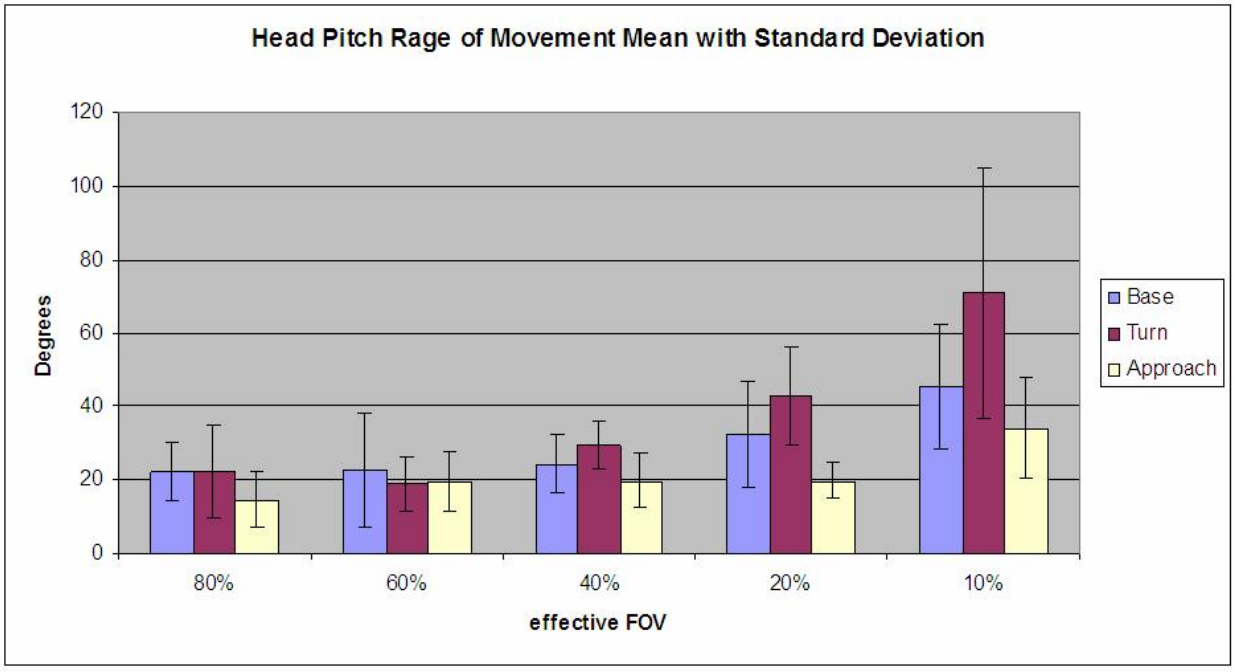

Figure 14: Pitch Effort Behavior

In Figure 15 one can also see the increasing trend in head yaw with decreasing eFOV. For all phases, significant change occurs below 40% eFOV, with the approach phase showing the greatest FOV effect.

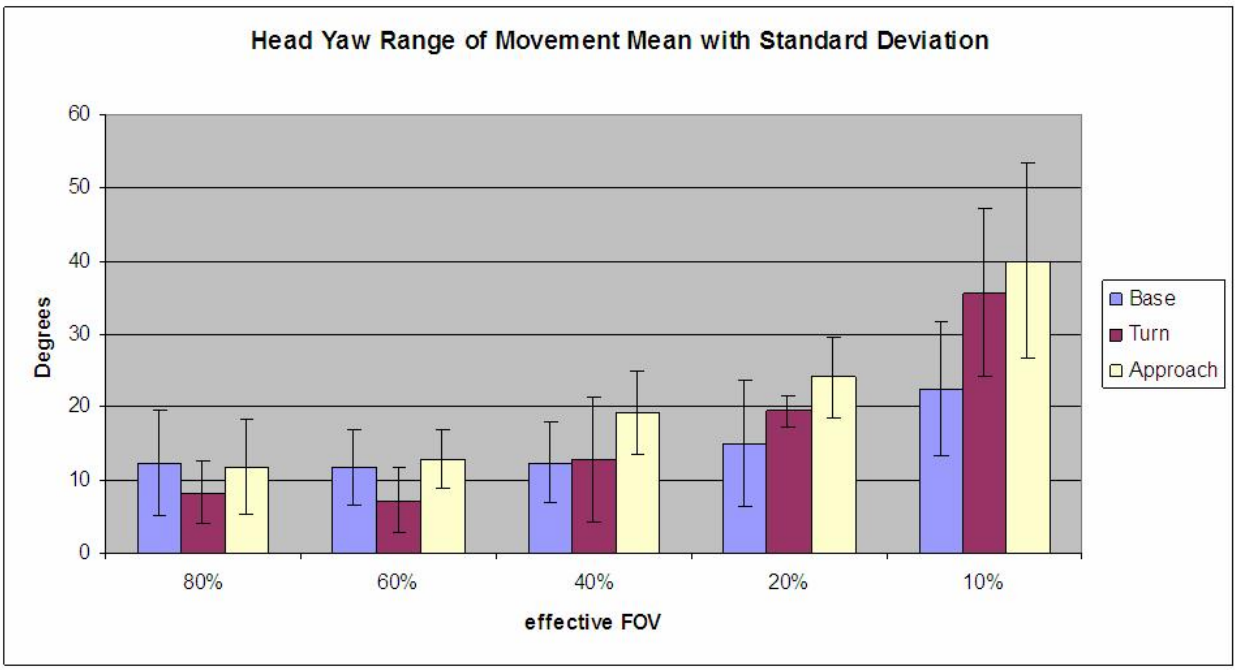

Figure 15: Yaw Effort Behavior

As described in the literature review (Gallimore et al., 2000), reduced eFOV had no effect on OKCR. However, the head role measurements taken by the head tracker for varying eFOV indicate a slight increasing trend in OKCR. The following Table 11 contains the calculated mean for pilot head roll movement range values by eFOV for each phase.

Table 11: Pilot Head Roll Movement Range Mean

eFOV	Roll (base)	Roll (turn)	Roll (apch)
10%	11.13	16.98	13.65
20%	6.43	9.58	8.84
40%	6.98	6.42	8.26
60%	5.96	6.47	7.44
80%	5.79	6.29	4.86

In Figure 16 one can see the increasing trend in head roll with decreasing eFOV. For all phases, significant change occurs below 20% eFOV, with the turn phase showing the greatest FOV effect.

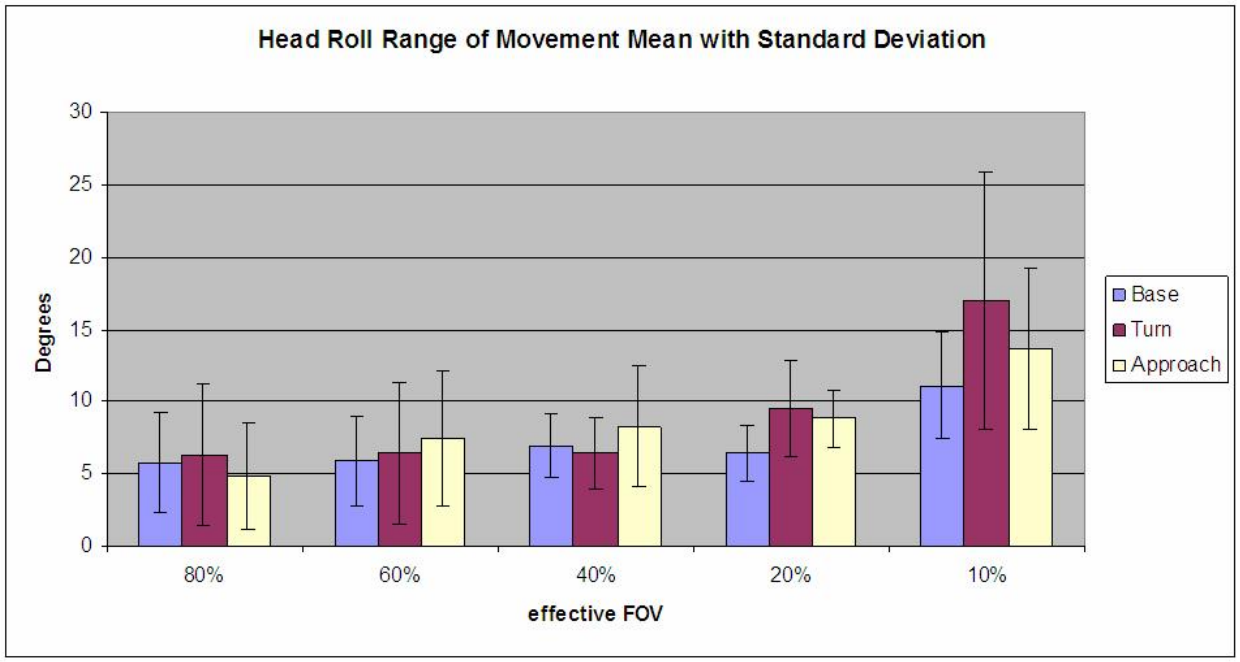

Figure 16: Roll Effort Behavior

Figure 17 contains the calculated average head movement maximum range and its associated standard deviations across the eFOVs tested for each phase of flight. The data indicate the original hypothesis of increased head movement to compensate for limited peripheral data was correct for all phases of all simulation flights. The head movement is most apparent during the turn phase. We infer that pilot effort to gather visual data tends to increase with a decreasing eFOV in all phases of the simulation run, but it is most significant in the turn phase to gather needed environmental data. Using a trend line function, a best fit curve for the turn phase head movement maximum range was a second order polynomial (y = 2.35x^2 -

22.384x + 66.78). For all phases, a significant change occurs below 40% eFOV, with the turn phase showing the greatest FOV effect. In summary, a decreasing eFOV reveals an overall increasing trend in head range of movement, with the most significant change occurring below a 40% eFOV that corresponds to an 80° h x 54° v FOV.

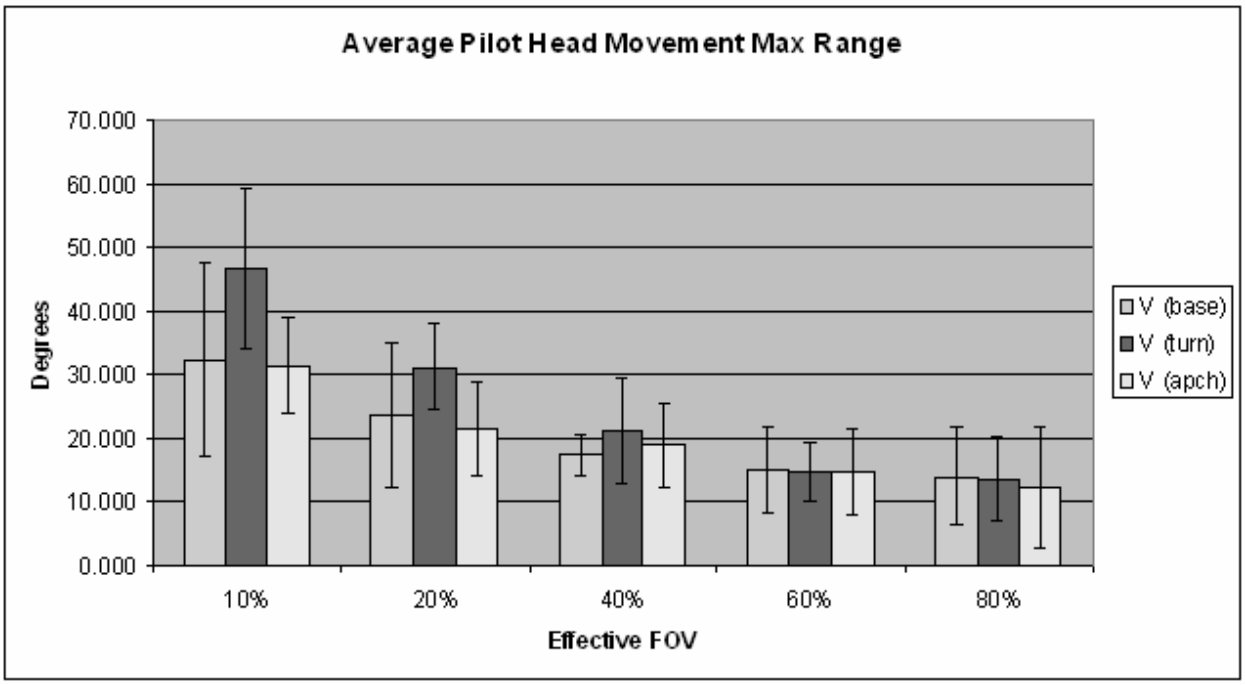

Figure 17: Average Head Movement Maximum Range

Normalized Head Movement Analysis

The maximum and minimum range values for each pilot in each phase and across all eFOVs were normalized and averaged to obtain Figure 18. From normalization, Figure 18 clearly shows a similar trend as the un-normalized Figure 17, with a decrease in standard deviation in the turn phase data at 10% eFOV. Figure 18 shows a statistically significant trend

for head movement in the turn phase only, modeled by a second order polynomial (y= 0.0527x^2 – 0.5122x + 1.4323).

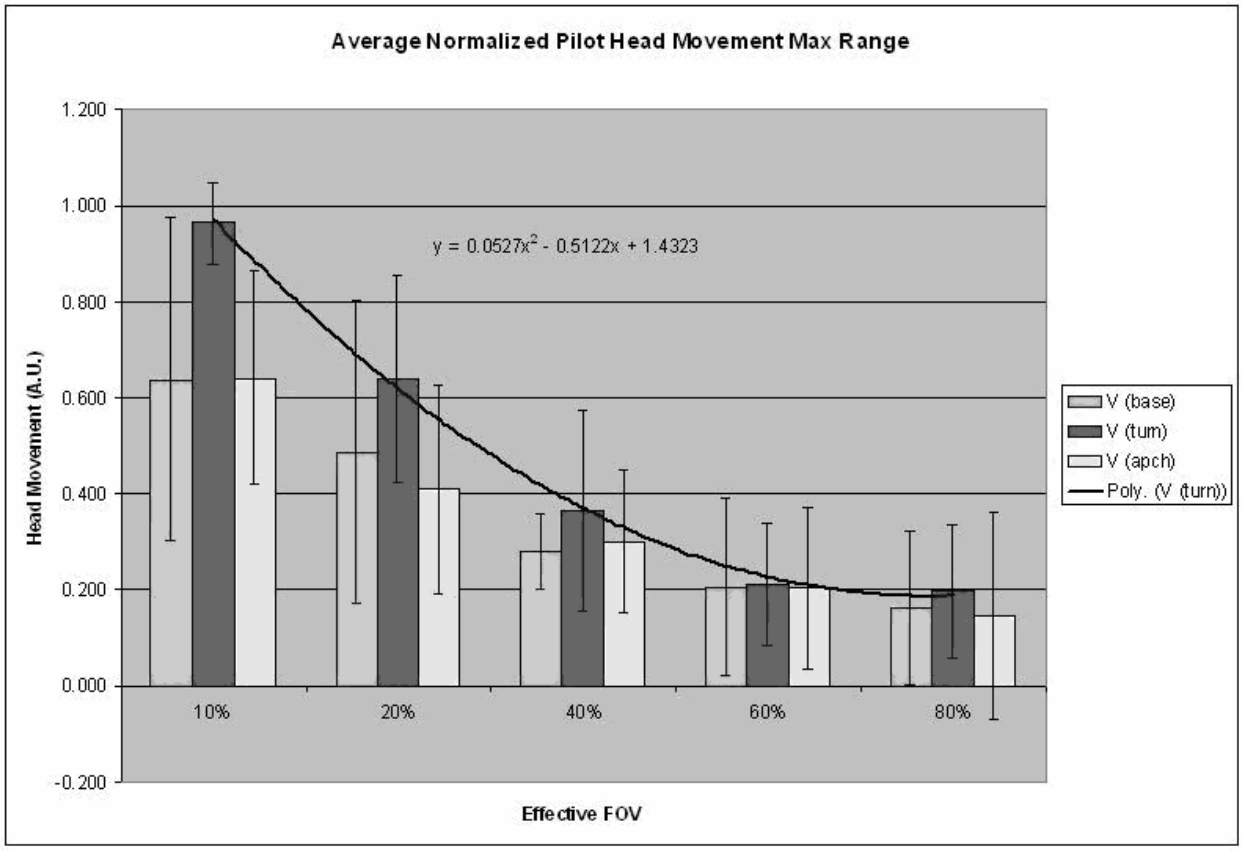

Figure 18: Average Normalized Head Movement Maximum Range with Turn Phase Statistically Significant Trend Curve

Importance Behavior

Every pilot tested had a tendency to increase their head movement velocity as the eFOV was decreased. The following Table 12 contains calculated mean for pilot head pitch and yaw rates of movement by eFOV for each phase. The data indicates that the original hypothesis of increased head rates of movement to compensate for limited peripheral data was correct for all

phases of the simulation runs. We infer that pilot urgency to obtain visual data tends to increase with a decreasing eFOV in all phases of the simulation run. It is to be noted that all head movement patterns seemed to show the greatest increase below 40% eFOV.

Table 12: Mean for Pilot Head Pitch and Yaw Rates of Movement

eFOV	Pitch (base)	Pitch (turn)	Pitch (apch)
10%	492.37	485.27	197.58
20%	172.55	222.43	76.53
40%	100.64	143.59	78.97
60%	92.28	62.64	66.91
80%	72.88	54.14	45.23
eFOV	Yaw (base)	Yaw (turn)	Yaw (apch)
10%	236.40	199.78	184.84
20%	65.78	90.74	124.92
40%	47.73	54.13	151.22
60%	38.85	22.84	33.76
80%	38.05	24.24	28.97

In Figure 19 one can see the increasing trend in head pitch rate of movement with decreasing eFOV. For all phases, significant change occurs below 40% eFOV, with the turn phase showing the greatest FOV effect.

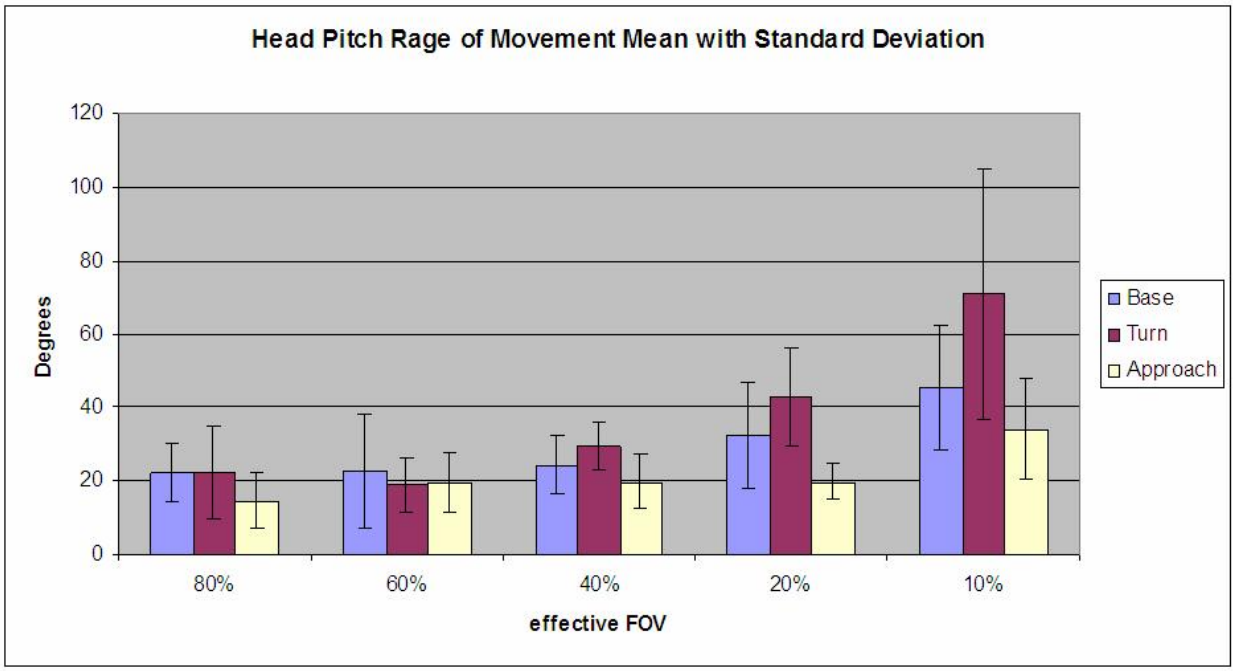

Figure 19: Pitch Importance Behavior

In Figure 20 one can see the increasing trend in head yaw rate of movement with decreasing eFOV. For all phases, significant change occurs below 40% eFOV, with the turn and approach phase showing the greatest FOV effect.

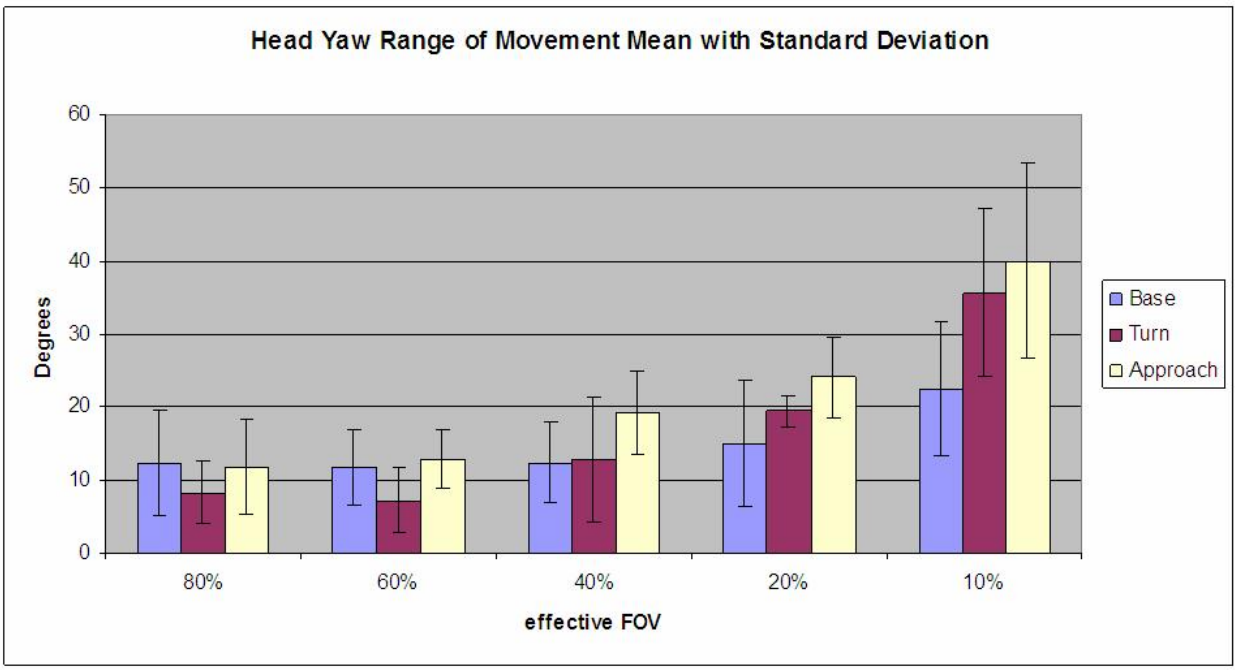

Figure 20: Yaw Importance Behavior

Figure 21 contains the calculated average maximum head velocity and the accompanying standard deviation by eFOV for each phase of flight. The data indicate the original hypothesis of increased head rates of movement to compensate for limited peripheral data was correct for all flight phases. It should be noted that two pilots only drove the standard deviations higher than normal for the 10% eFOV. We infer that pilot urgency to obtain visual data tends to increase with a decreasing eFOV in all phases of the simulation run, especially in the base and turn phase. It is to be noted that all head movement patterns seemed to show the greatest increase below 20% eFOV.

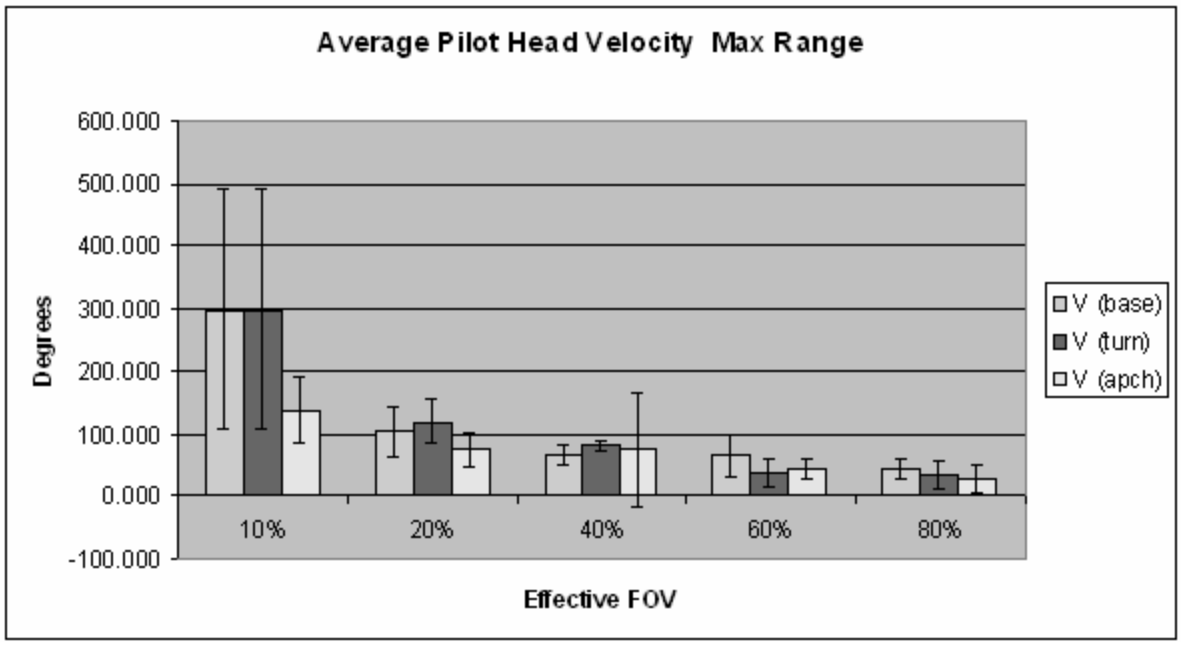

Figure 21: Average Head Velocity Maximum Range

Normalized Head Velocity Analysis

The maximum and minimum range values for each pilot in each phase and across all eFOVs were normalized and averaged to obtain Figure 22. The graph indicates a statistically significant trend for head velocity range in the base and turn phase only, modeled by two similar second order polynomials. ($y = 0.0712x^2 – 0.628x + 1.5047$ (Base phase) and $y = 0.0654x^2 – 0.6104x + 1.5086$ (Turn phase)).

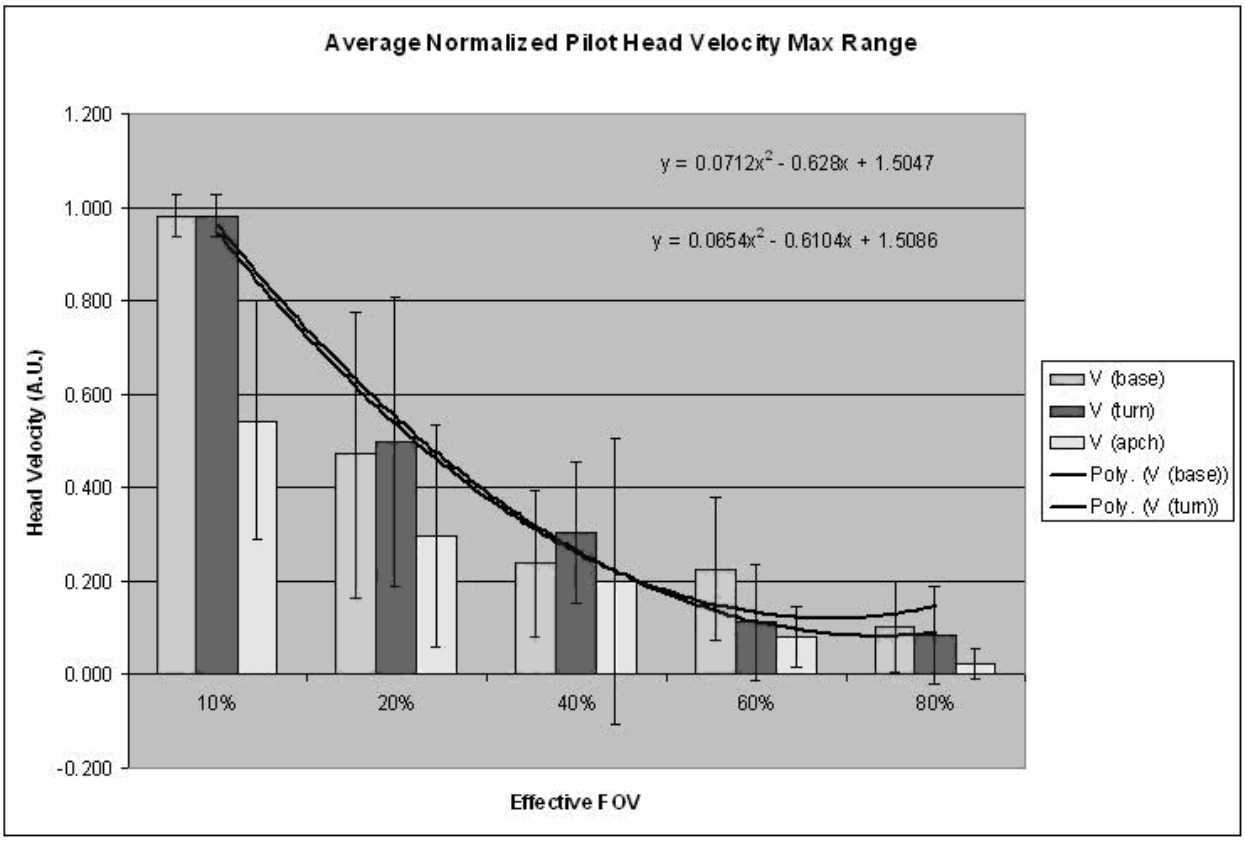

Figure 22: Average Normalized Head Velocity Maximum Range with Base and Turn Phase Statistically Significant Trend Curves

In summary, a decreasing eFOV reveals an overall increasing trend in head rate of movement, with the most significant change occurring below 20% eFOV, which corresponds to a 40° h x 27° v FOV. Recall we hypothesized a threshold exists while decreasing the eFOV at which a pilot can no longer compensate sufficiently to maintain an adequate cognitive mental image, thus leading to a measurable decrease in task performance. This proposed that participant's performance would deteriorate rapidly at a certain point as the eFOV is decreased.

Mean vs. Peak Values across Simulation Phases

When comparing data across simulation run phases shown in previous tables to the raw data (not reported here except a sample data in Figure 23), results show that the highest head movement range mean value and the highest head rate of movement mean value do not indicate the highest number of peak values in that phase. For example, looking at the data in Table 12, for a 40% eFOV the head yaw rates of movement mean increases from base (47.73), turn (54.13) and finally land (151.22) phase. However, looking at pilot head tracking raw data shows that there are only a few large peaks in the base leg, with more medium to large size peaks in the turn phase and finally many small peaks in the land phase. This finding is illustrated in Figure 23, which is a representative sample of one pilot simulation run with a 40% eFOV.

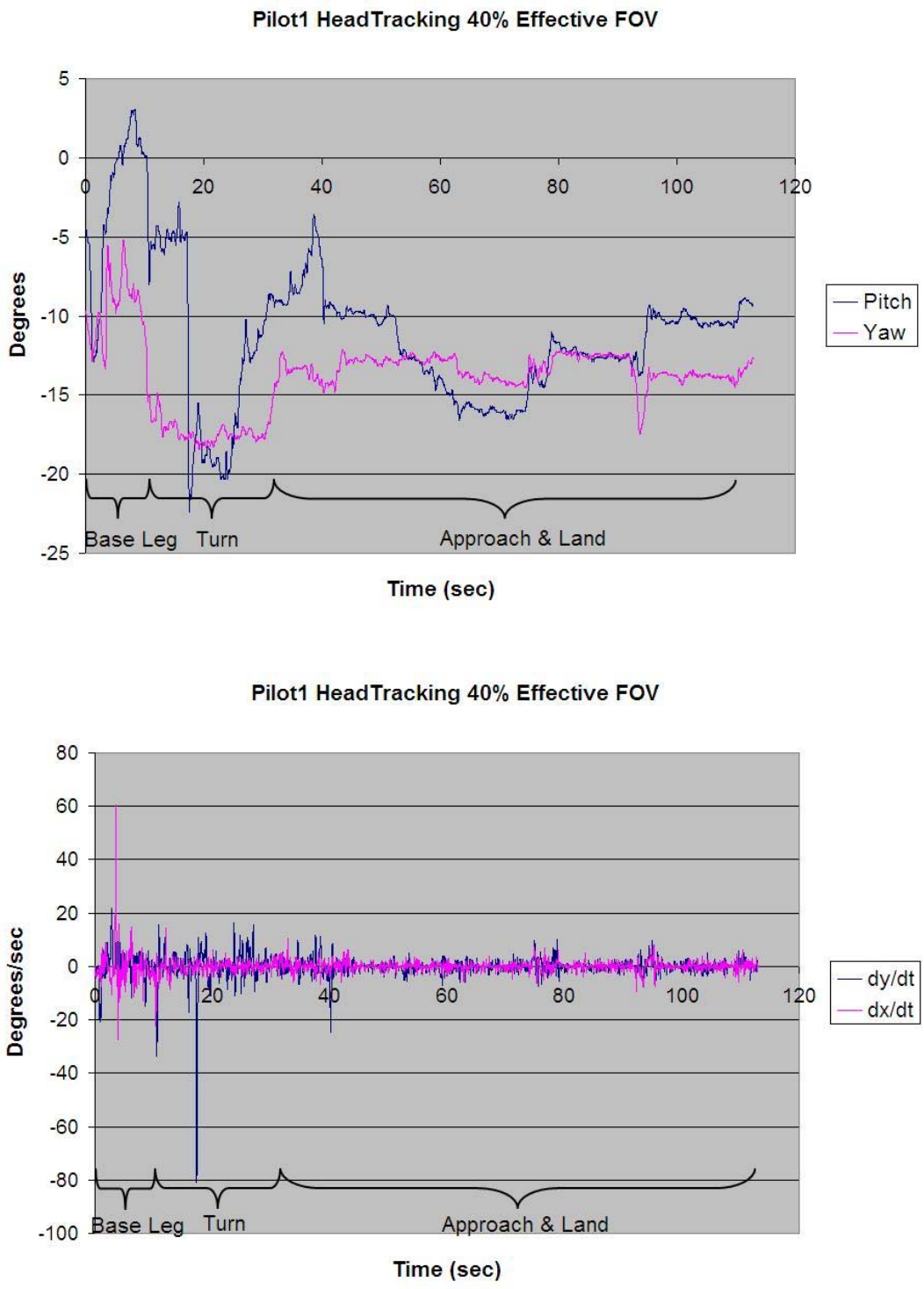

Figure 23: Sample Pilot Head Tracking Data

The base phase (approximately 10 seconds) indicates very few large peaks when the pilot is determining the best time to start the turn. The turn phase (approximately 20 seconds) indicates more medium size peaks, when the pilot has more need for gathering horizon and runway visual data. On the straight approach (approximately 90 seconds), the movement settles to very frequent small peaks, when the pilot is maintaining lineup and making quick checks on airspeed while calculating the descent to the landing spot.

Performance

Figure 24 and Figure 25 depict Pilot #6 aircraft course over ground (top portion) and the rate of descent (lower portion), which are representative of the majority of the pilot performance measurements from best performance (Figure 24) to worst (Figure 25). The green triangle represents a glide slope window for maintaining a safe instrument assisted approach. For a visual approach, it serves as a guide to analyze performance. The pilot was instructed to land at the runway intersection, which is further up the runway than the normal approach landing area. The green glide slope triangle would also have to be translated further up the runway. Since the pilot was instructed to land at the runway intersection, they will normally maintain a glide slope just above the green triangle on the lower portion.

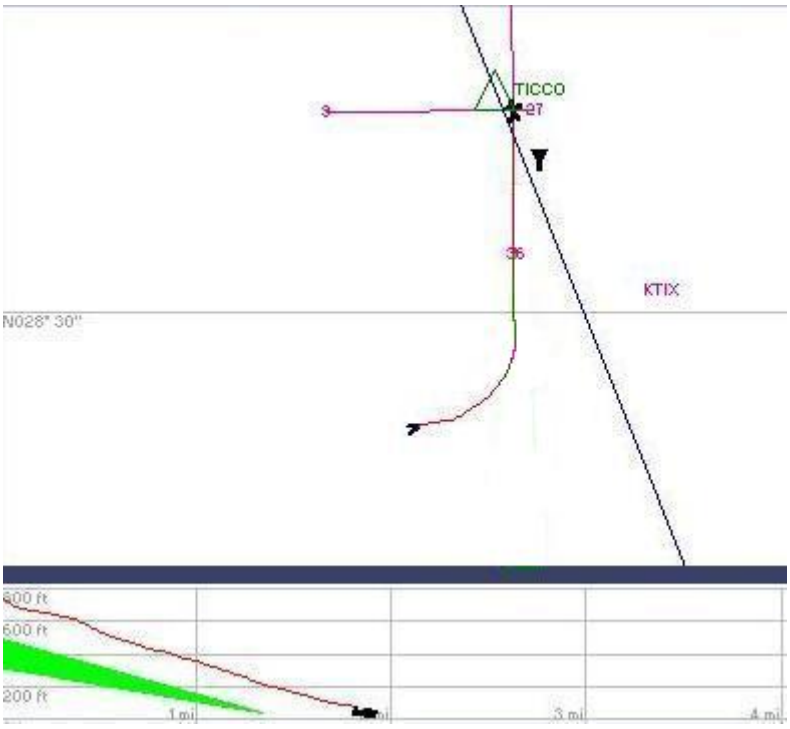

Figure 24: Pilot #6 80% effective FOV (eFOV) Performance

The pilots are taught in such scenarios to maintain base heading until at the position to make a standard left turn to approach. The decreasing eFOV clearly shows most started their turn too early, as seen in Figure 25 course over ground indicating a poor start for the straight-in approach, had trouble with runway lineup and also took less time to land by shortening the normal base leg turn. While struggling with lineup, the pilot also had trouble maintaining a steady rate of descent. Their normal visual approach scan pattern was disrupted by the restricted eFOV, as measured by the head tracker.

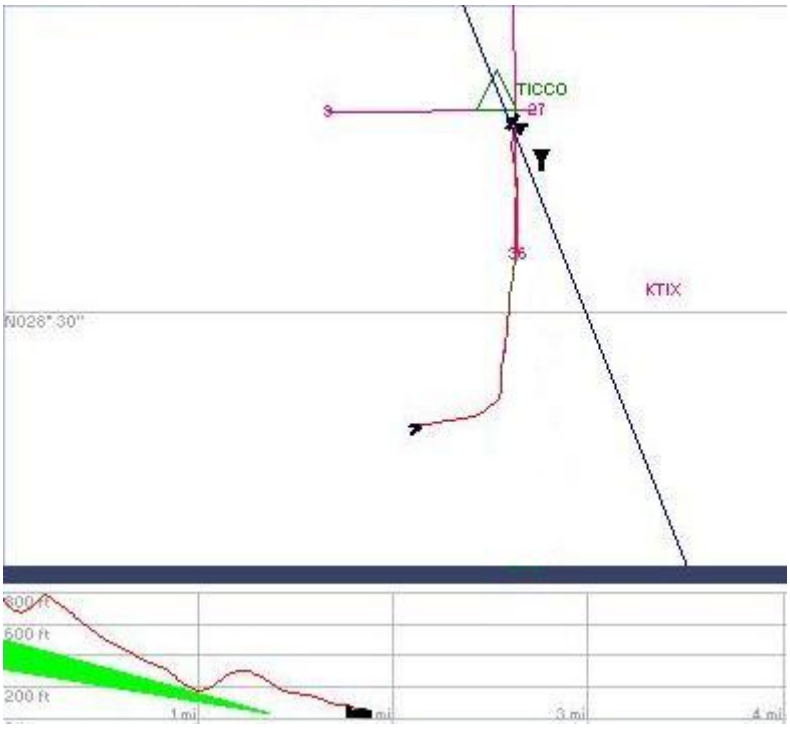

Figure 25: Pilot #6 10% effective FOV (eFOV) Performance

Runway Alignment Error (RAE)

The RAE was measured from each pilot and five eFOV depicted in Figure 26.

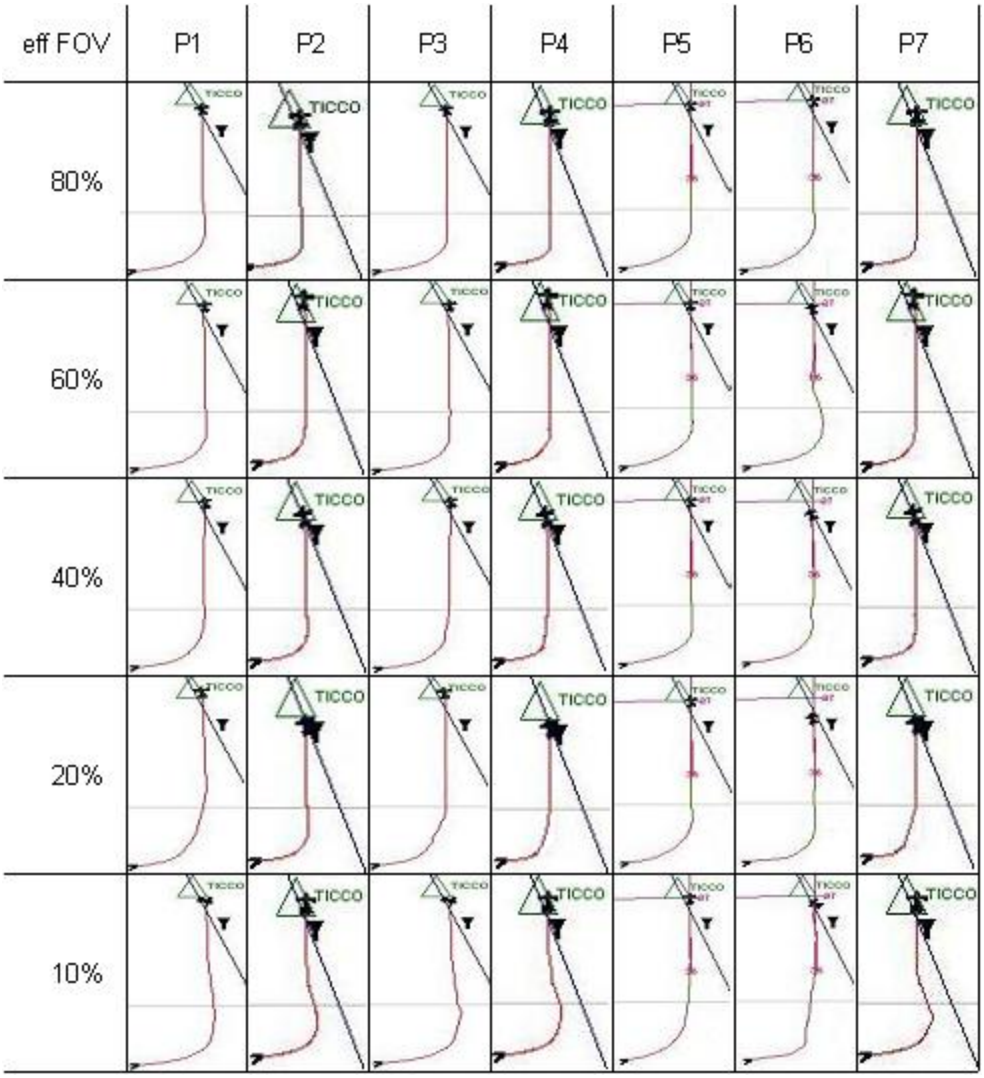

Figure 26: RAE Raw Data

A decreasing eFOV reveals an increasing trend in runway alignment error, which is shown in Figure 27. The increasing trend becomes significant below a 60% eFOV that corresponds to a 120° horizontal x 81° vertical FOV and follows a power function trend, graphed and analyzed for trend using the curve fit feature in Microsoft Excel. The best curve fit appears to be a power decay/growth function

$$y(x) = y_0 * x^{(k)}$$

where

y(x) is the RAE in degrees

y_0 is the normal RAE in degrees based on 100% eFOV

x is the eFOV

k is the decay/growth factor

Based on the power function model, one could predict a pilot will normally have a RAE of about 0.715° with unrestricted FOV.

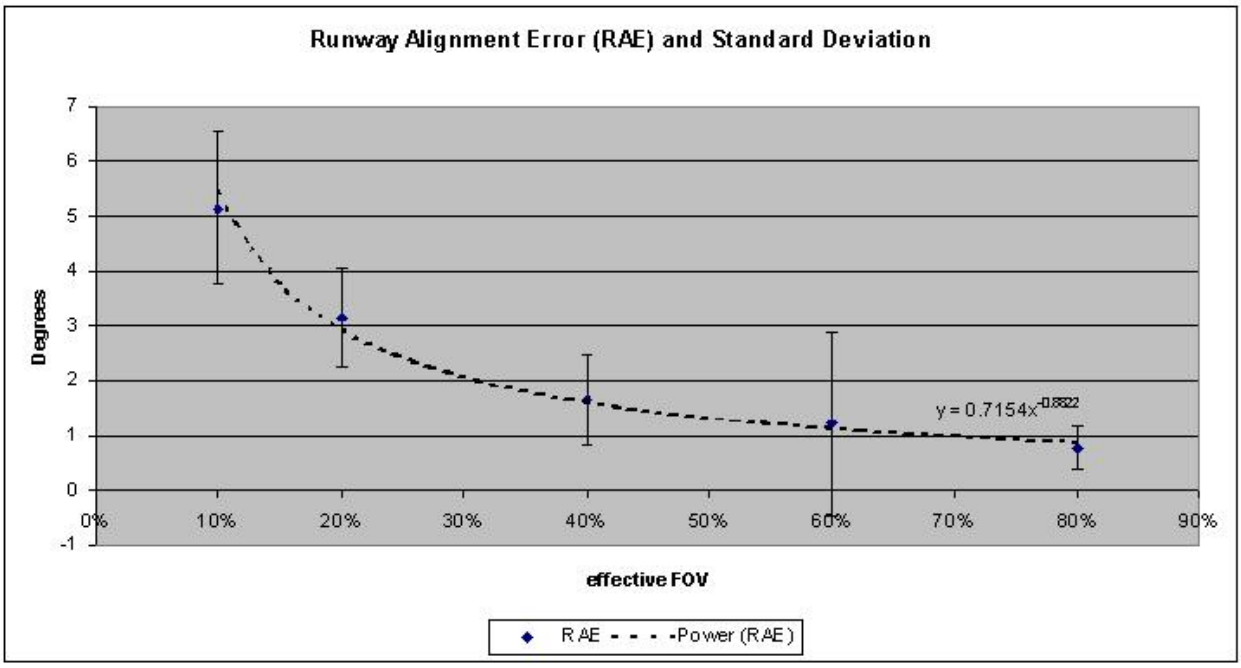

Figure 27: Measured RAE

Vertical Track Error (VTE)

The VTE was measured from each pilot and eFOV depicted in Figure 28

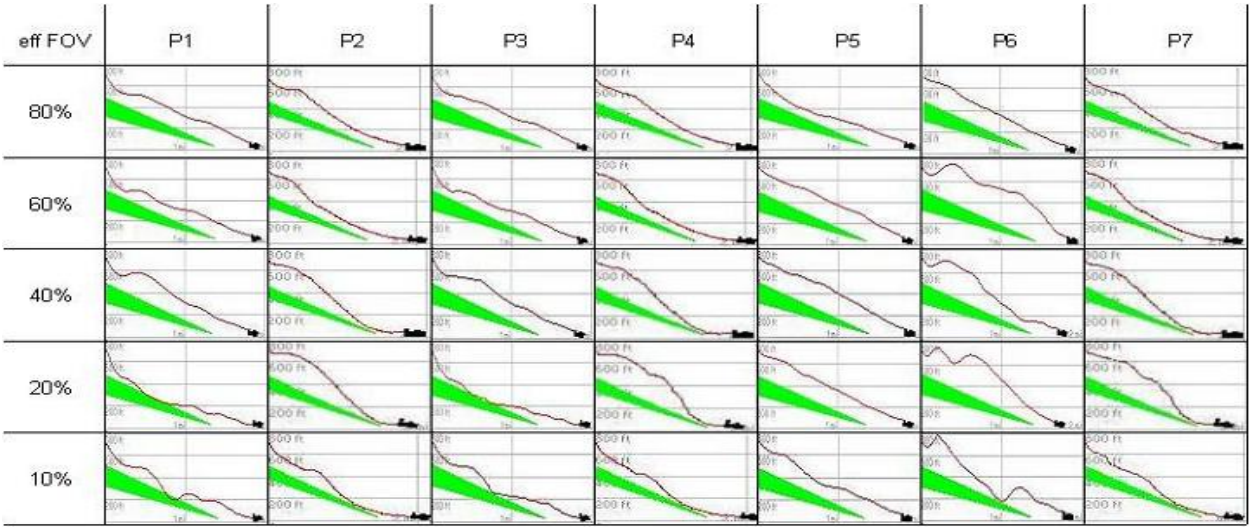

Figure 28: VTE Raw Data

Decreasing eFOV reveals an increasing (linear) trend in vertical track error as shown in Figure 29. The increasing trend becomes significant imediately (below 80% eFOV) and follows a linear function trend, graphed and analyzed for trend using the curve fit feature in Microsoft Excel. The best curve fit appears to be a linear function

$$y(x) = mx + y_0$$

where

y(x) is the VTE in degrees

y_0 is the intercept or worst case scenario VTE in degrees based on 0% eFOV

x is the eFOV

m is the slope or increase/decrease factor

Based on the linear function model, one could reasonably predict a pilot will crash prior to reaching the landing area with a VTE of about 14.54° with essentially 0% eFOV. In other words, if the aircraft has a VTE of greater than 14.54° at any time before reaching the landing area, they will have inadvertently flown through the ground. No one expects a pilot to fly blind, but interestingly enough the linear function seems to makes sense in all eFOV conditions. Based on the linear function model, one could predict a pilot will normally have a VTE of about 0.19° with unrestricted FOV.

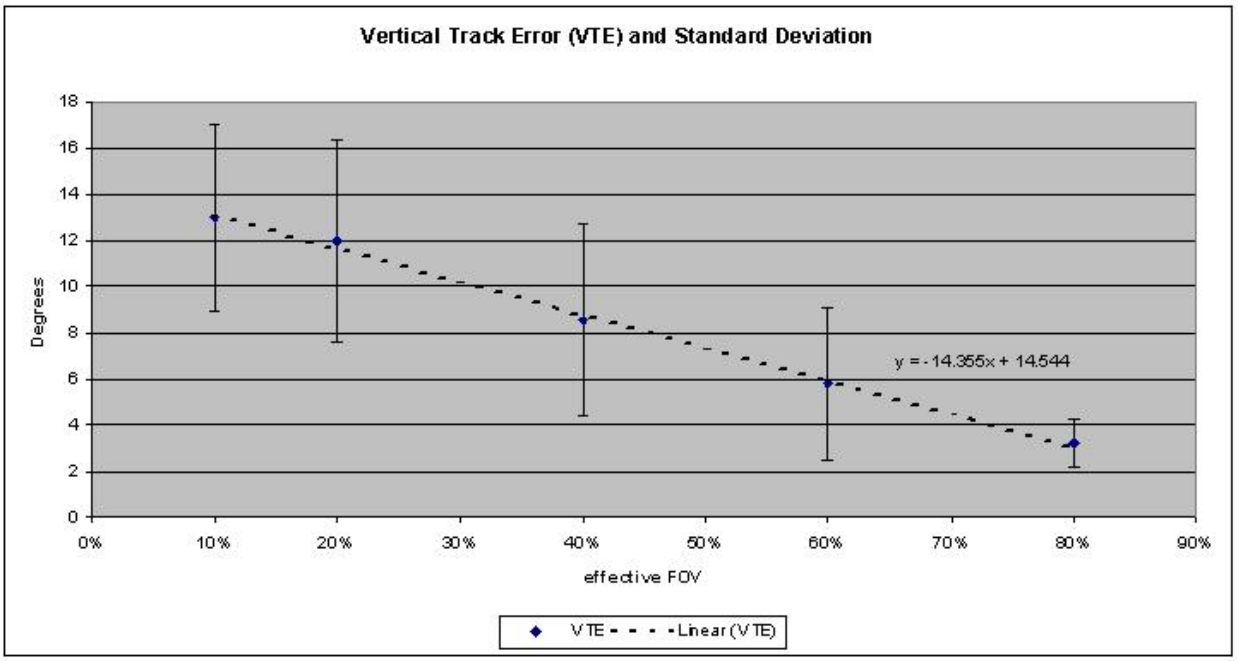

Figure 29: Measured VTE

The methodology used in this experiment was to influence the pilot's visual stimulus and situation awareness by controlling their eFOV and then quantifying the associated pilot behavior and performance response.

CHAPTER FIVE: CONCLUSION

Summary of Findings

Behavior and Performance Summary

Overall performance results indicate that a pilot will significantly alter their normal visual scan pattern, along with a significant head movement pattern change below 40% eFOV, which corresponds to 80° horizontal x 54° vertical. Results are based on pilot AOI, effort and importance behavior responses measured while varying the pilot's eFOV. An important behavior change to consider is the measured AOI behavior results. During the course of pilot training, a pilot develops a normal scan pattern for either visual meteorological conditions, or instrumented flight. For instrumented flight, the pilot does not normally use the out-the-window areas of interest. The AOI behavior results indicate that the limited eFOV forced an unnatural scan pattern behavior for simulated visual conditions, which is counterproductive in a training environment.

Based on measured pilot runway alignment error and vertical track error, performance results indicate that pilot basic task performance decreases significantly as the eFOV is decreased. This supports our original hypothesis. The runway alignment error became relatively large at less than 40% eFOV. However the vertical track error linearly increased as the eFOV was decreased. As a pilot's FOV was constrained, it appears that the primary focus of the pilot was to ensure they were lined up properly after their turn phase, and a steady rate of descent was a secondary concern. By limiting the pilot eFOV, additional workload and stress were also

assumed to increase for the pilot, measured by AOI, Effort and Importance behavior changes. As the eFOV was decreased, head movement range (in degrees) and head rate of movement (in degrees/second) increased to compensate for the reduced peripheral visual data.

It was also demonstrated, while decreasing the eFOV, that pilots had a noticeable threshold where they could no longer compensate sufficiently to maintain an adequate cognitive mental image due to a decreased amount of out-the-window visual information.

Experiment Limitations

The FOV masking process was actually similar to instrument flight rules check flight procedures where student pilots wore a mask that only allows them to see the instrument panel during navigation and approach, while the instructor pilot observes and can take over the controls during flight for safety. One limitation on our present work was testing time. While the pilots graciously volunteered, again free of any charge, it was only possible to test during their time off from their regular schedule. Therefore, the five simulation runs had to be brief, which limited the pilot's time in the simulator. Although the basic landing task using a familiar airport visual landing pattern collected valuable FOV effect data, further work is clearly needed on important performance tasks such as navigation, where previous experiments have indicated that a wide FOV is required. For this experiment design, low-level over land navigation tasks could be an important candidate scenario.

Lessons Learned

Sample Size Estimate

Although it was estimated that a minimum of nine participants were required to detect a significant FOV, the seven pilots that volunteered provided clear head and eye movement pattern change caused by the eFOV effect.

Scene Camera

The Arrington ViewPoint Scene Camera was extremely helpful in confirming the Intersense VisTracker head movement pattern eFOV effects, and also ensured that good MDD and DFA data were recorded for each simulation run. The ViewPoint EyeTracker software allowed one to define Region of Interest (ROI) boxes to automatically gather Information data like MDD and DFA. Although the eFOV masks were easy to change in between simulation runs, they interfered some with the ViewPoint EyeTracker camera and caused a slight offset to the calibration. Thus, the ViewPoint Scene Camera option was used, providing AVI recording of each run to track gaze position on the real world scene video being captured. Consequently, each of the 35 runs (7 participants, 5 eFOVs) was painstakingly analyzed for roughly one hour each, one by one and scene by scene, to ensure accurate MDD and DFA collection.

Space Limitation

The Arrington ViewPoint EyeTracker Video Capture Card required a tower computer with an empty Peripheral Computer Interface (PCI) slot. Therefore using a laptop was not an

option for easy daily equipment setup and breakdown when the simulator was available for the experiment. The tower, keyboard and monitor had to be set up in the very limited space offered in the instructor station.

Future Research

The significant FOV effect on the pilot's scan pattern behavior, coupled with the direct link to performance behavior, raises negative training concern over the use of narrow FOV HWD-based flight simulators. The driving force behind the research for this AR application is exploring the FOV requirements for the concept of embedded training with an HWD-based simulator; using actual operational vehicles and their subsystems in training mode to conduct deployable embedded training. The vision of aircrews being able to conduct flight simulations while deployed on a Navy aircraft carrier or destroyer emphasizes the need of having an inexpensive deployable simulation system that allows the warfighter to train in their weapon platform or an inexpensive emulation. The ultimate vision is using one common, deployable training solution; an HWD-based simulation system for all type of virtual simulations to conduct individual procedure training or coordinated interactive mission rehearsal. An environment fabric-free HWD also makes embedded AR training possible when dismounting a vehicle (Martins, Shaoulov, Ha, & Rolland, 2007).

The next step towards this vision is to design an AR usability experiment, along with development of the described prototype HWD-based simulator. The usability testing involves Human Factors research and experiments with AR, using existing HWDs and the latest ultra-lightweight HWD technology. The research will provide pros and cons of using AR displays

compared to conventional displays for this specific simulator application and will provide insight for other type of embedded virtual simulators that keep the "reality" in the simulation.

A proof of concept flight simulator is needed to conduct initial usability testing. An existing simulator test bed, the Chromakeyed Augmented Virtual Environment (ChrAVE) / Virtual Environment Helicopter (VEHELO) developed by the MOVES Institute was a proof of concept on how existing AR technology can be leveraged to save in development time and cost (Darken & Lennerton, 2003). A similar reconfigurable test bed could be developed to interchangeably use HWDs of varying quality, such as the optical see-through HWD being developed at the College of Optics and Photonics ODALab at the University of Central Florida (Rolland, Biocca, Hamza-Lup, & Martins, 2005; Cakmakci, & Rolland, 2007). This test bed allows experimental human centered task comparison when using either video see-through HMDs, the optical see-though HWDs or even some of the new retinal scan HWDs that are being used by the U.S. Army Striker Brigades. The concern for retinal scan HWDs is the relatively narrow FOV.

Head / Eye Movement Model Validation

A logical follow-on experiment is the validation of the baseline head/eye movement model for the unrestricted FOV desired. Although expensive, validation of this data could be accomplished by duplicating the experiment in actual helicopter flights. The eFOV masking process is actually similar to IFR check flight procedures where student pilots wear a mask that only allows them to see the IP during navigation and approach, while the instructor pilot observes and can take over the controls during flight, for safety.

Training Tasks Requiring Stereopsis

Other than the FOV effects in flight simulation, of additional interest is the importance of stereopsis or depth perception in actual flights and in flight simulation training. Advanced training tasks like formation flight or in-flight refueling can be trained in a simulator, where it is safe. The Rotorcraft Human Factors Research Branch at NASA Ames Research Center in Moffett Field, California conducted a review on how visual cues are important for routine low-level flight training as well as the development of simulator visual systems and enhanced or synthetic vision systems for aircraft cockpits. Along with the importance of FOV and FOR, functional stereopsis has been shown to be a useful depth cue for distances up to approximately 30 meters (Arditi, 1986). Replicating the FNPT II simulator experiment using a stereoscopic AR display system-based simulator instead of the conventional 2D projection display system and comparing head/eye movement patterns at comparable FOV restrictions will further validate the models. Additionally, comparing performance for similar tasks that require depth perception at the same FOV will provide an indication if functional stereopsis in flight simulation is more realistic training for such tasks (Rolland, Davis, Ha, Meyer, Shaoulov, Akcay, Zheng, Banks, & DelVento, 2002).

APPENDIX A: SUBJECTIVE OBSERVATIONS

Collective Observations

- All pilots seemed to perform and behave similarly with no FOV restrictions.
- One pilot (Pilot #5: the experienced instrument check-flight instructor) displayed little performance change with decreasing eFOV. However, head movements did appear to increase as eFOV decreased.
- The majority of pilots displayed rapid head movement increase and some performance decrease with eFOV decrease.
- The simulation run for two pilots with 10% eFOV resulted in a simulated aircraft crash landing.

Pilot #1 Observations

- Started with 80% eFOV (no mask). Very clean run with little noticeable head movement. Demonstrated clear orientation and navigation capabilities.
- Fitted subject with 20% eFOV mask. Very noticeable up and down head movement right away to look at horizon and at instruments at the start. Very noticeable head movement to gather orientation to runway during turn. Slight tendency to overshoot runway lineup after turn. Made slow corrections to regain lineup. Seemed to settle down at the end of the approach prior to landing.
- Fitted subject with 60% eFOV mask. Head movement not as noticeable as 20%. Made a good turn to line up with runway. Noticeable improvement over 20% eFOV.

- Fitted subject with 40% eFOV mask. Began noticeable head movement while in middle of turn to check on orientation to runway. Seems to be focusing more on instruments. Solid line up after turn and overall good landing.
- Fitted subject with 10% eFOV mask. Subject not very happy with FOV prior to start. Displayed noticeable up and down head movement again at the start. Very noticeable head movements to gather orientation to runway. Made large angle of bank turn to correct for poor lineup. Slowly corrected lineup. Very noticeable up and down head movements prior to land.

Pilot #2 Observations

- Fitted subject with 40% eFOV mask. Noticeable left and right head movement to gather orientation to runway. Started turn late and made big correction for lineup. Settled down after turn and made a nice landing.
- Fitted subject with 60% eFOV mask. Head movements to the left not as noticeable as 40%. Turn and approach also much better.
- Fitted subject with 20% eFOV mask. Making very rapid left to right head movements at the start. Settling down in the turn. Slight overshoot after turn. Made corrections and made a nice landing.
- Fitted subject with 10% eFOV mask. No one seems to like this mask. Very noticeable left to right head movements but with larger peaks and not as fast ast 20%. Started turn with too much angle of bank. Had to level out in middle of turn. Stayed level too long and over shot line up to runway. Settled down just prior to landing.

- Finished with 80% eFOV. Subject much happier. Much better performance than 10% and very little head movement. Good approach and landing.

Pilot #3 Observations

- Fitted subject with 60% eFOV mask. Made several up and down head movements prior to start to get used to mask. Noticeable large left to right head movements to gather orientation to runway. Pretty good lineup and solid approach.
- Fitted subject with 10% eFOV mask. Subject not happy. Again made several up and down head movements prior to start. Pilot seems to be using a visual landmark on the ground to start their turn. Seems to be relying on instruments during turn phase with some large head movements to gather orientation to runway. Overshot runway lineup after turn and slowly corrected back. Very noticeable up and down head movements in approach and land.
- Fitted subject with 40% eFOV mask. Noticeable left to right movement to gather orientation during turn. Nice job on lineup after turn. Settled down to solid approach and land.
- Fitted subject with 20% eFOV mask. Made several up, down left and right head movements prior to start to gather orientation (and visual landmark). Head movements very noticeable throughout. Level wings slightly during turn to compensate but managed to start with good line up after turn. Settled down and made a good approach and landing.
- Finished with 80% eFOV. Subject much happier. Very little head movement in comparison. Solid turn, approach and landing.

Pilot #4 Observations

- Started with 80% eFOV. Head movements hardly noticeable. Solid run with good performance.
- Fitted subject with 20% eFOV mask. Very noticeable head movements to gather orientation to runway and up and down movement from horizon to instruments. Turn needed corrections (leveled out angle of bank in turn) to regain lineup. Seemed to settle down just prior to landing but still made a very rough touch down.
- Fitted subject with 10% eFOV mask. Again, very noticeable head movements throughout. Misjudged turn and made big correction to regain lineup. Rough approach. Seemed to try landing with too much nose down attitude resulting in simulated aircraft crash landing (tipped forward and then rolled to the left). Pilot seemed surprised over the landing (i.e. how the simulator displayed the roll). Pilot ego slightly bruised but still willing to continue with experiment.
- Fitted subject with 40% eFOV mask. Head movements more relaxed. Up and down head movements to gather runway and instrument data. Not bad lineup and descent approach to land.
- Fitted subject with 60% eFOV mask. Head movements even more relaxed. Turn and approach more relaxed with solid landing.

Pilot #5 Observations

- Fitted subject with 10% eFOV mask. Noticeable head movements between runway and instruments. However, pilot seems much more relaxed than previous subjects. Undershot turn slightly but overall not a bad run considering the eFOV.

- Fitted subject with 20% eFOV mask. More relaxed but still noticeable head movements between runway and instruments. Pilot seems to be more relaxed than previous subjects in all conditions.
- Fitted subject with 40% eFOV mask. Same head movements but more smooth and relaxed. Very slight overshoot on lineup but overall solid performance.
- Fitted subject with 60% eFOV mask. Head movements not as noticeable but still seems to be smoothly transitioning between runway and instruments. This pilot seems to be using the instruments more effectively. Solid performance.
- Finished with 80% eFOV. Head movements hardly noticeable. Nice turn and lineup. Performance seems flawless.
- It should be noted that this instructor pilot is the instrument check-flight instructor that certifies all students in the simulator prior to the instrument check-flight. In other words, he has a lot of simulator flight time and very experienced in instrumented approaches.

Pilot #6 Observations

- Fitted subject with 20% eFOV mask. This was the only female and only instructor pilot tested that wore glasses. Started feeling uncomfortable right away with limited FOV. Head movements were very noticeable at start and during turn. Aircraft attitude erratic and angle of bank also very erratic in turn. Not a bad job salvaging a good lineup. Settled down once over the runway and made a good landing. Reported slight nausea after landing.

- Used 80% eFOV. Subject much happier with this. Head movements slightly noticeable. Leveled out in middle of turn slightly but corrected for overall solid approach and landing.
- Fitted subject with 60% eFOV mask. Head movements noticeable between runway and instruments during turn. Overshot runway lineup and seemed high in approach. Made corrections and settled down for a good landing.
- Fitted subject with 10% eFOV mask. Subject not happy at all. Head movements seemed erratic from the start and aircraft attitude fluctuated dramatically. Seemed to start turn but leveled angle of bank for a while then over compensated for a rough start of approach. Attempted to land with too much right angle of bank resulting in simulated aircraft crash landing (rolled the aircraft to the right). Subject was upset over performance but still willing to continue with last run.
- Fitted subject with 40% eFOV mask. Head movements noticeable between runway and instruments but with noticeable improvement in performance. Good lineup at end of turn and landing was much smoother.

Pilot #7 Observations

- Fitted subject with 40% eFOV mask. Head movements noticeable but relaxed. Up and down head movements to gather runway and instrument data. Not a bad lineup and approach to land.
- Fitted subject with 10% eFOV mask. It's no secret; nobody likes 10% eFOV. Head movements very noticeable. Seems to be relying on instruments during turn phase like

most of the subjects. Overshot runway lineup after turn and made slow corrections back. Head movements remain noticeable in approach and land.

- Fitted subject with 20% eFOV mask. Head movements still rapid at the start. Settling down some in the turn. Slight overshoot after turn. Made corrections to get back and made a good landing.
- Used 80% eFOV. Head movements hardly noticeable compared to previous run. Nice turn and lineup. Performance seems very good.
- Fitted subject with 60% eFOV mask. Head movement increased slightly from previous run. Good turn and line up with runway. Solid run.

APPENDIX B: TREND CURVES

Information Behavior

DFA

OTW

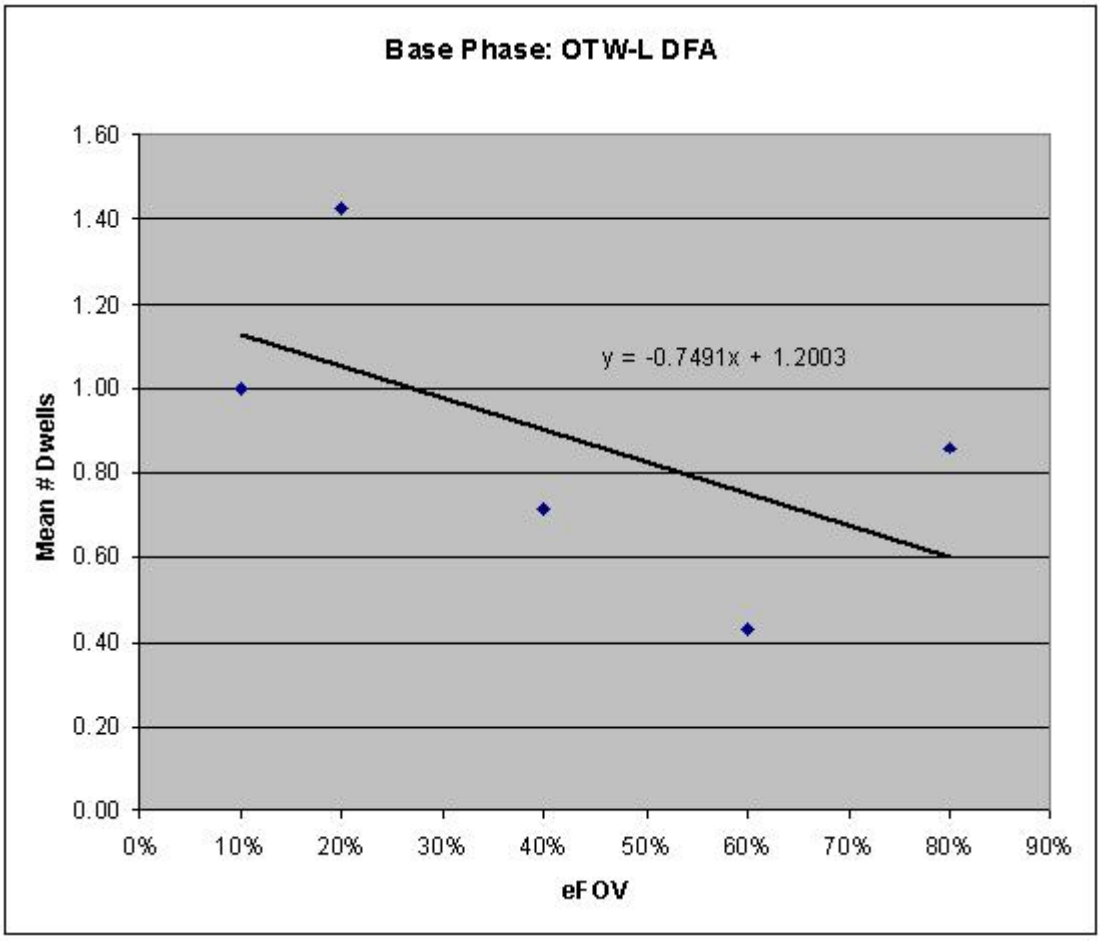

Figure 30: DFA Trend - OTW-L Base Phase

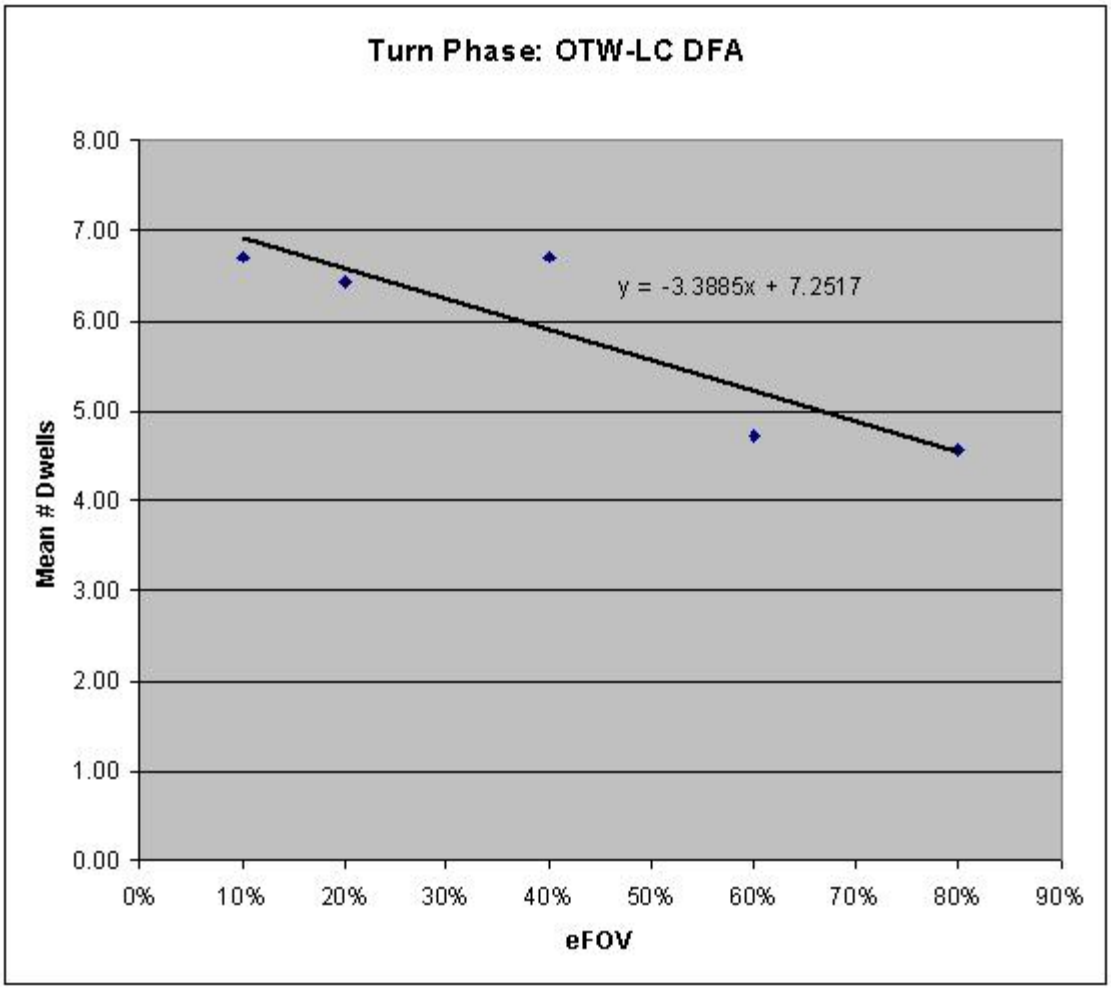

Figure 31: DFA Trend – OTW-LC Turn Phase

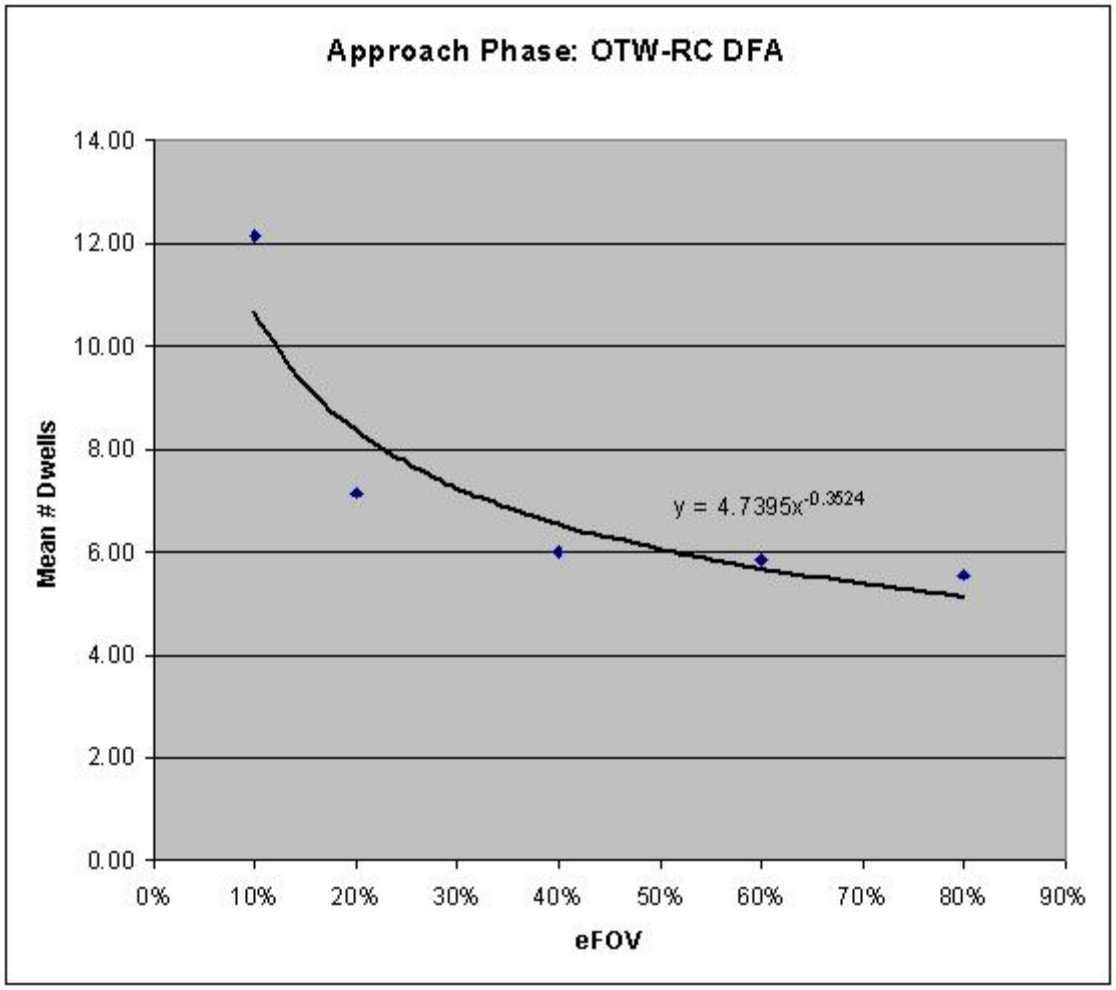

Figure 32: DFA Trend - OTW-RC Approach Phase

IP

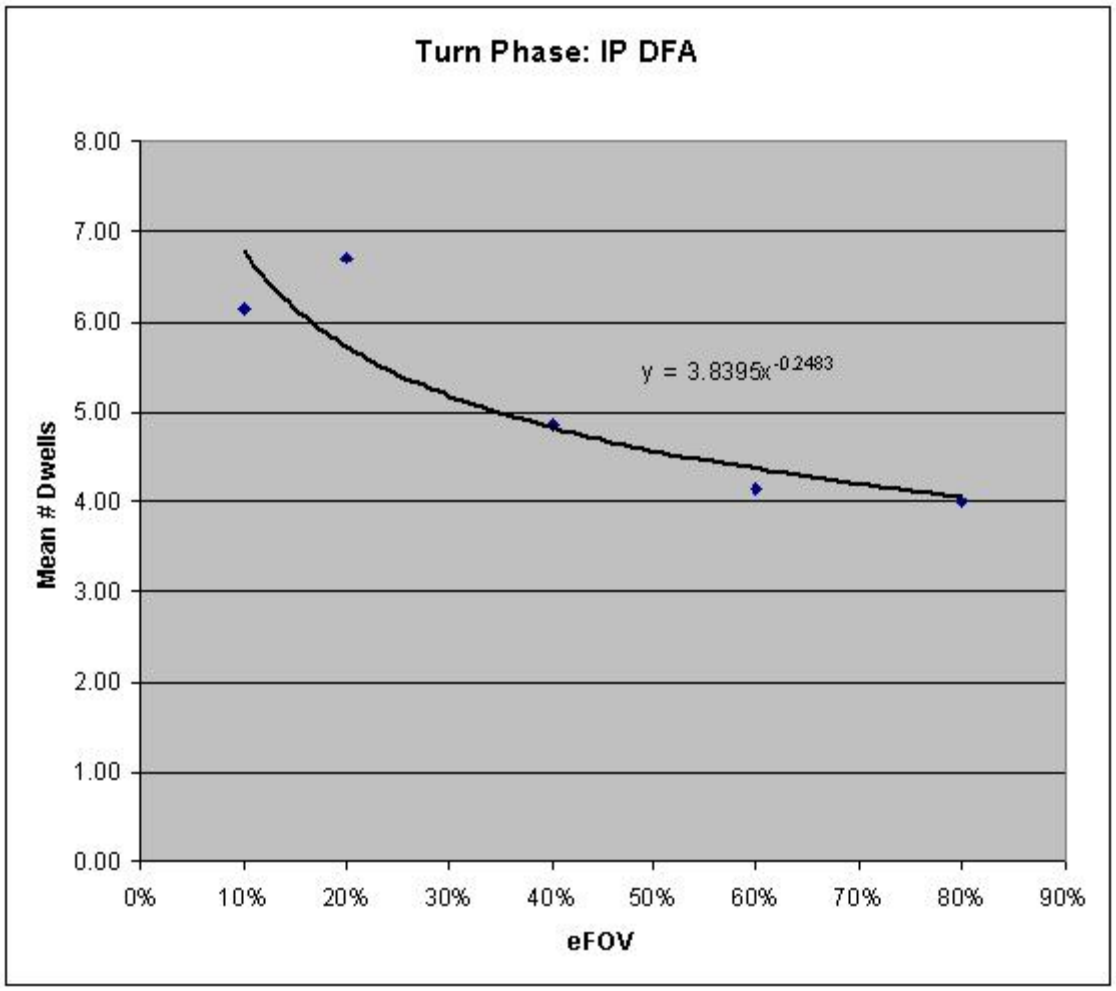

Figure 33: DFA Trend - IP Turn Phase

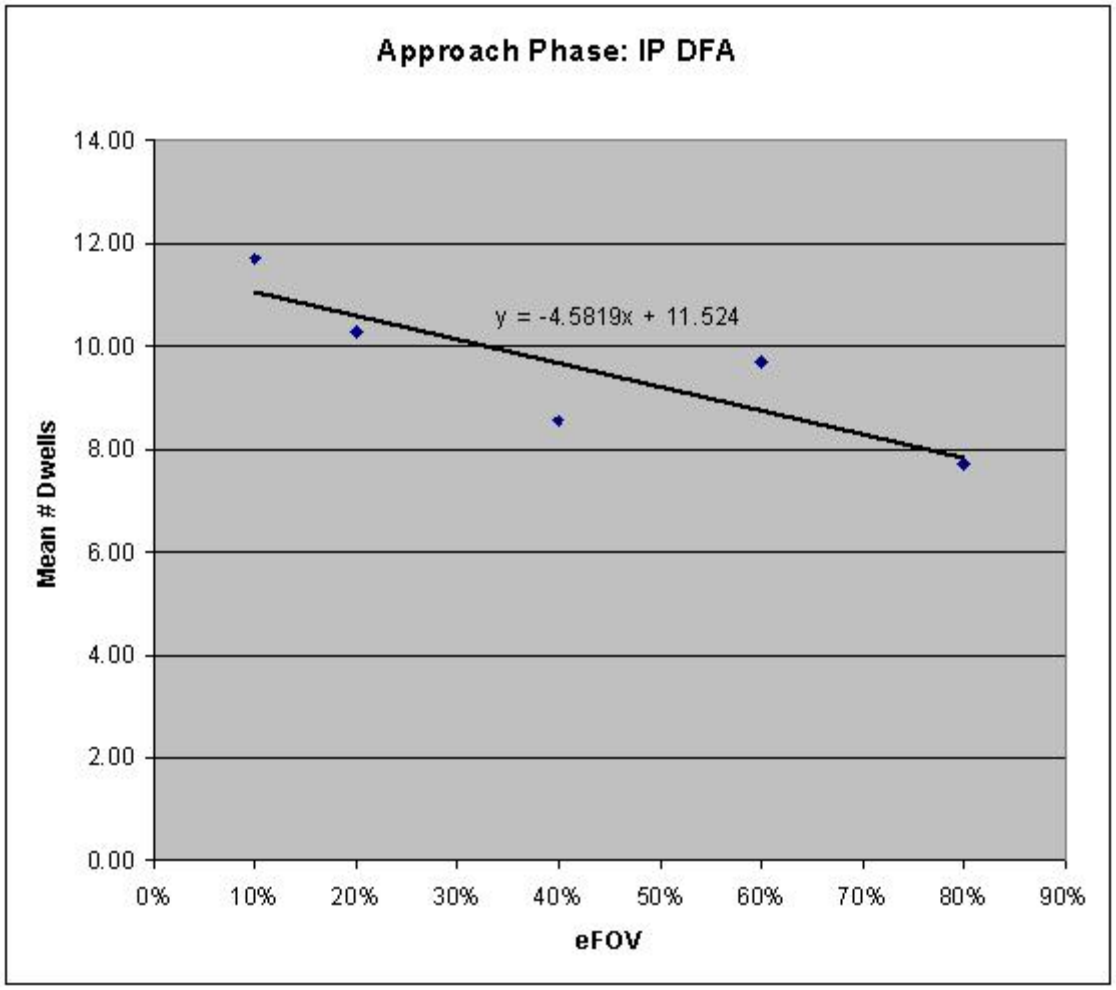

Figure 34: DFA Trend - IP Approach Phase

MDD

OTW

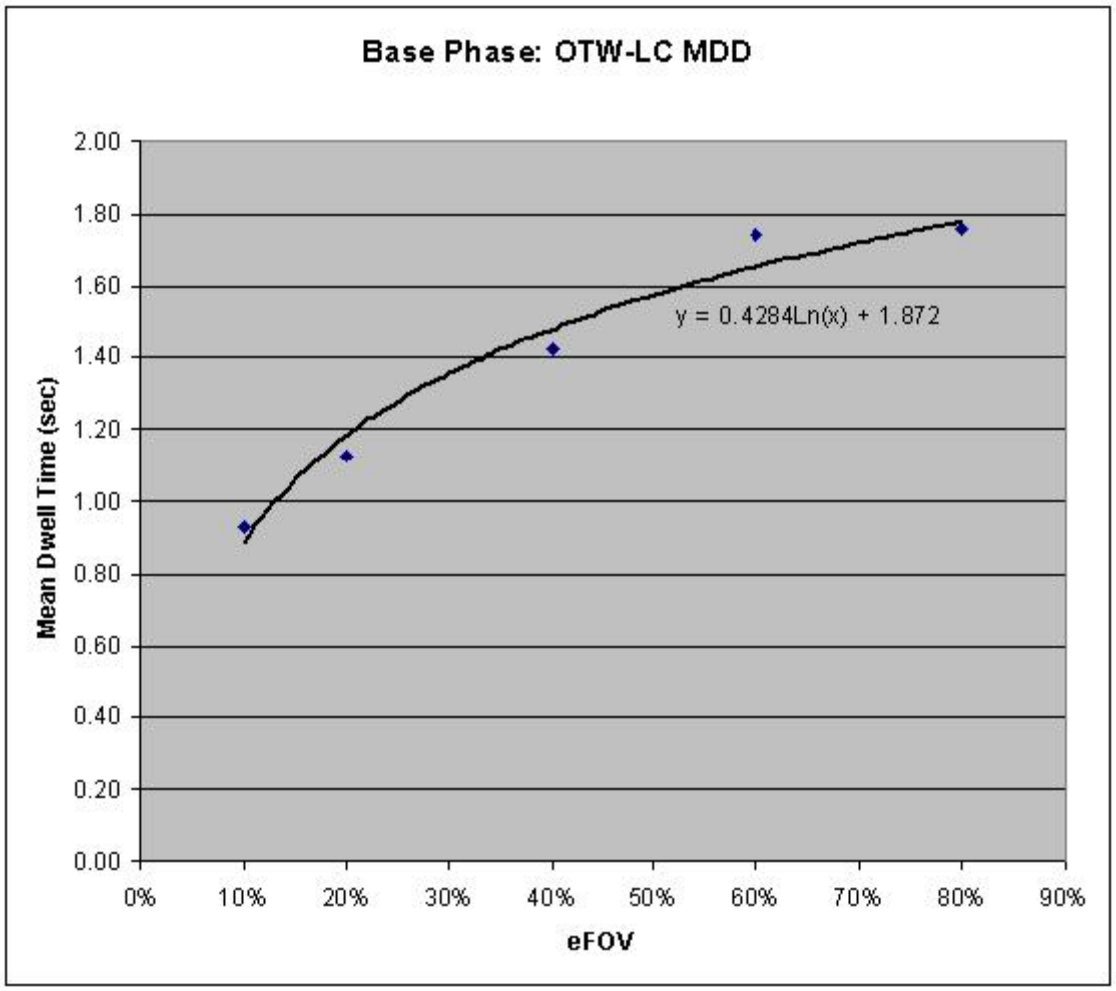

Figure 35: MDD Trend - OTW-LC Base Phase

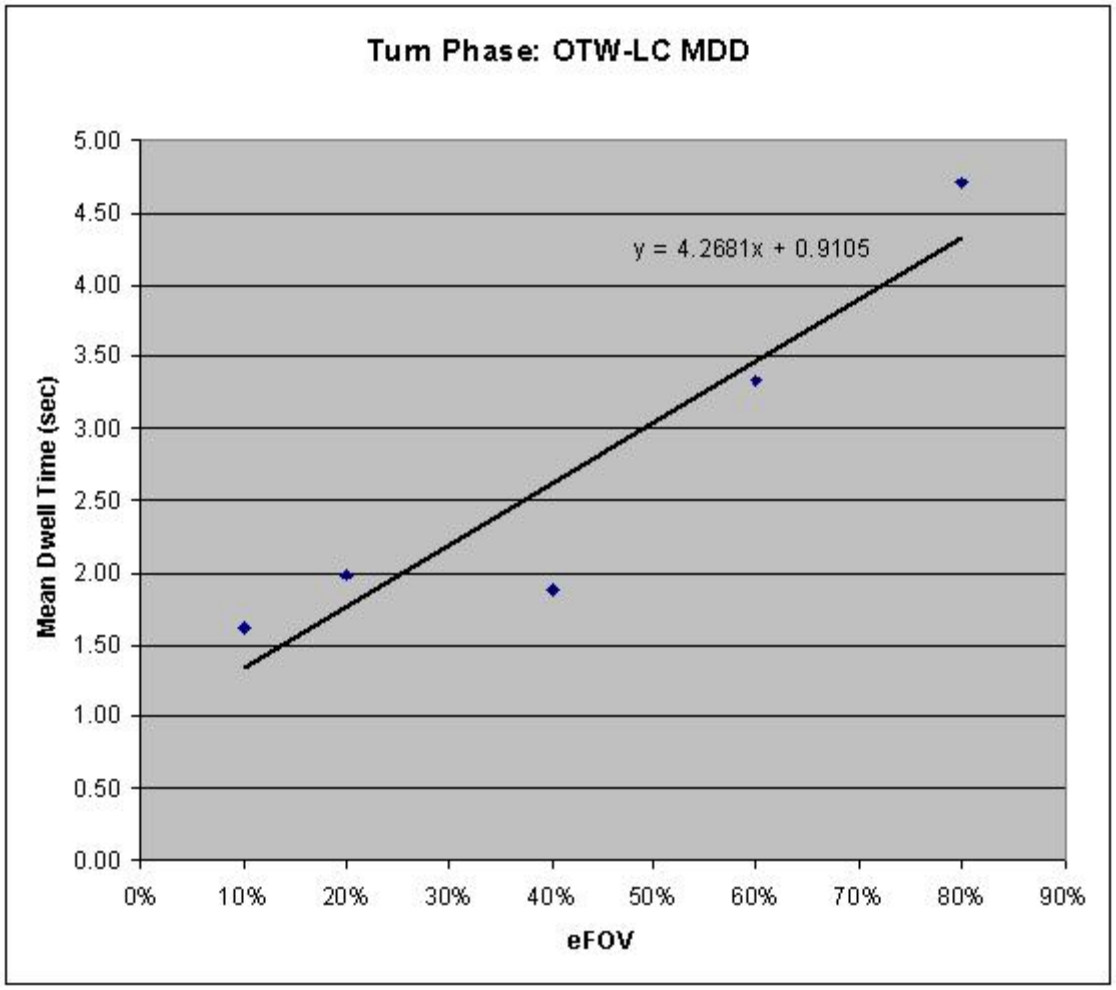

Figure 36: MDD Trend - OTW-LC Turn Phase

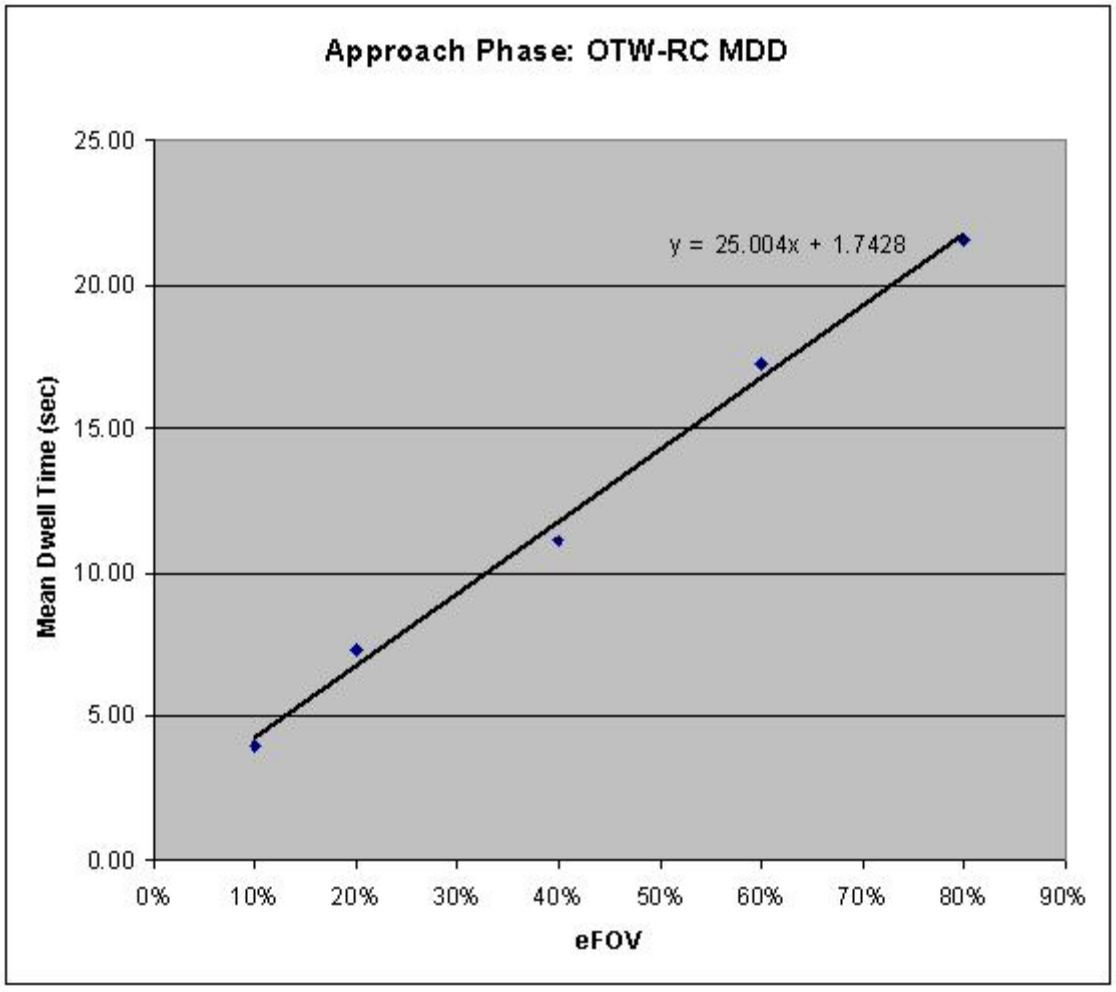

Figure 37: MDD Trend - OTW-RC Approach Phase

IP

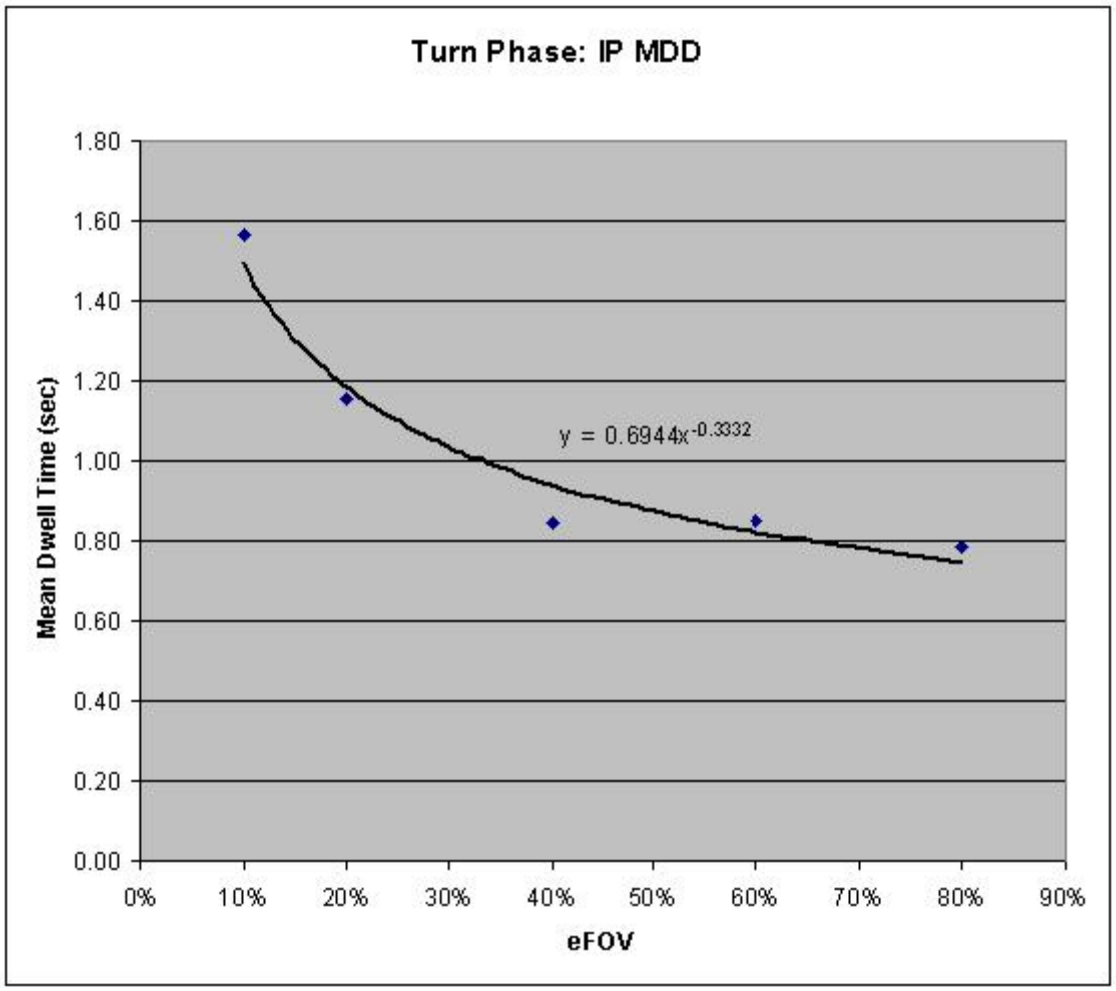

Figure 38: MDD Trend - IP Turn Phase

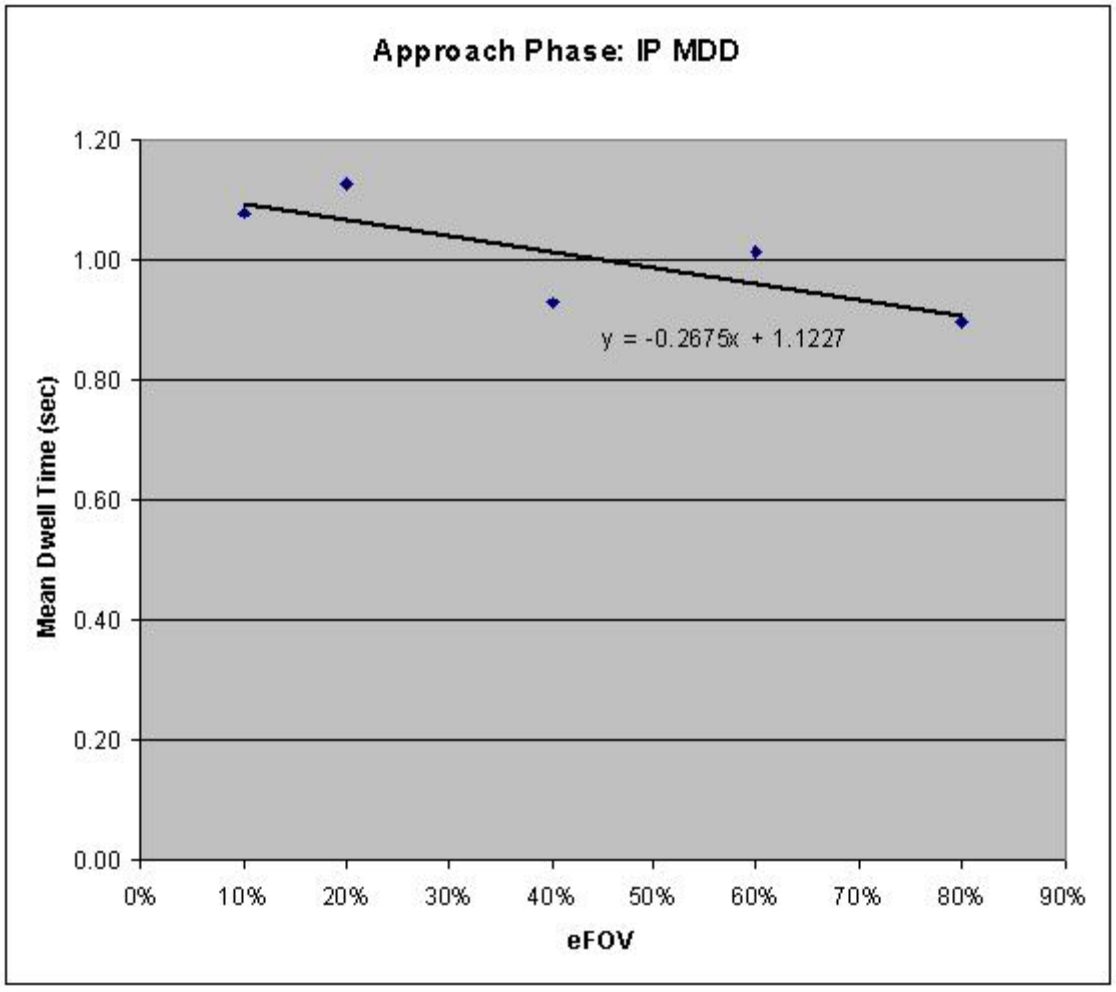

Figure 39: MDD Trend - IP Approach Phase

Effort Behavior

Pitch

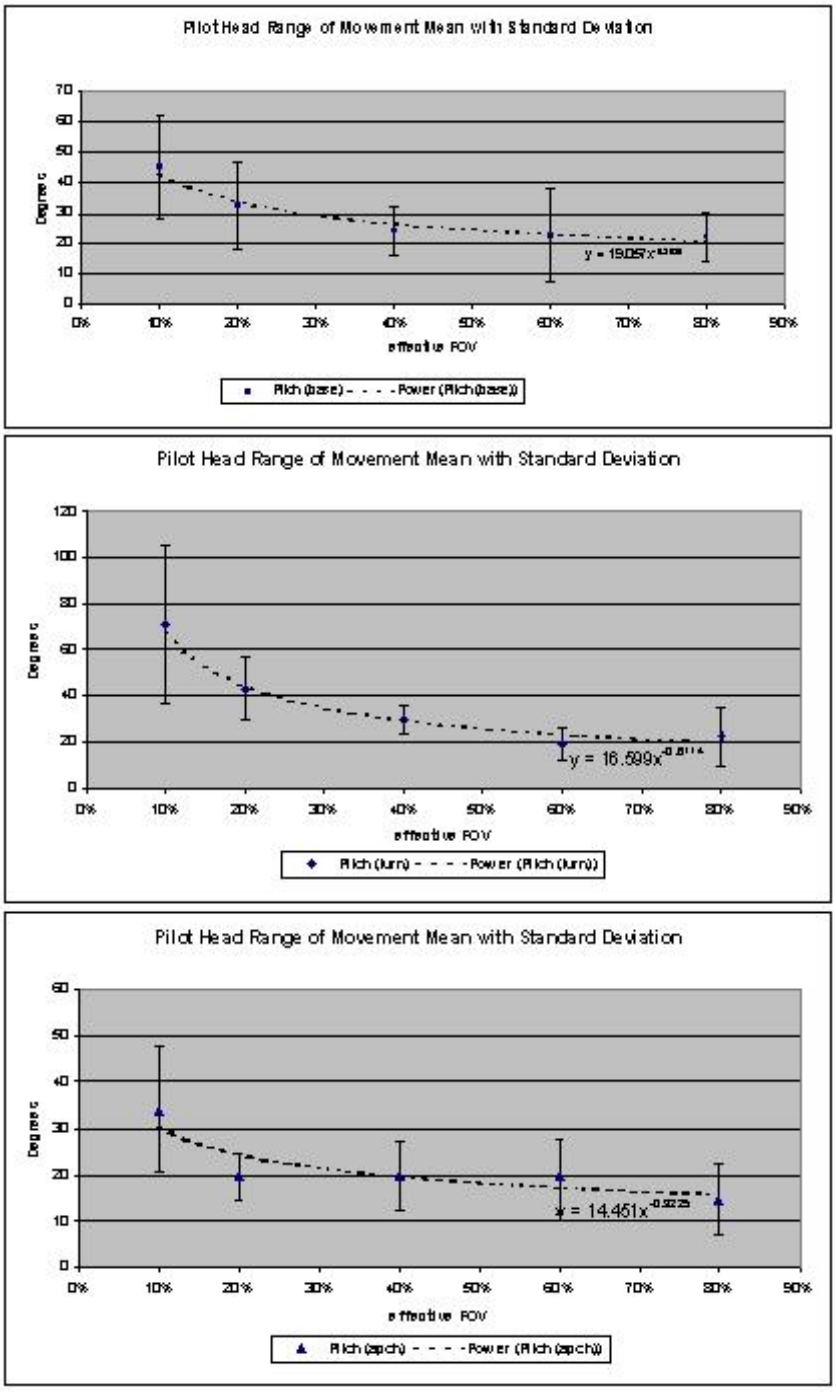

Figure 40: Pitch Effort Trend

Yaw

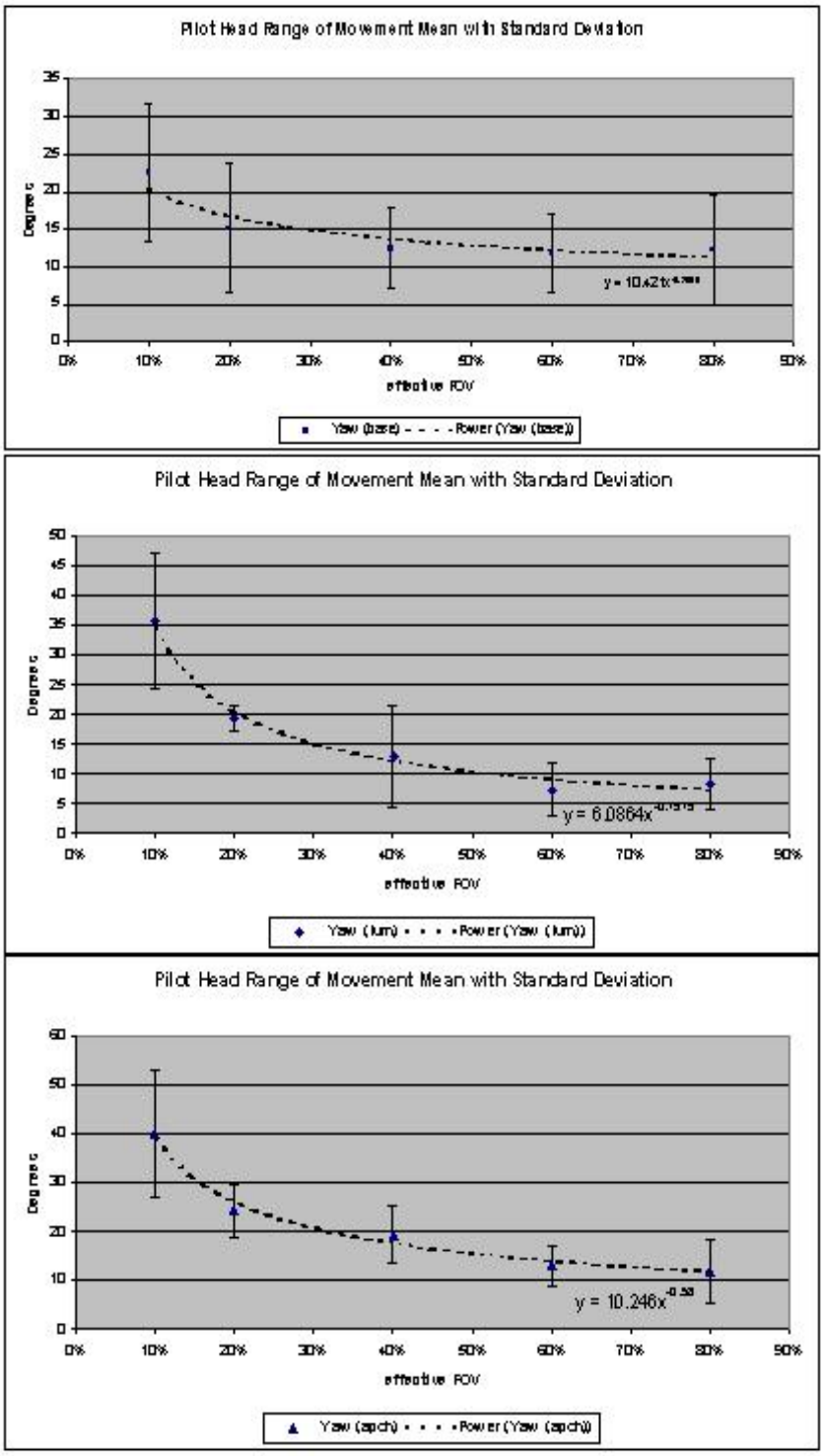

Figure 41: Yaw Effort Trend

Roll

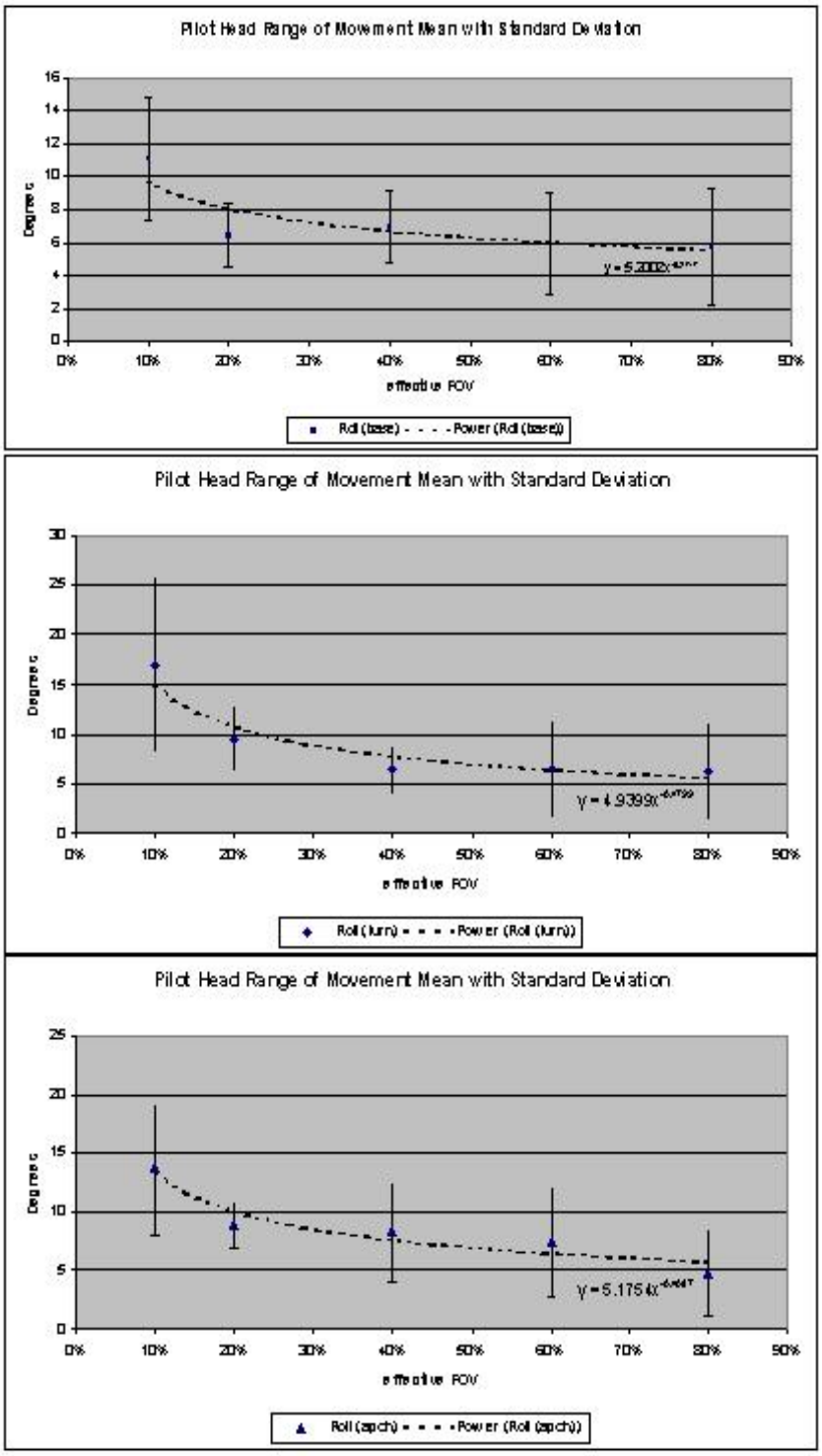

Figure 42: Roll Effort Trend

Importance Behavior

Pitch

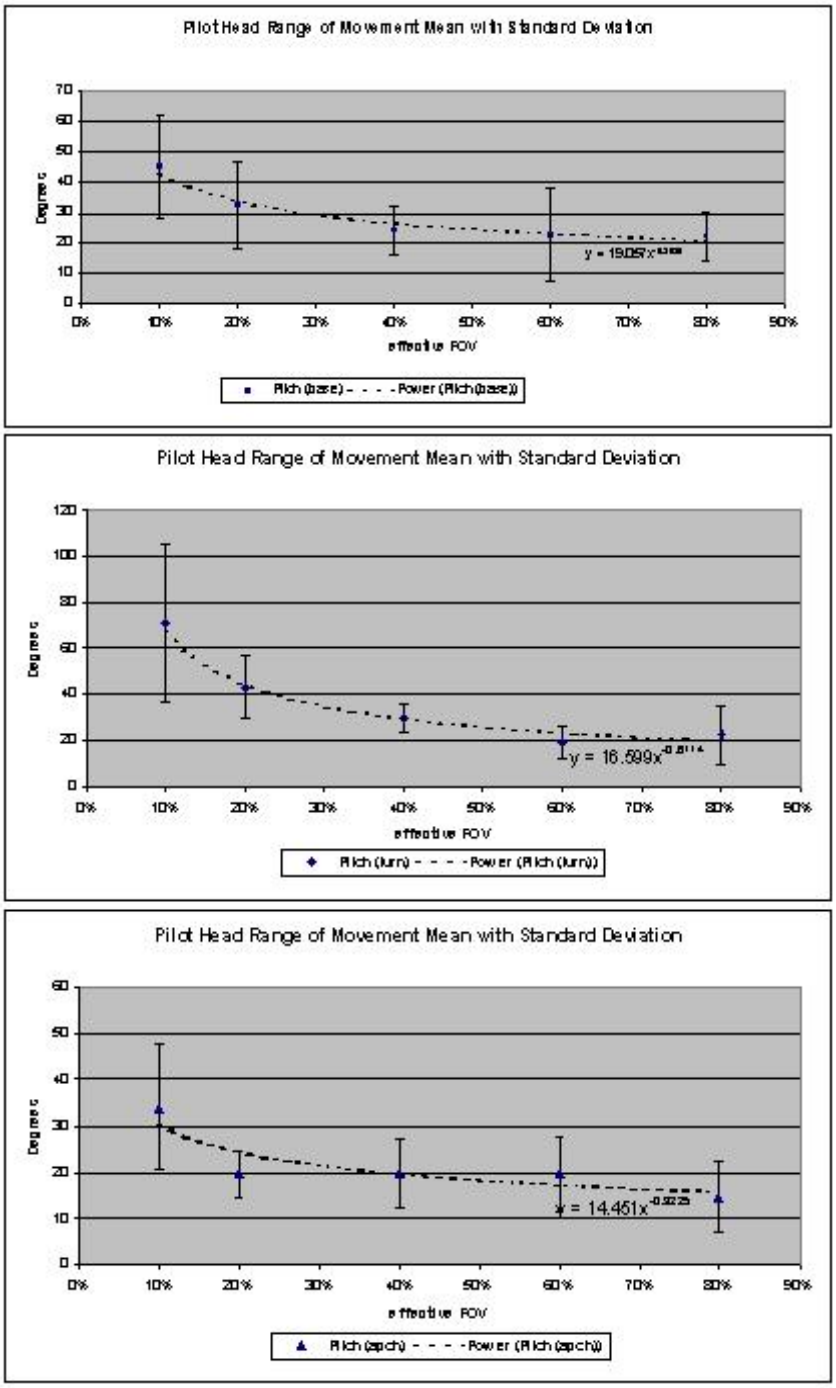

Figure 43: Pitch Importance Trend

Yaw

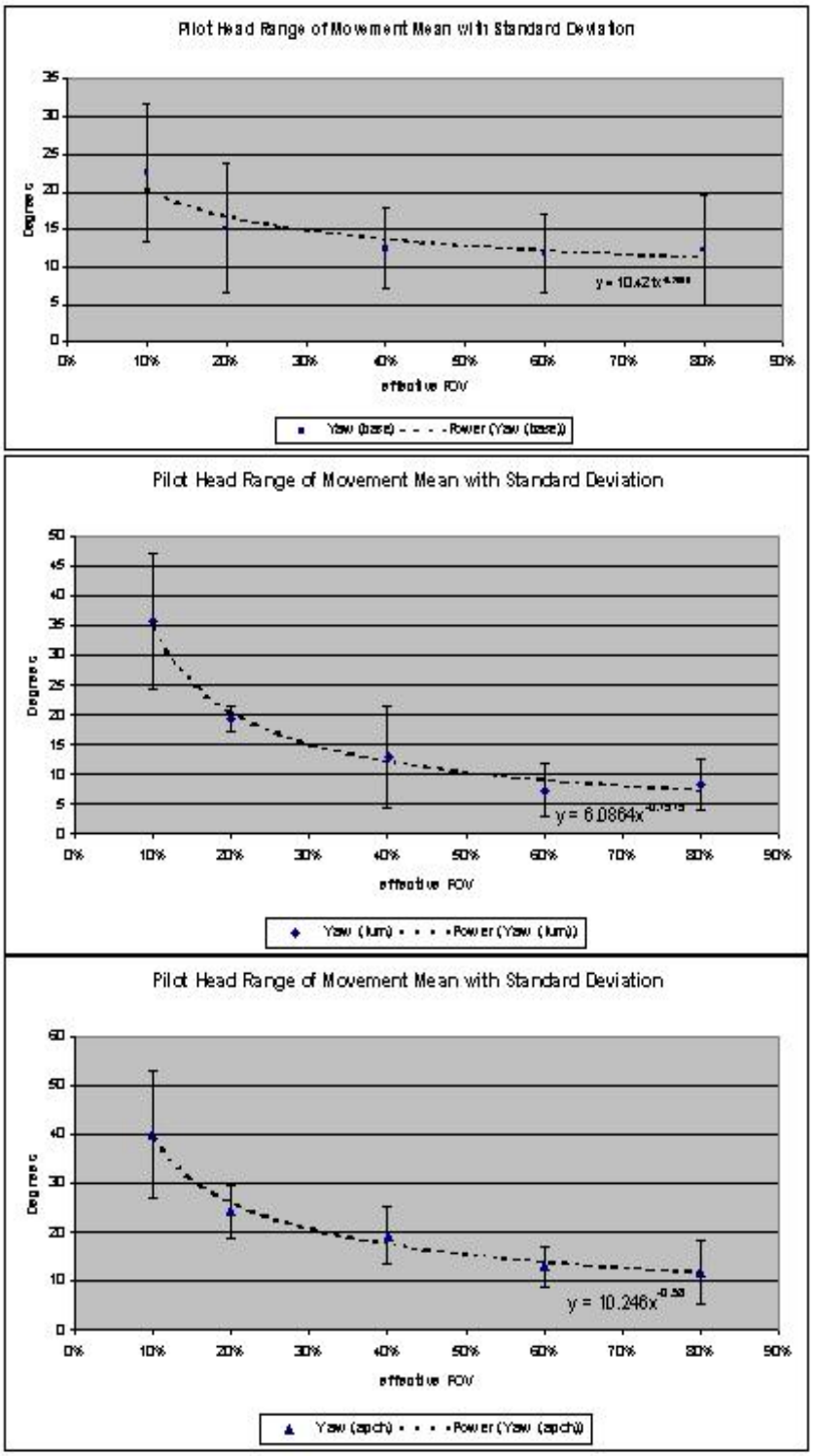

Figure 44: Yaw Importance Trend

Roll

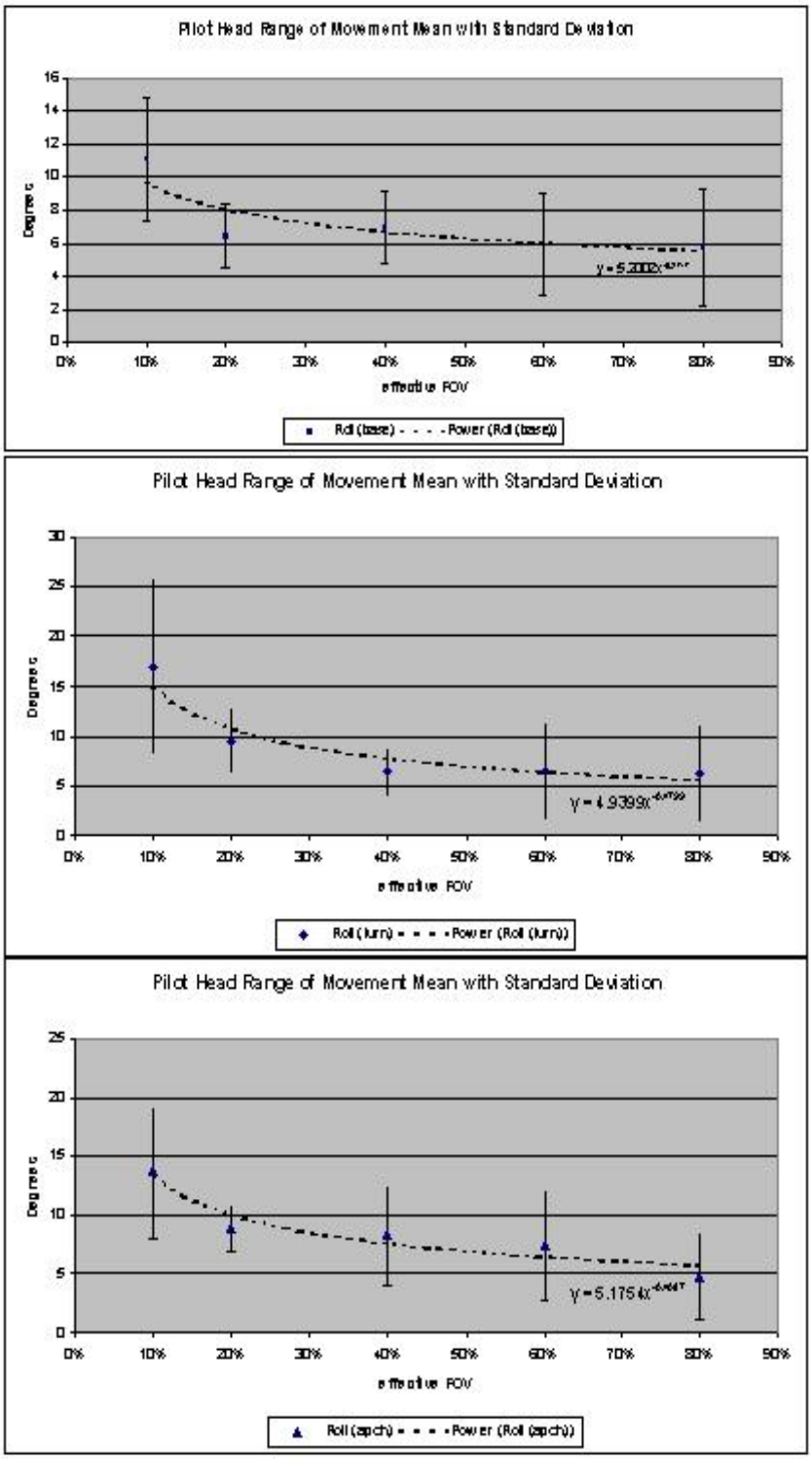

Figure 45: Roll Importance Trend

Pilot Raw Data

Pilot #1

Information

Table 13: Pilot #1 DFA

effective FOV	Dwell Frequency per AOI (DFA)						
	OW-L	OW-LC	OW-RC	OW-R	IP	OW-LL	OW-LR
10%	3	13	18	0	15	0	0
20%	1	20	11	0	15	0	1
40%	2	23	6	0	21	0	2
60%	0	26	11	0	21	0	0
80%	2	32	10	0	21	0	0

Table 14: Pilot #1 MDD

effective FOV	Mean Dwell Duration (MDD)						
	OW-L	OW-LC	OW-RC	OW-R	IP	OW-LL	OW-LR
10%	1.3764	1.3764	1.3764	1.3764	1.3764	1.3764	1.3764
20%	0.7992	2.176155	2.67005455		1.27872		5.328
40%	1.68165	3.04912174	1.83705		1.09097143		6.327
60%		2.58203077	0.65389091		1.05608571		
80%	0.4329	3.25819688	0.70596		0.96252857		

Effort

Table 15: Pilot #1 Effort

Max eFOV	Eye Offset (rad)	
	X Gaze	Y Gaze
10%	0.6766	0.6521
20%	0.5594	0.6
40%	0.6266	0.6167
60%	0.6313	0.6437
80%	0.7203	0.5375

Max eFOV	Head Offset (deg)		
	Pitch	Yaw	Roll
10%	12.602	3.964	26.133
20%	-0.64	10.005	13.562
40%	3.076	-5.188	12.313
60%	23.838	0	12.373
80%	-2.312	-13.011	10.949

Min	Eye Offset (rad)	
eFOV	X Gaze	Y Gaze
10%	0.3797	0.2708
20%	0.3172	0.2792
40%	0.3047	0.2333
60%	0.2797	0.2937
80%	0.2344	0.2667

Min	Head Offset (deg)		
eFOV	Pitch	Yaw	Roll
10%	-61.389	-46.258	-2.205
20%	-37.421	-24.07	8.045
40%	-22.416	-18.419	3.065
60%	-0.194	-18.116	0
80%	-14.085	-18.667	6.611

Range	Eye Offset (rad)	
eFOV	X Gaze	Y Gaze
10%	0.2969	0.3813
20%	0.2422	0.3208
40%	0.3219	0.3834
60%	0.3516	0.35
80%	0.4859	0.2708

Range	Head Offset (deg)		
eFOV	Pitch	Yaw	Roll
10%	73.991	50.222	28.338
20%	36.781	34.075	5.517
40%	25.492	13.231	9.248
60%	24.032	18.116	12.373
80%	11.773	5.656	4.338

Mean	Eye Offset (rad)	
eFOV	X Gaze	Y Gaze
10%	0.45866126	0.47523393
20%	0.36575253	0.43044619
40%	0.38665871	0.40125361
60%	0.36198011	0.36151554
80%	0.36159072	0.36337404

Mean	Head Offset (deg)		
eFOV	Pitch	Yaw	Roll
10%	-9.1820426	-21.473705	11.3556952
20%	-9.039381	-15.025989	10.617981
40%	-11.051637	-13.621528	8.59554959
60%	8.57776405	-14.99684	9.40606517
80%	-4.8625174	-17.114469	8.12201634

Variance	Eye Offset (rad)	
eFOV	X Gaze	Y Gaze
10%	0.00067163	0.00222276
20%	0.00140222	0.0025065
40%	0.00219146	0.00707183
60%	0.00277305	0.00272958
80%	0.00215234	0.00240976

Variance	Head Offset (deg)		
eFOV	Pitch	Yaw	Roll
10%	123.721264	84.2594689	7.24446289
20%	31.9693582	25.5924892	1.44866149
40%	20.9822331	4.55968945	4.66663772
60%	10.4177245	7.84524286	2.0077427
80%	9.69679829	0.61811254	1.04157229

Std Dev	Eye Offset (rad)	
eFOV	X Gaze	Y Gaze
10%	0.02591579	0.04714613
20%	0.03744629	0.05006492
40%	0.04681304	0.08409416
60%	0.05265979	0.05224538
80%	0.04639334	0.04908935

Std Dev	Head Offset (deg)		
eFOV	Pitch	Yaw	Roll
10%	11.1230061	9.17929567	2.69155399
20%	5.65458552	5.05917742	1.20369876
40%	4.58063676	2.2317735	2.30973196
60%	3.22764999	2.80093607	1.41694838
80%	3.11396825	0.78620133	1.02057449

Importance

Table 16: Pilot #1 Importance

Max	Eye Vel (rad/sec)	
eFOV	dy/dt	dx/dt
10%	2.34131737	3.11676647
20%	3.48192771	2.5045045
40%	6.99399399	2.62762763
60%	2.2042042	5.44144144
80%	9.15015015	2.68181818

Max	Head Vel (deg/sec)		
eFOV	dy/dt	dx/dt	dz/dt
10%	237.636364	198.363636	120.363636
20%	54.4471894	56.6322577	12.7638822
40%	150.870056	204.657217	131.605041
60%	52.2481153	19.5252472	13.0168315
80%	16.0803011	16.6825596	8.36363636

Min	Eye Vel (rad/sec)	
eFOV	dy/dt	dx/dt
10%	-1.8318318	-1.8247734
20%	-2.760479	-3.003003
40%	-4.2252252	-2.3783784
60%	-2.5795796	-2.6276276
80%	-9.1501502	-2.5045045

Min	Head Vel (deg/sec)		
eFOV	dy/dt	dx/dt	dz/dt
10%	-252.22472	-283.27273	-74.666667
20%	-107.66374	-73.400466	-21.634095
40%	-80.699031	-458.63455	-195.79484
60%	-27.118399	-19.412759	-18.678389
80%	-32.727273	-14.939351	-7.4545455

Range	Eye Vel (rad/sec)	
eFOV	dy/dt	dx/dt
10%	4.1731492	4.94153988
20%	6.24240675	5.50750751
40%	11.2192192	5.00600601
60%	4.78378378	8.06906907
80%	18.3003003	5.18632269

Range	Head Vel (deg/sec)		
eFOV	dy/dt	dx/dt	dz/dt
10%	489.861083	481.636364	195.030303
20%	162.110928	130.032724	34.3979776
40%	231.569087	663.29177	327.399881
60%	79.3665142	38.9380063	31.6952201
80%	48.8075739	31.6219108	15.8181818

Mean	Eye Vel (rad/sec)	
eFOV	dy/dt	dx/dt
10%	5.3909E-06	-0.0004603
20%	0.00048721	0.00066764
40%	0.00038239	0.00085472
60%	8.4379E-05	-0.000421
80%	-0.0006389	-0.0002159

Mean	Head Vel (deg/sec)		
eFOV	dy/dt	dx/dt	dz/dt
10%	0.53105707	0.17439633	-0.0301867
20%	0.0373391	0.01660256	-0.008028
40%	-0.0440049	-0.0274422	-0.0051377
60%	0.00014822	-0.0590828	-0.0136353
80%	0.02163561	-0.0349731	0.00132565

Variance	Eye Vel (rad/sec)	
eFOV	dy/dt	dx/dt
10%	0.06483267	0.08451801
20%	0.07291048	0.0796184
40%	0.10350299	0.09480671
60%	0.05989217	0.11832304
80%	0.09842028	0.07333238

Variance	Head Vel (deg/sec)		
eFOV	dy/dt	dx/dt	dz/dt
10%	1024.21186	457.094585	86.0897847
20%	64.7350892	86.9090294	4.66742471
40%	20.7406229	75.8339263	13.5218046
60%	10.1332642	3.69597112	2.04170864
80%	5.0086462	1.64324409	0.73067148

Std Dev	Eye Vel (rad/sec)	
eFOV	dy/dt	dx/dt
10%	0.2546226	0.29071981
20%	0.2700194	0.28216733
40%	0.3217188	0.30790699
60%	0.24472877	0.34398116
80%	0.31372007	0.27079953

Std Dev	Head Vel (deg/sec)		
eFOV	dy/dt	dx/dt	dz/dt
10%	32.0033102	21.3797705	9.2784581
20%	8.0458119	9.32250124	2.16042235
40%	4.5541874	2.90756353	1.5163696
60%	3.18327885	1.92249086	1.4288837
80%	2.23800049	1.28189083	0.85479324

Performance

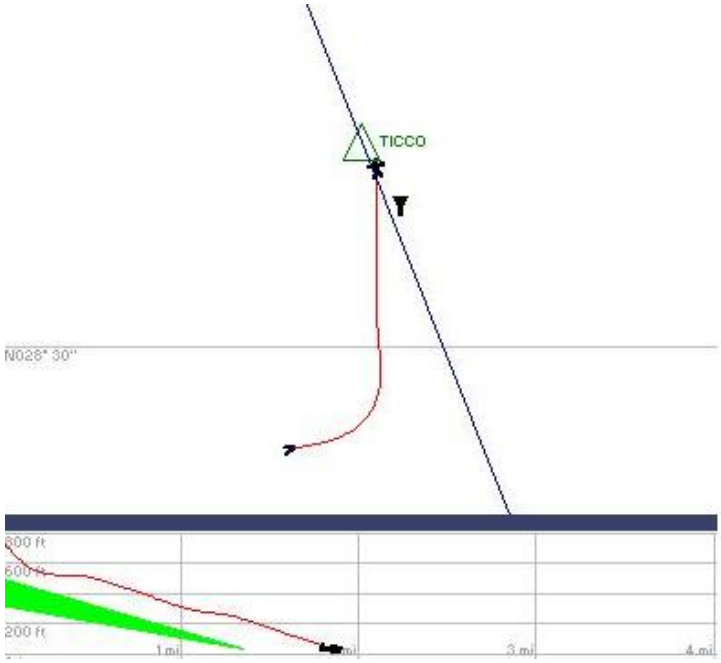

Figure 46: Pilot #1 Performance at 80% eFOV

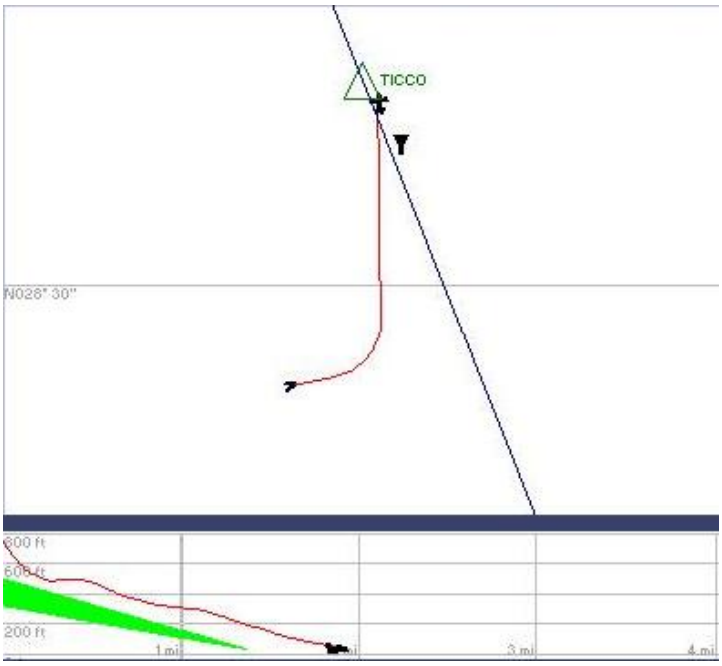

Figure 47: Pilot #1 Performance at 60% eFOV

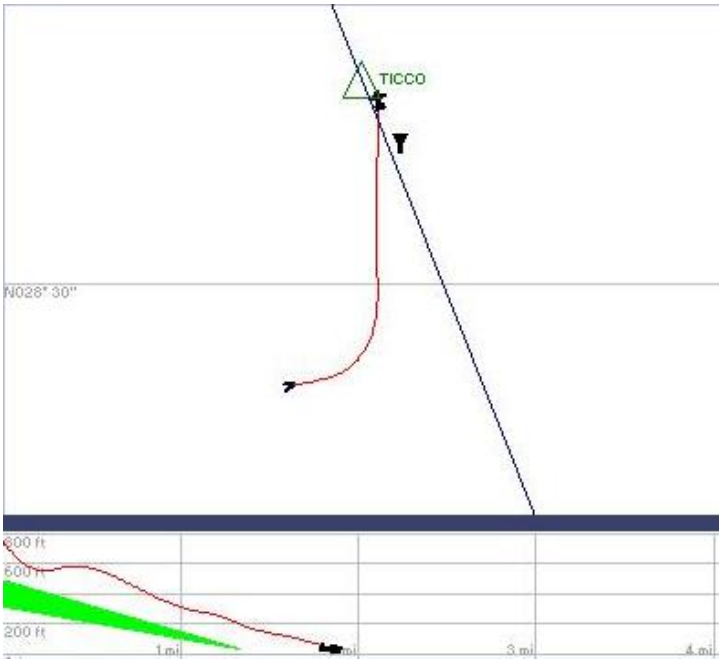

Figure 48: Pilot #1 Performance at 40% eFOV

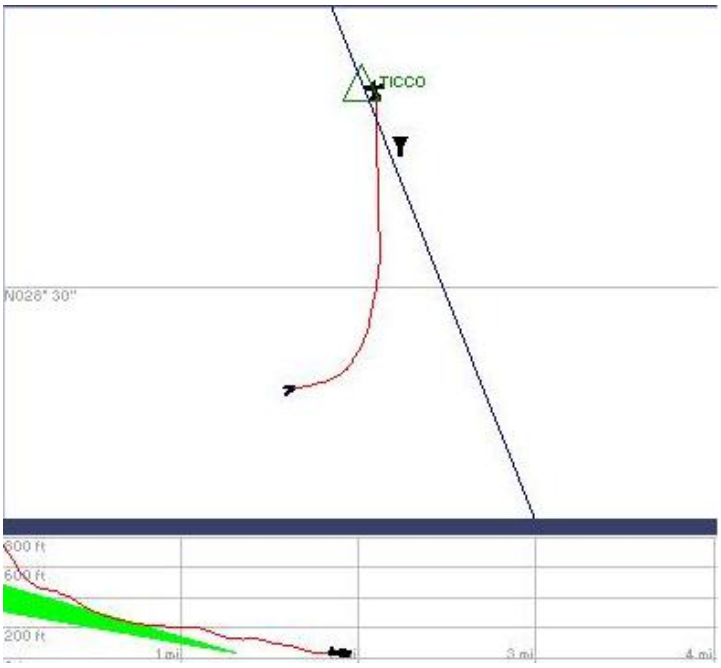

Figure 49: Pilot #1 Performance at 20% eFOV

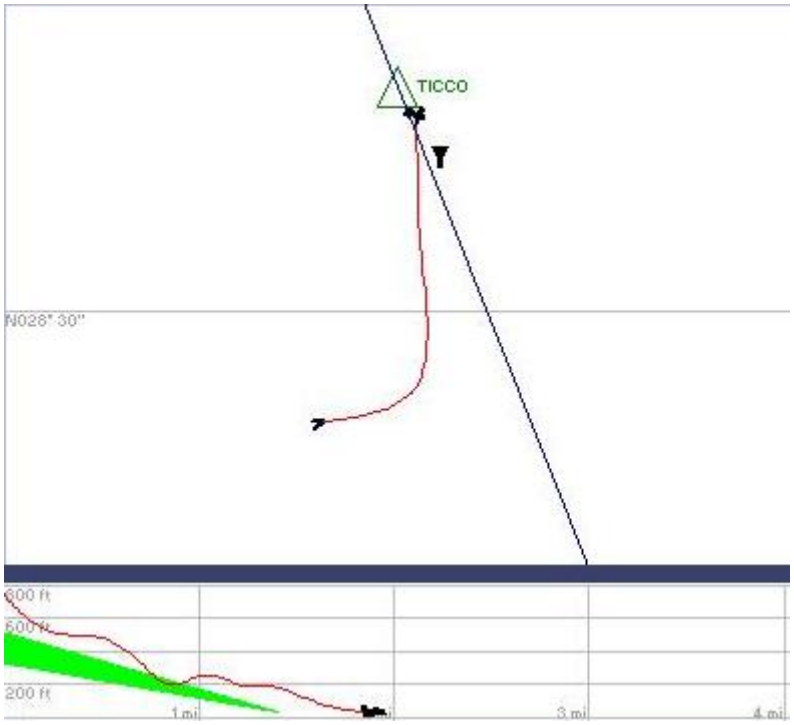

Figure 50: Pilot #1 Performance at 10% eFOV

Pilot #2

Information

Table 17: Pilot #2 DFA

effective FOV	Dwell Frequency per AOI (DFA)						
	OW-L	OW-LC	OW-RC	OW-R	IP	OW-LL	OW-LR
10%	4	20	2	0	16	0	0
20%	4	26	1	0	21	0	0
40%	3	20	4	0	15	0	0
60%	2	25	2	0	21	0	0
80%	0	21	5	0	17	0	0

Table 18: Pilot #2 MDD

effective FOV	Mean Dwell Duration (MDD)						
	OW-L	OW-LC	OW-RC	OW-R	IP	OW-LL	OW-LR
10%	1.0989	1.0989	1.0989	1.0989	1.0989	1.0989	1.0989
20%	0.857475	3.93580385	0.5328		0.79761429		
40%	0.888	4.940055	3.538125		0.87468		
60%	3.4299	4.211784	2.0646		0.81347143		
80%		5.30262857	3.48984		0.91477059		

Effort

Table 19: Pilot #2 Effort

Max eFOV	Eye Offset (rad)	
	X Gaze	Y Gaze
10%	0.4437	0.5458
20%	0.5578	0.7292
40%	0.55	0.6542
60%	0.6203	0.7042
80%	0.7453	0.775

Max eFOV	Head Offset (deg)		
	Pitch	Yaw	Roll
10%	7.624	-2.766	12.732
20%	6.285	-4.234	14.909
40%	-2.76	-6.283	10.23
60%	1.295	-4.73	10.829
80%	-0.493	-0.216	10.271

Min eFOV	Eye Offset (rad)	
	X Gaze	Y Gaze
10%	0.2438	0.3125
20%	0.2609	0.4417
40%	0.2109	0.4146
60%	0.2359	0.4833
80%	0.2734	0.6104

Min eFOV	Head Offset (deg)		
	Pitch	Yaw	Roll
10%	-41.443	-27.91	2.783
20%	-36.449	-23.035	2.34
40%	-30.208	-16.727	4.185
60%	-29.021	-17.234	4.589
80%	-16.606	-13.903	4.202

Range eFOV	Eye Offset (rad)	
	X Gaze	Y Gaze
10%	0.1999	0.2333
20%	0.2969	0.2875
40%	0.3391	0.2396
60%	0.3844	0.2209
80%	0.4719	0.1646

Range eFOV	Head Offset (deg)		
	Pitch	Yaw	Roll
10%	49.067	25.144	9.949
20%	42.734	18.801	12.569
40%	27.448	10.444	6.045
60%	30.316	12.504	6.24
80%	16.113	13.687	6.069

Mean eFOV	Eye Offset (rad)	
	X Gaze	Y Gaze
10%	0.31687428	0.37278982
20%	0.36259808	0.50515472
40%	0.32654514	0.48448704
60%	0.3705996	0.57327763
80%	0.36908039	0.6782092

Mean eFOV	Head Offset (deg)		
	Pitch	Yaw	Roll
10%	-2.7138338	-16.686576	7.51051168
20%	-3.5580528	-14.241256	7.16359632
40%	-7.2801286	-13.520243	7.99371172
60%	-5.9202739	-13.360398	6.01769108
80%	-5.1992887	-10.953614	6.95829739

Variance eFOV	Eye Offset (rad)	
	X Gaze	Y Gaze
10%	0.00012149	0.00074097
20%	0.00106619	0.00176061
40%	0.00183225	0.00164165
60%	0.00270262	0.00270825
80%	0.00220196	0.00104803

Variance eFOV	Head Offset (deg)		
	Pitch	Yaw	Roll
10%	73.3189531	27.3432084	1.83620799
20%	102.583365	13.1651731	3.52190383
40%	45.8398199	3.21261245	0.58248108
60%	53.7376493	4.85213507	0.69843799
80%	16.0006307	5.12771707	1.27438033

Std Dev eFOV	Eye Offset (rad)	
	X Gaze	Y Gaze
10%	0.01102209	0.02722085
20%	0.03265256	0.04195958
40%	0.04280475	0.04051727
60%	0.05198677	0.05204085
80%	0.04692499	0.03237327

Std Dev eFOV	Head Offset (deg)		
	Pitch	Yaw	Roll
10%	8.56264872	5.22907338	1.35506752
20%	10.1283447	3.62838436	1.87667361
40%	6.77051105	1.7923762	0.76320448
60%	7.33059679	2.20275624	0.83572603
80%	4.00007884	2.26444631	1.12888455

Importance

Table 20: Pilot #2 Importance

Max	Eye Vel (rad/sec)	
eFOV	dy/dt	dx/dt
10%	1.64264264	4.69069069
20%	2.90990991	4.31831832
40%	2.11111111	3.37837838
60%	3.98798799	3.11976048
80%	10.5105105	2.25225225

Max	Head Vel (deg/sec)		
eFOV	dy/dt	dx/dt	dz/dt
10%	129.989876	94.3739021	25.1297163
20%	105.253656	73.8387103	23.9059179
40%	70.2727273	17.4545455	12
60%	34.7272727	18.3111111	10.3636364
80%	20.476788	11.2727273	7.19101124

Min	Eye Vel (rad/sec)	
eFOV	dy/dt	dx/dt
10%	-1.6396396	-2.3682635
20%	-2.9908815	-2.734375
40%	-2.6756757	-3.1291291
60%	-2.8618619	-3.6276276
80%	-8.5598802	-2.6046512

Min	Head Vel (deg/sec)		
eFOV	dy/dt	dx/dt	dz/dt
10%	-167.23315	-68.555557	-24.572146
20%	-104.71015	-54.960949	-21.845098
40%	-73.427136	-23.316583	-15.93985
60%	-65.924812	-16	-14.222222
80%	-14	-14.363636	-12.567127

Range	Eye Vel (rad/sec)	
eFOV	dy/dt	dx/dt
10%	3.28228228	7.05895416
20%	5.90079137	7.05269332
40%	4.78678679	6.50750751
60%	6.84984985	6.74738811
80%	19.0703908	4.85690342

Range	Head Vel (deg/sec)		
eFOV	dy/dt	dx/dt	dz/dt
10%	297.223026	162.929459	49.7018619
20%	209.963807	128.799659	45.7510163
40%	143.699863	40.7711284	27.9398496
60%	100.652085	34.3111111	24.5858586
80%	34.476788	25.6363636	19.758138

Mean	Eye Vel (rad/sec)	
eFOV	dy/dt	dx/dt
10%	-0.0001007	0.00032815
20%	4.3815E-05	0.00023396
40%	-3.866E-05	0.00045575
60%	-0.0002143	0.00045868
80%	-0.0002022	-0.0005023

Mean	Head Vel (deg/sec)		
eFOV	dy/dt	dx/dt	dz/dt
10%	0.09732503	-0.0303189	0.00263584
20%	0.08692655	-0.0800806	-0.0074263
40%	0.02975706	0.07553978	0.00548759
60%	-0.0142573	-0.0090358	-0.0220027
80%	0.02303678	-0.0330757	-0.0002148

Variance	Eye Vel (rad/sec)	
eFOV	dy/dt	dx/dt
10%	0.0163639	0.06524037
20%	0.06309839	0.10410311
40%	0.06464938	0.08978148
60%	0.08075969	0.11329046
80%	0.14333115	0.05811236

Variance	Head Vel (deg/sec)		
eFOV	dy/dt	dx/dt	dz/dt
10%	238.020139	117.667868	8.39818903
20%	127.818233	48.8528838	7.54164152
40%	49.5701104	4.61285533	2.06570309
60%	14.1110692	4.64160378	1.85032521
80%	3.56057964	2.38673849	1.2638253

Std Dev	Eye Vel (rad/sec)	
eFOV	dy/dt	dx/dt
10%	0.12792146	0.25542194
20%	0.25119393	0.32265013
40%	0.25426241	0.29963558
60%	0.2841825	0.33658648
80%	0.37859101	0.24106506

Std Dev	Head Vel (deg/sec)		
eFOV	dy/dt	dx/dt	dz/dt
10%	15.4279013	10.8474821	2.89796291
20%	11.3056726	6.9894838	2.74620493
40%	7.04060441	2.14775588	1.4372554
60%	3.75647031	2.15443816	1.36026659
80%	1.88694983	1.54490727	1.12419985

Performance

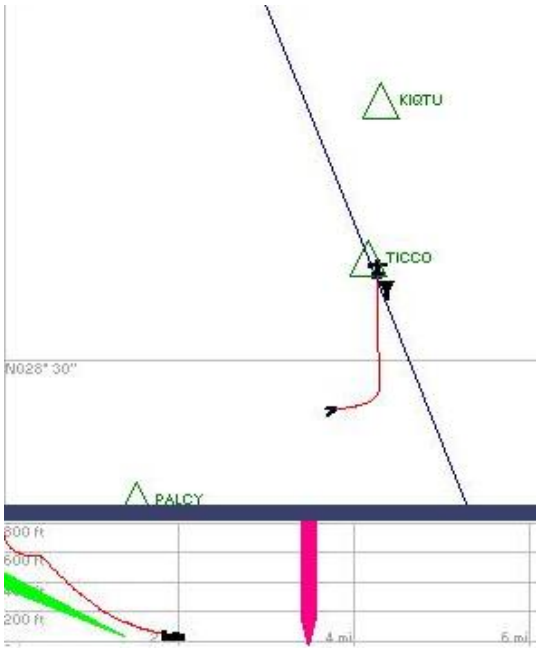

Figure 51: Pilot #2 Performance at 80% eFOV

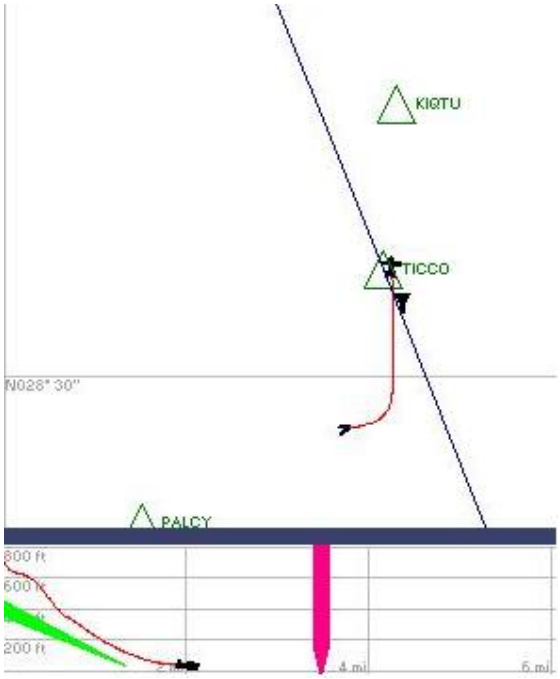

Figure 52: Pilot #2 Performance at 60% eFOV

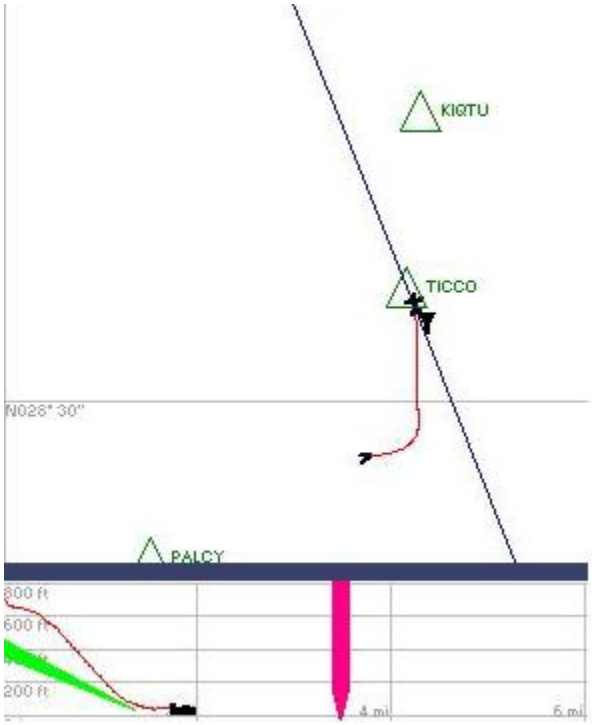

Figure 53: Pilot #2 Performance at 40% eFOV

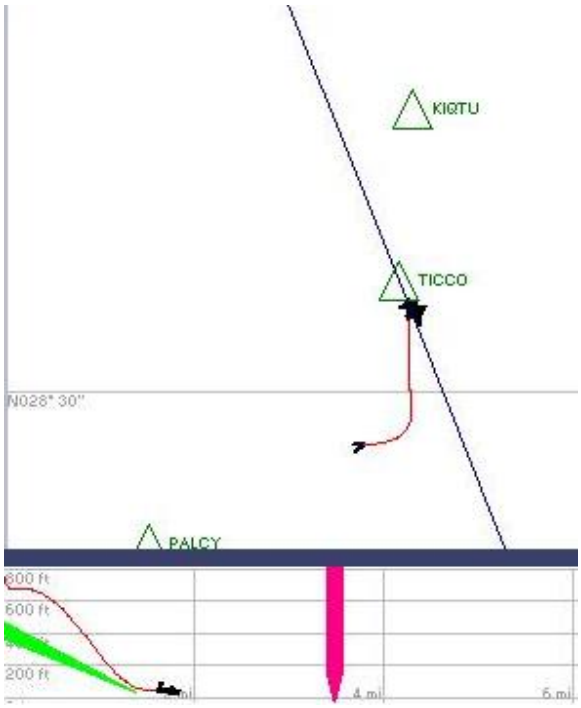

Figure 54: Pilot #2 Performance at 20% eFOV

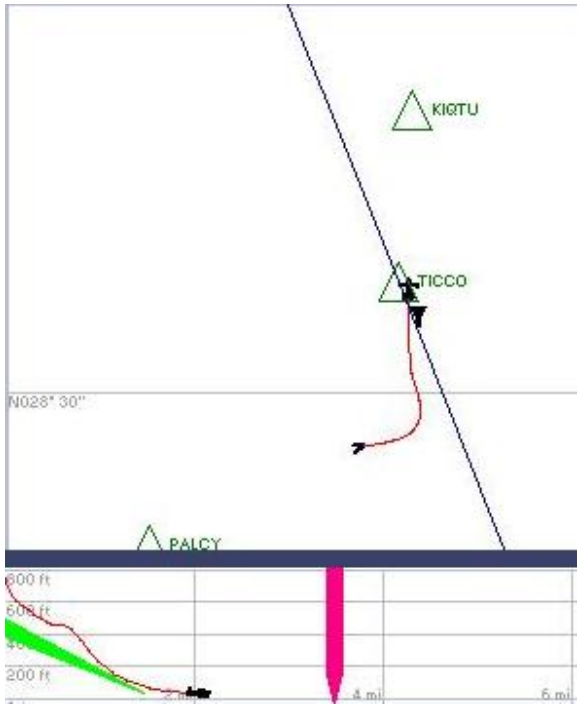

Figure 55: Pilot #2 Performance at 10% eFOV

Pilot #3

Information

Table 21: Pilot #3 DFA

effective FOV	Dwell Frequency per AOI (DFA)						
	OW-L	OW-LC	OW-RC	OW-R	IP	OW-LL	OW-LR
10%	5	20	13	0	23	0	0
20%	4	22	17	1	29	0	0
40%	1	12	22	0	22	0	0
60%	0	8	16	0	12	0	0
80%	2	29	9	0	19	0	0

Table 22: Pilot #3 MDD

effective FOV	Mean Dwell Duration (MDD)						
	OW-L	OW-LC	OW-RC	OW-R	IP	OW-LL	OW-LR
10%	1.43856	1.43856	1.43856	1.43856	1.43856	1.43856	1.43856
20%	1.207125	1.24572273	3.10669412	0.7326	1.08971379		
40%	1.5984	1.578975	7.06716818		0.74925		
60%		1.789875	7.434225		0.8103		
80%	0.4329	3.19335517	0.5513		1.00425789		

Effort

Table 23: Pilot #3 Effort

Max eFOV	Eye Offset (rad)	
	X Gaze	Y Gaze
10%	0.6172	0.6187
20%	0.7047	0.6917
40%	0.6234	0.575
60%	0.775	0.7167
80%	0.6766	0.525

Max eFOV	Head Offset (deg)		
	Pitch	Yaw	Roll
10%	56.535	19.113	28.752
20%	7.038	-14.403	19.569
40%	7.049	-15.413	13.322
60%	33.132	-15.354	14.092
80%	5.813	-10.782	14.385

Min	Eye Offset (rad)	
eFOV	X Gaze	Y Gaze
10%	0.3047	0.3146
20%	0.2281	0.2417
40%	0.2375	0.2417
60%	0.2063	0.2042
80%	0.2641	0.2271

Min	Head Offset (deg)		
eFOV	Pitch	Yaw	Roll
10%	-63.144	-42.667	3.4
20%	-51.54	-38.141	3.645
40%	-28.353	-37.137	4.453
60%	-18.842	-37.52	3.602
80%	-25.716	-38.408	3.33

Range	Eye Offset (rad)	
eFOV	X Gaze	Y Gaze
10%	0.3125	0.3041
20%	0.4766	0.45
40%	0.3859	0.3333
60%	0.5687	0.5125
80%	0.4125	0.2979

Range	Head Offset (deg)		
eFOV	Pitch	Yaw	Roll
10%	119.679	61.78	25.352
20%	58.578	23.738	15.924
40%	35.402	21.724	8.869
60%	51.974	22.166	10.49
80%	31.529	27.626	11.055

Mean	Eye Offset (rad)	
eFOV	X Gaze	Y Gaze
10%	0.44927171	0.49121769
20%	0.35396709	0.44694641
40%	0.38676357	0.3810571
60%	0.45128279	0.28693925
80%	0.44676685	0.32612367

Mean	Head Offset (deg)		
eFOV	Pitch	Yaw	Roll
10%	-3.2828696	-25.090636	9.65591476
20%	-0.2436973	-25.924106	7.58453184
40%	-0.9878371	-27.303868	7.82495578
60%	4.46092727	-28.373342	9.32677986
80%	-4.1518721	-29.733088	8.21665884

Variance	Eye Offset (rad)	
eFOV	X Gaze	Y Gaze
10%	0.00072337	0.00167593
20%	0.00886291	0.01246106
40%	0.00163959	0.00453265
60%	0.00330517	0.00178515
80%	0.0035874	0.0036015

Variance	Head Offset (deg)		
eFOV	Pitch	Yaw	Roll
10%	111.014735	53.27459	9.0721122
20%	92.019791	25.5913809	4.31757714
40%	20.2189023	17.6774695	2.24657661
60%	26.9498268	14.4127227	3.24432387
80%	23.6670546	23.8092075	3.48005897

Std Dev	Eye Offset (rad)	
eFOV	X Gaze	Y Gaze
10%	0.02689558	0.04093815
20%	0.09414302	0.11162911
40%	0.04049191	0.06732499
60%	0.05749065	0.042251
80%	0.05989494	0.06001253

Std Dev	Head Offset (deg)		
eFOV	Pitch	Yaw	Roll
10%	10.536353	7.29894444	3.01199472
20%	9.59269467	5.05879244	2.07787804
40%	4.49654337	4.20445829	1.49885844
60%	5.19132226	3.79640918	1.80120068
80%	4.86487971	4.87946796	1.86549162

Importance

Table 24: Pilot #3 Importance

Max	Eye Vel (rad/sec)	
eFOV	dy/dt	dx/dt
10%	2.95495495	2.62762763
20%	9.87125749	4.9251497
40%	2.95495495	3.7993921
60%	9.05705706	14.0780781
80%	2.57185629	3.5045045

Max	Head Vel (deg/sec)		
eFOV	dy/dt	dx/dt	dz/dt
10%	355.69697	123.454545	135.272727
20%	166.363636	57.8305085	57.8090452
40%	65.0909091	46.235589	13.8591549
60%	121.454545	33.1457286	16.5454545
80%	66.9090909	46.3517588	22.3636364

Min	Eye Vel (rad/sec)	
eFOV	dy/dt	dx/dt
10%	-2.3453453	-2.6906907
20%	-5.2072072	-2.8566978
40%	-3.003003	-3.8798799
60%	-6.0540541	-13.138138
80%	-4.6456456	-4.1445783

Min	Head Vel (deg/sec)		
eFOV	dy/dt	dx/dt	dz/dt
10%	-543.63636	-120.18182	-70.512563
20%	-122	-57.724311	-34.909091
40%	-72.363636	-21.636364	-16.181818
60%	-82	-40.181818	-18.276056
80%	-68.545455	-26.086957	-13.636364

Range	Eye Vel (rad/sec)	
eFOV	dy/dt	dx/dt
10%	5.3003003	5.31831832
20%	15.0784647	7.78184752
40%	5.95795796	7.67927198
60%	15.1111111	27.2162162
80%	7.21750193	7.64908282

Range	Head Vel (deg/sec)		
eFOV	dy/dt	dx/dt	dz/dt
10%	899.333333	243.636364	205.78529
20%	288.363636	115.554819	92.7181361
40%	137.454545	67.8719526	30.0409731
60%	203.454545	73.3275468	34.8215109
80%	135.454545	72.4387153	36

Mean	Eye Vel (rad/sec)	
eFOV	dy/dt	dx/dt
10%	-0.0004479	-0.0008337
20%	0.00178379	-0.0006668
40%	-5.816E-06	-0.0003635
60%	9.0449E-05	2.8197E-05
80%	-7.09E-05	0.0005756

Mean	Head Vel (deg/sec)		
eFOV	dy/dt	dx/dt	dz/dt
10%	0.49170532	0.09363277	-0.1200291
20%	0.14366787	-0.014649	-0.0121825
40%	0.04386283	0.00497837	0.00524857
60%	-0.0156838	0.00832103	-0.0202008
80%	0.00868723	0.03114571	0.00188161

Variance	Eye Vel (rad/sec)	
eFOV	dy/dt	dx/dt
10%	0.06959362	0.12484958
20%	0.29331518	0.1647464
40%	0.09193176	0.20379878
60%	0.31697837	0.32222567
80%	0.12066698	0.16772915

Variance	Head Vel (deg/sec)		
eFOV	dy/dt	dx/dt	dz/dt
10%	729.871751	402.243937	54.2469535
20%	388.307295	136.972551	16.8589664
40%	47.5303924	15.1663424	5.77046957
60%	67.0739404	15.8185516	7.26464938
80%	43.1145461	19.3050127	6.66726383

Std Dev	Eye Vel (rad/sec)	
eFOV	dy/dt	dx/dt
10%	0.26380604	0.3533406
20%	0.5415858	0.40588964
40%	0.30320251	0.45144078
60%	0.56300832	0.56764925
80%	0.34737153	0.4095475

Std Dev	Head Vel (deg/sec)		
eFOV	dy/dt	dx/dt	dz/dt
10%	27.0161387	20.05602	7.36525312
20%	19.7055143	11.7035273	4.10596717
40%	6.89422892	3.89439885	2.40218017
60%	8.18986815	3.97725428	2.69530135
80%	6.56616677	4.39374701	2.58210453

Performance

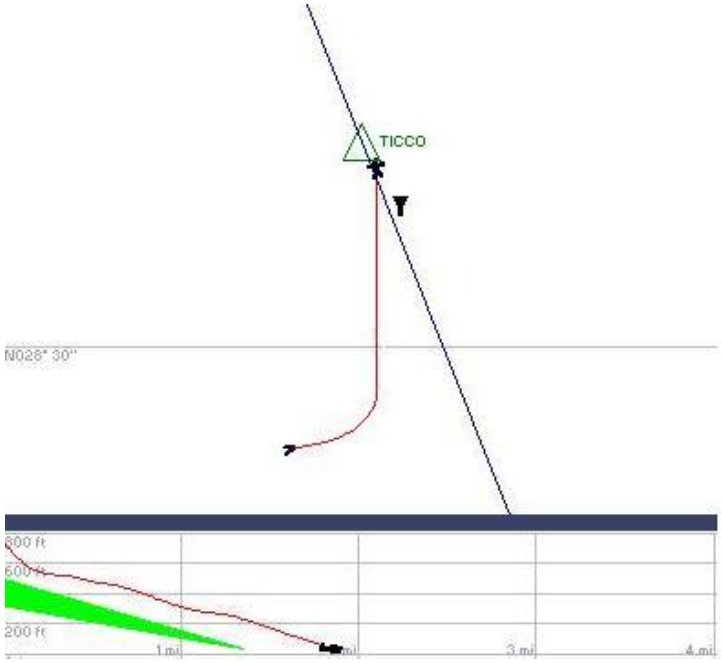

Figure 56: Pilot #3 Performance at 80% eFOV

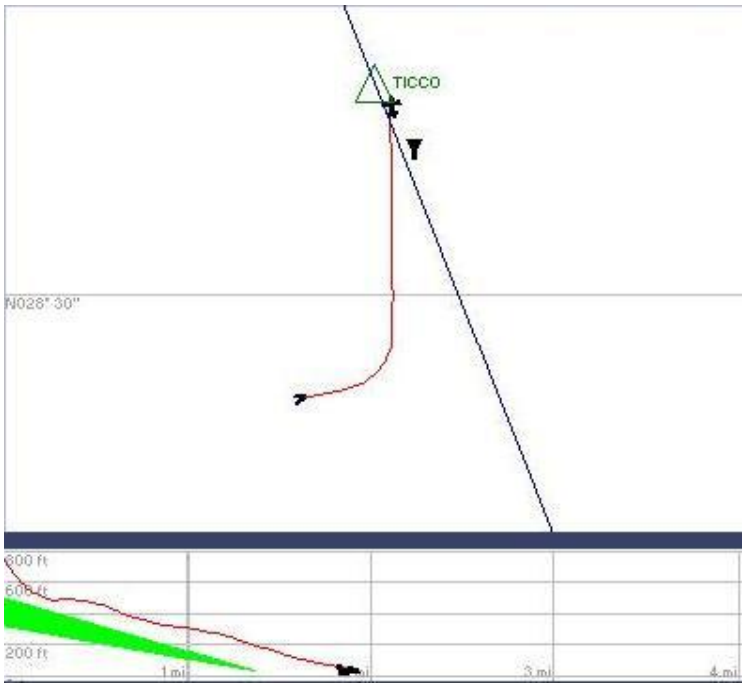

Figure 57: Pilot #3 Performance at 60% eFOV

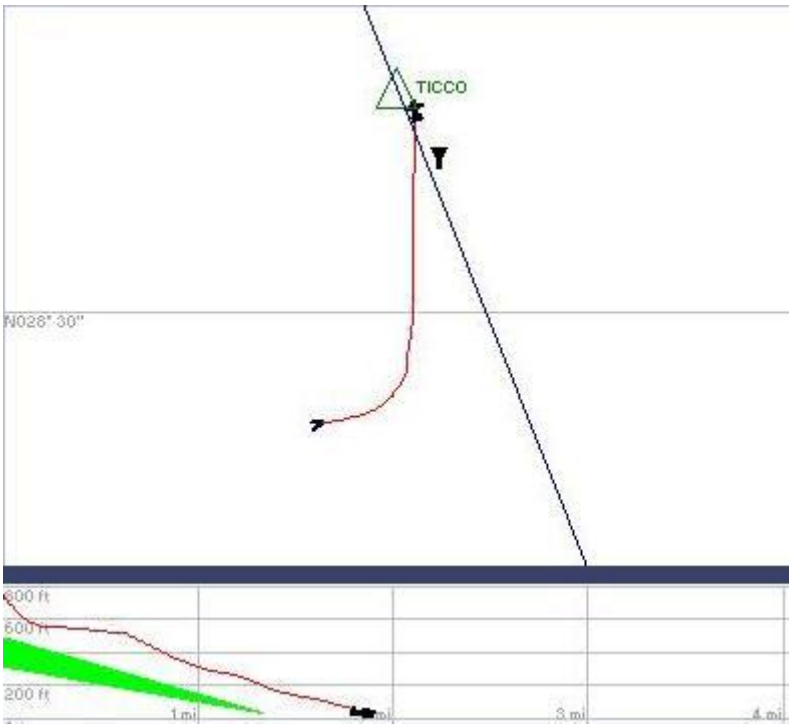

Figure 58: Pilot #3 Performance at 40% eFOV

Figure 59: Pilot #3 Performance at 20% eFOV

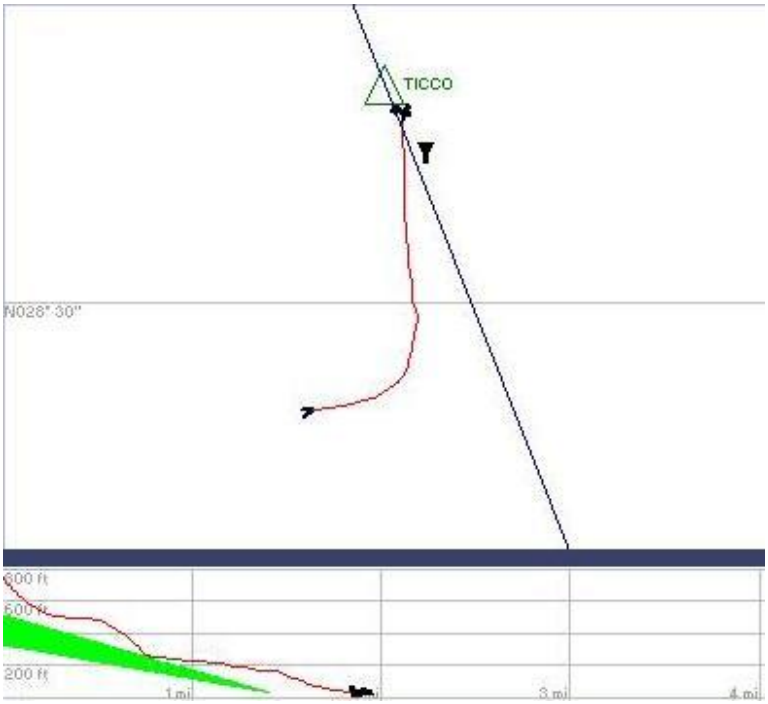

Figure 60: Pilot #3 Performance at 10% eFOV

Pilot #4

Information

Table 25: Pilot #4 DFA

effective FOV	Dwell Frequency per AOI (DFA)						
	OW-L	OW-LC	OW-RC	OW-R	IP	OW-LL	OW-LR
10%	3	8	17	0	18	0	0
20%	2	11	16	0	21	0	0
40%	3	20	4	0	15	0	0
60%	2	23	0	0	21	0	0
80%	1	10	11	0	16	0	0

Table 26: Pilot #4 MDD

effective FOV	Mean Dwell Duration (MDD)						
	OW-L	OW-LC	OW-RC	OW-R	IP	OW-LL	OW-LR
10%	1.1877	1.0323	3.684547		1.3579		
20%	0.88245	1.374382	3.754575		1.371643		
40%	0.888	3.534795	3.538125		0.87468		
60%	3.4299	3.374883			0.813471		
80%	0.2997	3.07692	4.910236		0.690975		

Effort

Table 27: Pilot #4 Effort

Max eFOV	Eye Offset (rad)	
	X Gaze	Y Gaze
10%	0.7625	0.7875
20%	0.675	0.7729
40%	0.5781	0.6396
60%	0.6406	0.7688
80%	0.6609	0.7167

Max eFOV	Head Offset (deg)		
	Pitch	Yaw	Roll
10%	13.855	-0.681	26.284
20%	8.693	-11.737	16.099
40%	6.615	-13.207	17.187
60%	8.21	-10.145	21.174
80%	8.575	-11.047	21.433

Min	Eye Offset (rad)	
eFOV	X Gaze	Y Gaze
10%	0.2828	0.5
20%	0.2141	0.3438
40%	0.2594	0.2875
60%	0.2688	0.3625
80%	0.2766	0.3812

Min	Head Offset (deg)		
eFOV	Pitch	Yaw	Roll
10%	-45.784	-43.271	2.735
20%	-34.484	-41.553	1.84
40%	-37.692	-40.641	3.063
60%	-20.726	-34.483	2.549
80%	-26.268	-33.821	6.091

Range	Eye Offset (rad)	
eFOV	X Gaze	Y Gaze
10%	0.4797	0.2875
20%	0.4609	0.4291
40%	0.3187	0.3521
60%	0.3718	0.4063
80%	0.3843	0.3355

Range	Head Offset (deg)		
eFOV	Pitch	Yaw	Roll
10%	59.639	42.59	23.549
20%	43.177	29.816	14.259
40%	44.307	27.434	14.124
60%	28.936	24.338	18.625
80%	34.843	22.774	15.342

Mean	Eye Offset (rad)	
eFOV	X Gaze	Y Gaze
10%	0.394436	0.686322
20%	0.280194	0.684728
40%	0.339313	0.433909
60%	0.405124	0.648347
80%	0.381958	0.553769

Mean	Head Offset (deg)		
eFOV	Pitch	Yaw	Roll
10%	-2.502226	-25.61183	8.553666
20%	-1.275634	-28.36238	7.651538
40%	-3.842217	-28.92667	9.154678
60%	-3.511302	-22.89411	8.262394
80%	-5.850767	-23.39339	11.15888

Variance	Eye Offset (rad)	
eFOV	X Gaze	Y Gaze
10%	0.00172	0.000421
20%	0.000669	0.000755
40%	0.001466	0.003166
60%	0.002528	0.002744
80%	0.002803	0.005024

Variance	Head Offset (deg)		
eFOV	Pitch	Yaw	Roll
10%	69.8323	64.65415	7.982306
20%	31.80336	45.52434	4.905474
40%	43.49293	28.8159	9.430641
60%	40.49124	34.13952	16.56315
80%	55.77995	21.44533	11.46515

Std Dev	Eye Offset (rad)	
eFOV	X Gaze	Y Gaze
10%	0.041472	0.020526
20%	0.025863	0.027474
40%	0.038283	0.056266
60%	0.05028	0.052381
80%	0.052944	0.070882

Std Dev	Head Offset (deg)		
eFOV	Pitch	Yaw	Roll
10%	8.356572	8.040781	2.825298
20%	5.639447	6.769425	2.194244
40%	6.594917	5.368044	3.070935
60%	6.363273	5.842903	4.069785
80%	7.468598	4.630911	3.386023

Importance

Table 28: Pilot #4 Importance

Max	Eye Vel (rad/sec)	
eFOV	dy/dt	dx/dt
10%	7.225225	3.189189
20%	12.1369	11.52632
40%	5.303303	4.816817
60%	6.295522	5.613772
80%	3.003003	4.003003

Max	Head Vel (deg/sec)		
eFOV	dy/dt	dx/dt	dz/dt
10%	166.1818	123.2727	60.54545
20%	142	133.9148	19.81818
40%	84.36364	60.29379	20.13483
60%	19.07345	41.16854	11.81818
80%	36.88169	21.74153	8

Min	Eye Vel (rad/sec)	
eFOV	dy/dt	dx/dt
10%	-7.084084	-2.745509
20%	-8.782609	-10.94895
40%	-5.444444	-5.069069
60%	-8.162162	-9.202985
80%	-3.189189	-3.441441

Min	Head Vel (deg/sec)		
eFOV	dy/dt	dx/dt	dz/dt
10%	-166.0905	-102.0351	-33.81818
20%	-131.8545	-66.96045	-24
40%	-77.8427	-56.36364	-21.57303
60%	-36.90909	-18.58647	-16.72727
80%	-36.51944	-20.42919	-15.59849

Range	Eye Vel (rad/sec)	
eFOV	dy/dt	dx/dt
10%	14.30931	5.934698
20%	20.91951	22.47526
40%	10.74775	9.885886
60%	14.45768	14.81676
80%	6.192192	7.444444

Range	Head Vel (deg/sec)		
eFOV	dy/dt	dx/dt	dz/dt
10%	332.2723	225.3078	94.36364
20%	273.8545	200.8752	43.81818
40%	162.2063	116.6574	41.70787
60%	55.98254	59.75501	28.54545
80%	73.40113	42.17072	23.59849

Mean	Eye Vel (rad/sec)	
eFOV	dy/dt	dx/dt
10%	-0.001245	0.000578
20%	-0.000645	0.004062
40%	0.001163	-0.001519
60%	-2.05E-05	-0.000821
80%	-0.000197	-0.000187

Mean	Head Vel (deg/sec)		
eFOV	dy/dt	dx/dt	dz/dt
10%	0.090009	0.163444	-0.017825
20%	0.012945	-0.027662	-0.013521
40%	0.011425	-0.030548	-0.030634
60%	0.031122	0.010128	-0.017905
80%	0.033112	-0.027047	-0.004589

Variance	Eye Vel (rad/sec)	
eFOV	dy/dt	dx/dt
10%	0.206574	0.072317
20%	0.37558	0.403766
40%	0.221993	0.341023
60%	0.19747	0.189615
80%	0.134223	0.169797

Variance	Head Vel (deg/sec)		
eFOV	dy/dt	dx/dt	dz/dt
10%	359.46	492.4332	22.86245
20%	160.961	196.4969	9.945226
40%	76.84384	67.18699	9.801334
60%	11.90126	11.65367	4.613251
80%	12.52451	6.8798	3.282702

Std Dev	Eye Vel (rad/sec)	
eFOV	dy/dt	dx/dt
10%	0.454504	0.268918
20%	0.612846	0.635426
40%	0.471162	0.583972
60%	0.444376	0.435448
80%	0.366365	0.412064

Std Dev	Head Vel (deg/sec)		
eFOV	dy/dt	dx/dt	dz/dt
10%	18.95943	22.19084	4.781469
20%	12.68704	14.01774	3.153605
40%	8.766062	8.196767	3.130708
60%	3.44982	3.413748	2.147848
80%	3.538998	2.622937	1.811823

Performance

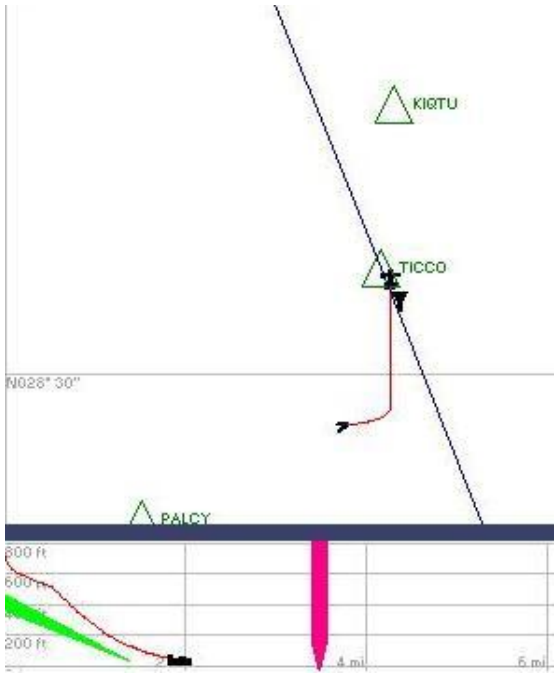

Figure 61: Pilot #4 Performance at 80% eFOV

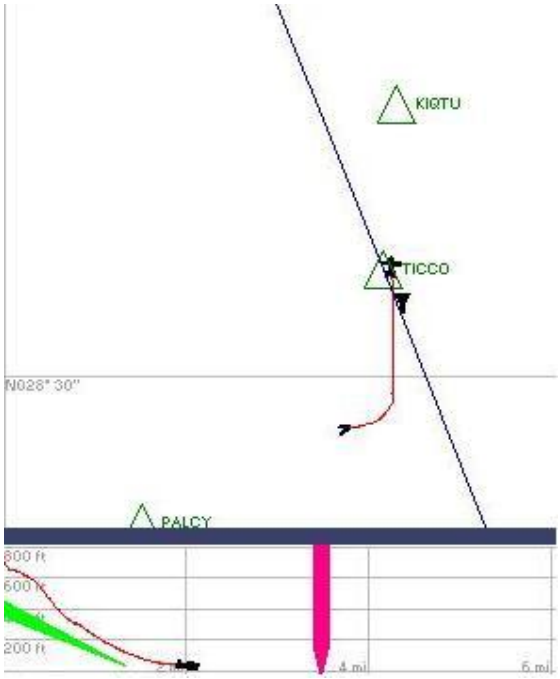

Figure 62: Pilot #4 Performance at 60% eFOV

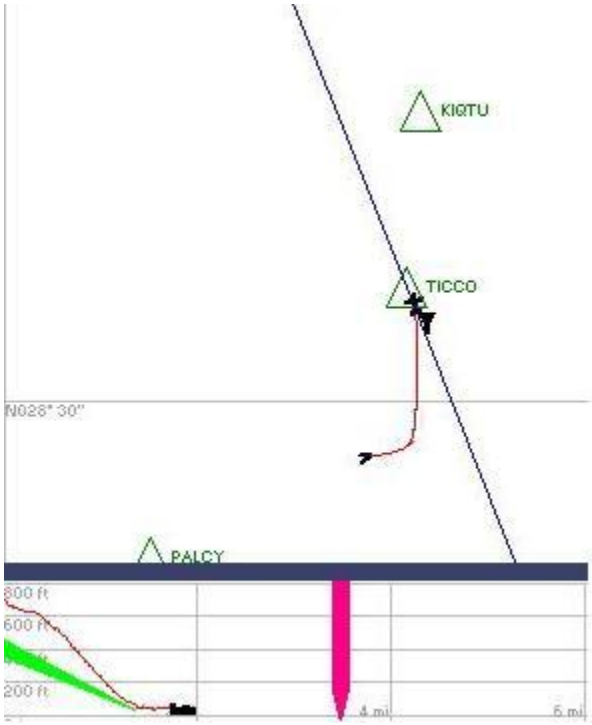

Figure 63: Pilot #4 Performance at 40% eFOV

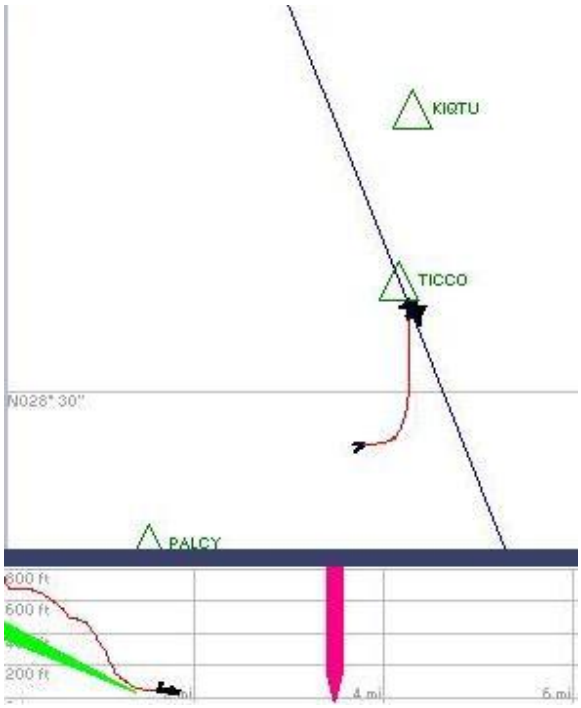

Figure 64: Pilot #4 Performance at 20% eFOV

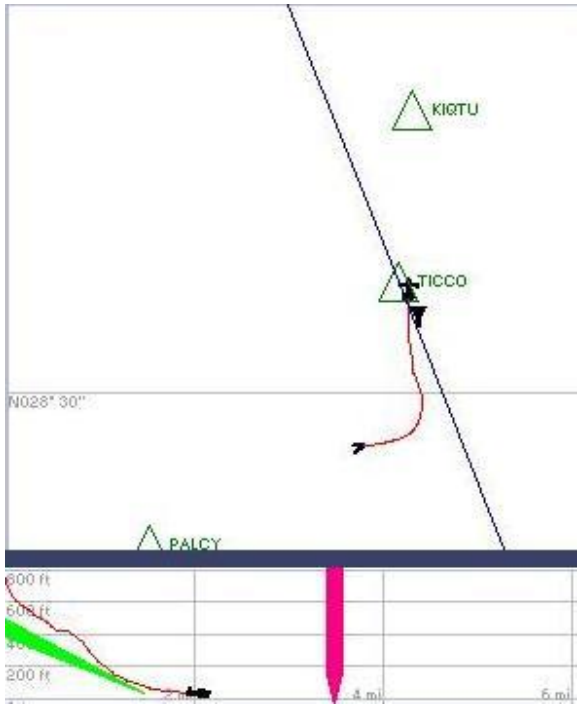

Figure 65: Pilot #4 Performance at 10% eFOV

Pilot #5

Information

Table 29: Pilot #5 DFA

effective FOV	Dwell Frequency per AOI (DFA)						
	OW-L	OW-LC	OW-RC	OW-R	IP	OW-LL	OW-LR
10%	2	9	12	1	16	0	1
20%	3	8	8	1	13	0	0
40%	3	6	9	1	9	0	1
60%	2	6	5	1	6	0	1
80%	1	9	13	0	12	0	0

Table 30: Pilot #5 MDD

effective FOV	Mean Dwell Duration (MDD)						
	OW-L	OW-LC	OW-RC	OW-R	IP	OW-LL	OW-LR
10%	0.6993	1.6613	5.591625	0.4329	1.250831		0.6993
20%	1.1988	2.060438	8.945213	0.3996	1.301262		
40%	1.3542	3.0414	8.4064	0.6993	1.4467		2.7972
60%	0.7992	3.8073	11.96802	0.6993	0.8991		3.1302
80%	1.2321	1.554	5.233223		1.3209		

Effort

Table 31: Pilot #5 Effort

Max eFOV	Eye Offset (rad)	
	X Gaze	Y Gaze
10%	0.7531	0.5542
20%	0.6594	0.7688
40%	0.7391	0.6979
60%	0.7734	0.6708
80%	0.7797	0.7563

Max eFOV	Head Offset (deg)		
	Pitch	Yaw	Roll
10%	23.247	-11.508	10.167
20%	18.693	-13.707	10.951
40%	11.726	-17.719	11.984
60%	6.756	-17.585	6.816
80%	12.362	-9.159	4.766

Min	Eye Offset (rad)	
eFOV	X Gaze	Y Gaze
10%	0.3313	0.3125
20%	0.2812	0.3812
40%	0.2922	0.3875
60%	0.3484	0.2292
80%	0.325	0.4271

Min	Head Offset (deg)		
eFOV	Pitch	Yaw	Roll
10%	-43.414	-50.254	-3.436
20%	-46.745	-43.214	-0.307
40%	-33.018	-40.07	0.141
60%	-15.537	-28.812	-1.273
80%	-23.633	-24.776	-3.693

Range	Eye Offset (rad)	
eFOV	X Gaze	Y Gaze
10%	0.4218	0.2417
20%	0.3782	0.3876
40%	0.4469	0.3104
60%	0.425	0.4416
80%	0.4547	0.3292

Range	Head Offset (deg)		
eFOV	Pitch	Yaw	Roll
10%	66.661	38.746	13.603
20%	65.438	29.507	11.258
40%	44.744	22.351	11.843
60%	22.293	11.227	8.089
80%	35.995	15.617	8.459

Mean	Eye Offset (rad)	
eFOV	X Gaze	Y Gaze
10%	0.553717	0.425731
20%	0.452116	0.481425
40%	0.46915	0.51655
60%	0.502538	0.456184
80%	0.620488	0.584106

Mean	Head Offset (deg)		
eFOV	Pitch	Yaw	Roll
10%	-0.45683	-33.91008	3.224125
20%	-1.978235	-31.56155	5.091366
40%	-4.614155	-30.52085	4.716771
60%	0.621737	-25.54847	3.143522
80%	0.932495	-19.74642	1.550897

Variance	Eye Offset (rad)	
eFOV	X Gaze	Y Gaze
10%	0.000788	0.001121
20%	0.002346	0.001889
40%	0.005245	0.003787
60%	0.006291	0.006837
80%	0.005196	0.004368

Variance	Head Offset (deg)		
eFOV	Pitch	Yaw	Roll
10%	92.91251	75.26694	4.399481
20%	98.26134	44.13183	2.90807
40%	52.36053	15.0617	2.711248
60%	22.29297	4.741683	1.962787
80%	26.24074	9.374411	1.518903

Std Dev	Eye Offset (rad)	
eFOV	X Gaze	Y Gaze
10%	0.028077	0.033483
20%	0.04843	0.043458
40%	0.072424	0.061536
60%	0.079319	0.082684
80%	0.072082	0.066091

Std Dev	Head Offset (deg)		
eFOV	Pitch	Yaw	Roll
10%	9.639114	8.675652	2.097494
20%	9.912686	6.643179	1.705306
40%	7.236058	3.880941	1.646587
60%	4.721543	2.177541	1.400995
80%	5.122572	3.061766	1.232438

Importance

Table 32: Pilot #5 Importance

Max	Eye Vel (rad/sec)	
eFOV	dy/dt	dx/dt
10%	3.084142	3.431138
20%	5.256173	5.595679
40%	4.324723	4.218354
60%	11.82282	6.069069
80%	4.244565	3.776435

Max	Head Vel (deg/sec)		
eFOV	dy/dt	dx/dt	dz/dt
10%	113.6364	76.18182	42.33708
20%	112.3596	57.63636	17.09091
40%	84.18182	31.63636	12.72727
60%	59.11811	17.1753	12.65525
80%	40.6776	26.03366	17.84781

Min	Eye Vel (rad/sec)	
eFOV	dy/dt	dx/dt
10%	-3.368263	-2.876877
20%	-4.716981	-2.753754
40%	-4.197761	-3.964789
60%	-3.569132	-3.688525
80%	-4.185185	-4.695364

Min	Head Vel (deg/sec)		
eFOV	dy/dt	dx/dt	dz/dt
10%	-140	-70.75556	-24
20%	-115.6364	-65.63636	-20.49438
40%	-76.54545	-34.8764	-13.63636
60%	-78.28319	-13.73999	-12.47469
80%	-66.75031	-21.51393	-21.51393

Range	Eye Vel (rad/sec)	
eFOV	dy/dt	dx/dt
10%	6.452406	6.308015
20%	9.973154	8.349433
40%	8.522484	8.183143
60%	15.39195	9.757594
80%	8.42975	8.471799

Range	Head Vel (deg/sec)		
eFOV	dy/dt	dx/dt	dz/dt
10%	253.6364	146.9374	66.33708
20%	227.9959	123.2727	37.58529
40%	160.7273	66.51277	26.36364
60%	137.4013	30.91529	25.12994
80%	107.4279	47.54759	39.36174

Mean	Eye Vel (rad/sec)	
eFOV	dy/dt	dx/dt
10%	9.53E-05	-0.000117
20%	0.002169	0.003065
40%	-3.04E-05	-0.000901
60%	-2.76E-05	-0.001488
80%	0.000296	-0.001168

Mean	Head Vel (deg/sec)		
eFOV	dy/dt	dx/dt	dz/dt
10%	-0.018879	-0.055037	-0.021914
20%	0.008011	0.076634	-0.007844
40%	-0.049454	0.067632	0.016902
60%	0.046845	0.053445	-0.0239
80%	-0.033525	-0.016481	0.015897

Variance	Eye Vel (rad/sec)	
eFOV	dy/dt	dx/dt
10%	0.10085	0.088509
20%	0.134598	0.113137
40%	0.173448	0.145359
60%	0.203897	0.18033
80%	0.159999	0.115952

Variance	Head Vel (deg/sec)		
eFOV	dy/dt	dx/dt	dz/dt
10%	417.0756	238.0081	19.06456
20%	300.6788	86.59398	10.35402
40%	81.16959	22.59113	3.463418
60%	44.36911	6.864166	3.644203
80%	43.06749	9.497839	6.471603

Std Dev eFOV	Eye Vel (rad/sec) dy/dt	dx/dt
10%	0.31757	0.297505
20%	0.366876	0.336358
40%	0.416471	0.38126
60%	0.45155	0.424653
80%	0.399998	0.340517

Std Dev eFOV	Head Vel (deg/sec) dy/dt	dx/dt	dz/dt
10%	20.42243	15.42751	4.366298
20%	17.34009	9.305589	3.217766
40%	9.009417	4.753012	1.861026
60%	6.661014	2.619955	1.908979
80%	6.562583	3.081856	2.543935

Performance

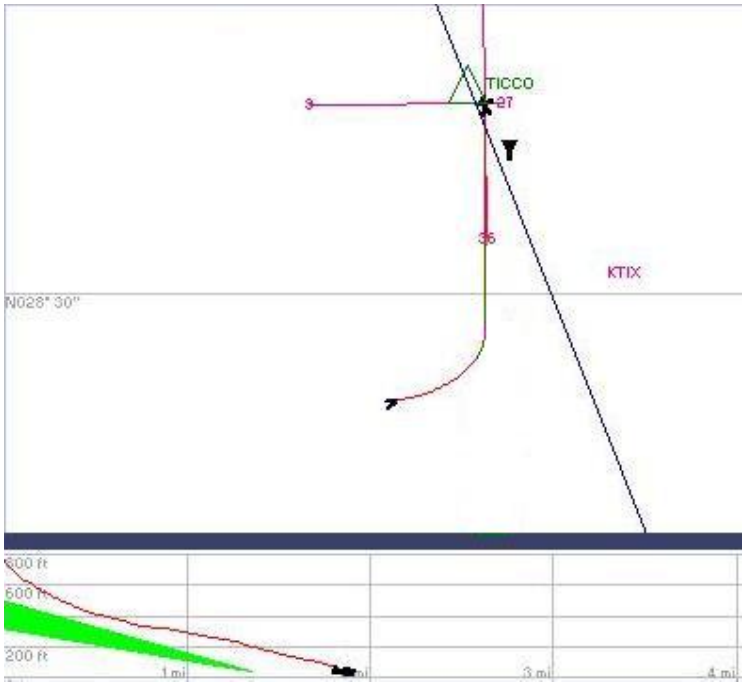

Figure 66: Pilot #5 Performance at 80% eFOV

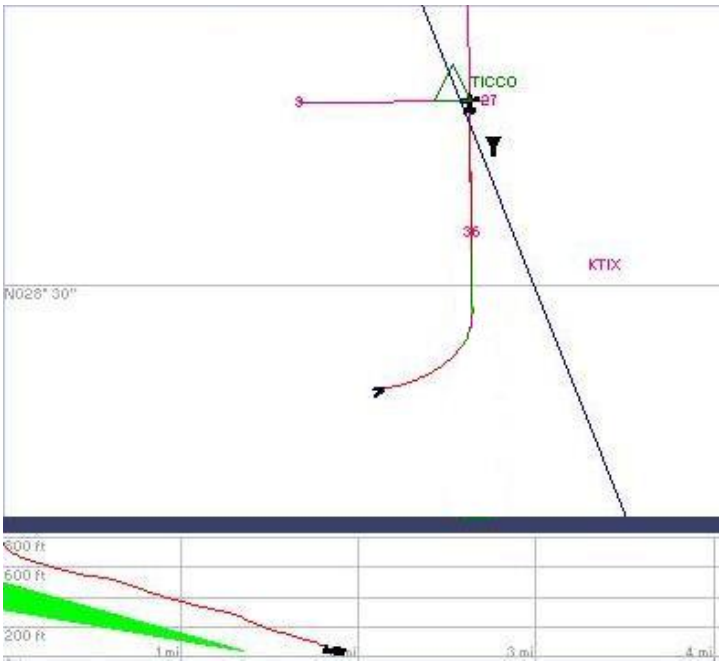

Figure 67: Pilot #5 Performance at 60% eFOV

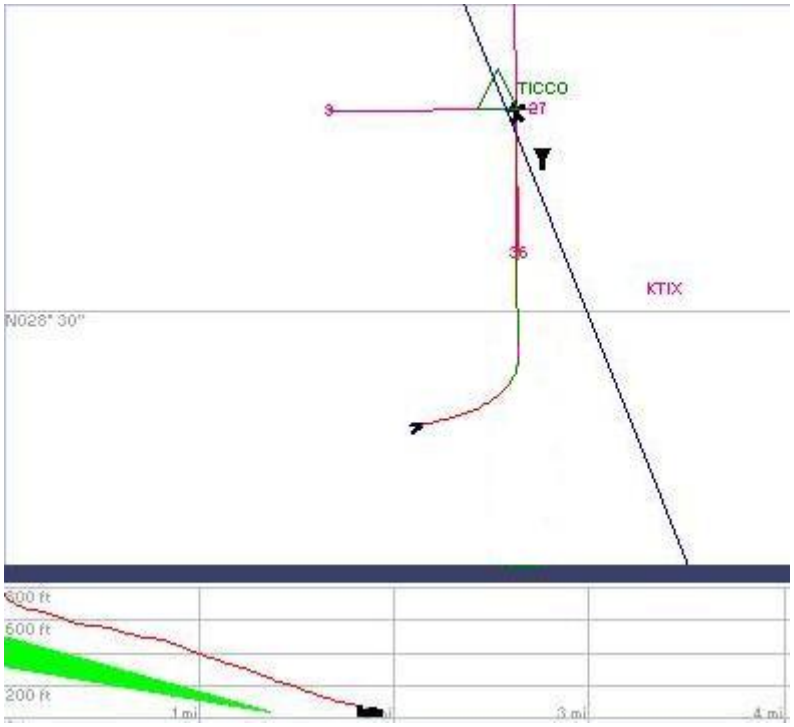

Figure 68: Pilot #5 Performance at 40% eFOV

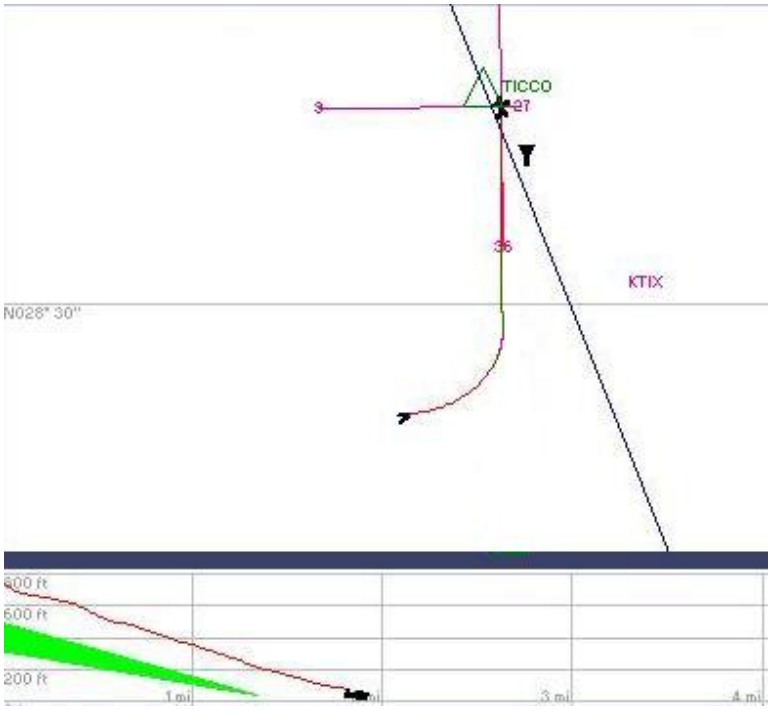

Figure 69: Pilot #5 Performance at 20% eFOV

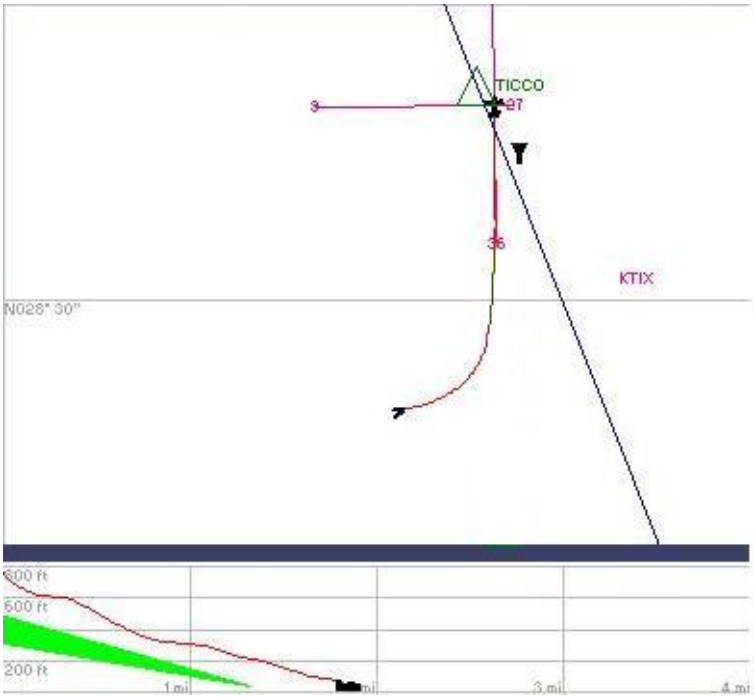

Figure 70: Pilot #5 Performance at 10% eFOV

Pilot #6

Information

Table 33: Pilot #6 DFA

effective FOV	Dwell Frequency per AOI (DFA)						
	OW-L	OW-LC	OW-RC	OW-R	IP	OW-LL	OW-LR
10%	3	7	26	0	32	0	1
20%	3	10	10	0	18	0	0
40%	4	15	4	0	16	0	0
60%	4	4	3	1	4	0	0
80%	2	6	4	0	5	0	0

Table 34: Pilot #6 MDD

effective FOV	Mean Dwell Duration (MDD)						
	OW-L	OW-LC	OW-RC	OW-R	IP	OW-LL	OW-LR
10%	1.4763	1.056086	2.341246		1.642106		0.4329
20%	1.0767	0.85914	9.45387		1.20065		
40%	0.7326	0.97014	24.30068		0.8991		
60%	1.61505	2.3976	30.0255	0.333	0.6993		
80%	0.88245	4.9395	30.7359		1.01232		

Effort

Table 35: Pilot #6 Effort

Max eFOV	Eye Offset (rad)	
	X Gaze	Y Gaze
10%	0.5	0.6771
20%	0.6266	0.5896
40%	0.6094	0.7146
60%	0.7016	0.6208
80%	0.5625	0.75

Max eFOV	Head Offset (deg)		
	Pitch	Yaw	Roll
10%	9.589	-21.563	11.455
20%	8.434	-16.372	15.077
40%	9.169	-25.018	10.295
60%	8.865	-29.834	11.236
80%	14.326	-28.621	12.214

Min	Eye Offset (rad)	
eFOV	X Gaze	Y Gaze
10%	0.3266	0.4875
20%	0.3609	0.2917
40%	0.3391	0.2771
60%	0.375	0.2937
80%	0.3344	0.3458

Min	Head Offset (deg)		
eFOV	Pitch	Yaw	Roll
10%	-37.99	-55.797	0.675
20%	-50.979	-47.005	0.667
40%	-29.175	-45.605	-0.45
60%	-28.074	-43.913	-0.383
80%	-23.886	-40.523	1.105

Range	Eye Offset (rad)	
eFOV	X Gaze	Y Gaze
10%	0.1734	0.1896
20%	0.2657	0.2979
40%	0.2703	0.4375
60%	0.3266	0.3271
80%	0.2281	0.4042

Range	Head Offset (deg)		
eFOV	Pitch	Yaw	Roll
10%	47.579	34.234	10.78
20%	59.413	30.633	14.41
40%	38.344	20.587	10.745
60%	36.939	14.079	11.619
80%	38.212	11.902	11.109

Mean	Eye Offset (rad)	
eFOV	X Gaze	Y Gaze
10%	0.384207	0.53858
20%	0.484563	0.406467
40%	0.449077	0.411803
60%	0.466352	0.332407
80%	0.401964	0.50559

Mean	Head Offset (deg)		
eFOV	Pitch	Yaw	Roll
10%	-2.146302	-37.97228	5.235131
20%	-2.727978	-37.33329	6.129749
40%	-0.791885	-39.66178	6.107485
60%	-3.645455	-38.83103	6.404971
80%	-1.458606	-35.41534	5.419834

Variance	Eye Offset (rad)	
eFOV	X Gaze	Y Gaze
10%	0.000252	0.001425
20%	0.000279	0.001133
40%	0.000919	0.00184
60%	0.000766	0.001237
80%	0.001584	0.003672

Variance	Head Offset (deg)		
eFOV	Pitch	Yaw	Roll
10%	79.07574	53.89324	3.489927
20%	65.47235	24.35586	4.312385
40%	32.96224	18.32358	2.376346
60%	52.00601	10.26136	3.254715
80%	39.40737	6.273679	6.082526

Std Dev	Eye Offset (rad)	
eFOV	X Gaze	Y Gaze
10%	0.015867	0.037751
20%	0.016713	0.033661
40%	0.030308	0.0429
60%	0.027678	0.035176
80%	0.039797	0.060597

Std Dev	Head Offset (deg)		
eFOV	Pitch	Yaw	Roll
10%	8.892454	7.341202	1.868135
20%	8.091499	4.935166	2.076628
40%	5.741275	4.280605	1.54154
60%	7.211519	3.203336	1.804083
80%	6.277529	2.504731	2.466278

Importance

Table 36: Pilot #6 Importance

Max	Eye Vel (rad/sec)	
eFOV	dy/dt	dx/dt
10%	2.708978	3.87988
20%	3.801802	5.613772
40%	4.27027	7.961194
60%	4.724551	5.441441
80%	3.660661	7.047904

Max	Head Vel (deg/sec)		
eFOV	dy/dt	dx/dt	dz/dt
10%	153.0909	89.09091	22.75556
20%	159.1111	53.45455	39.81818
40%	81.27273	32.6015	19.09091
60%	69.12563	25.74874	16.90909
80%	65.09091	20.36364	16

Min	Eye Vel (rad/sec)	
eFOV	dy/dt	dx/dt
10%	-1.823353	-3.504505
20%	-4.504505	-4.567568
40%	-3.612613	-5.882883
60%	-4.318318	-4.318318
80%	-2.720721	-4.802395

Min	Head Vel (deg/sec)		
eFOV	dy/dt	dx/dt	dz/dt
10%	-121.8182	-61.63636	-25.45455
20%	-171.6364	-46.57778	-36.18182
40%	-82.36364	-16.72727	-18.54545
60%	-78.97744	-14.05514	-15.28889
80%	-61.24294	-13.81818	-14.73684

Range	Eye Vel (rad/sec)	
eFOV	dy/dt	dx/dt
10%	4.532332	7.384384
20%	8.306306	10.18134
40%	7.882883	13.84408
60%	9.042869	9.75976
80%	6.381381	11.8503

Range	Head Vel (deg/sec)		
eFOV	dy/dt	dx/dt	dz/dt
10%	274.9091	150.7273	48.2101
20%	330.7475	100.0323	76
40%	163.6364	49.32878	37.63636
60%	148.1031	39.80388	32.19798
80%	126.3338	34.18182	30.73684

Mean	Eye Vel (rad/sec)	
eFOV	dy/dt	dx/dt
10%	0.000708	-0.000367
20%	-0.000231	-0.000344
40%	6.23E-05	0.000131
60%	-0.000491	-0.000296
80%	0.000741	0.000157

Mean	Head Vel (deg/sec)		
eFOV	dy/dt	dx/dt	dz/dt
10%	0.087426	-0.064508	-0.015264
20%	0.023907	-0.007507	-0.019671
40%	0.037502	0.008665	-0.007732
60%	0.045533	0.00243	0.013995
80%	0.055335	-0.052768	0.007688

Variance	Eye Vel (rad/sec)	
eFOV	dy/dt	dx/dt
10%	0.152665	0.813397
20%	0.296264	0.749782
40%	0.550582	1.471696
60%	0.326958	0.812866
80%	0.709183	2.084064

Variance	Head Vel (deg/sec)		
eFOV	dy/dt	dx/dt	dz/dt
10%	342.116	299.2352	15.28681
20%	482.2402	87.94979	25.36771
40%	129.7469	10.03598	6.956584
60%	64.01699	5.989426	5.652627
80%	41.80063	5.815432	4.675086

Std Dev eFOV	Eye Vel (rad/sec) dy/dt	dx/dt
10%	0.390724	0.901885
20%	0.544301	0.8659
40%	0.742012	1.213135
60%	0.571802	0.901591
80%	0.84213	1.443629

Std Dev eFOV	Head Vel (deg/sec) dy/dt	dx/dt	dz/dt
10%	18.49638	17.29842	3.909835
20%	21.95997	9.378155	5.036637
40%	11.39065	3.167962	2.637534
60%	8.001062	2.44733	2.377525
80%	6.465341	2.411521	2.162195

Performance

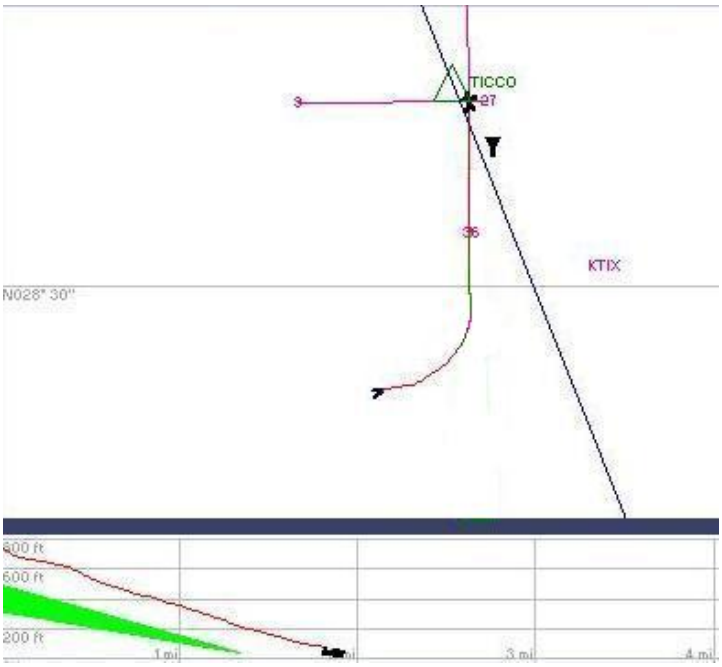

Figure 71: Pilot #6 Performance at 80% eFOV

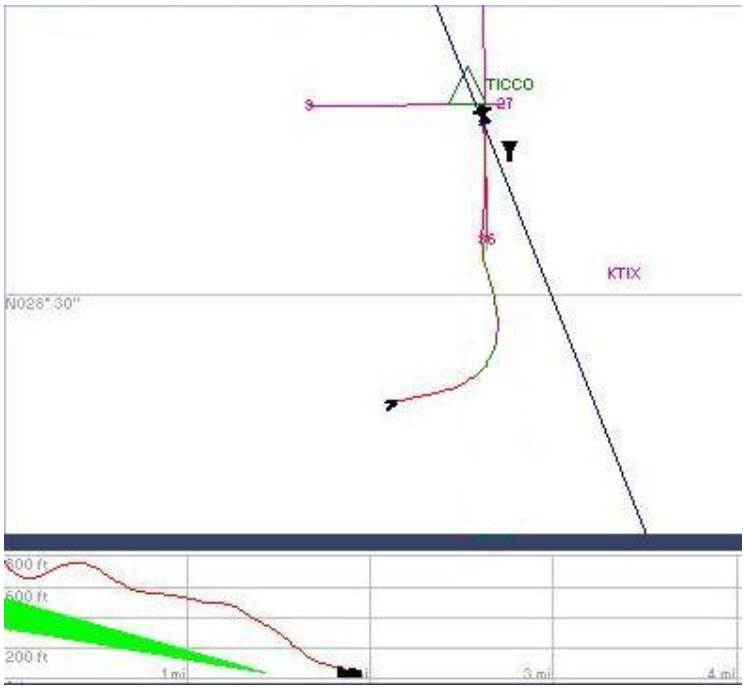

Figure 72: Pilot #6 Performance at 60% eFOV

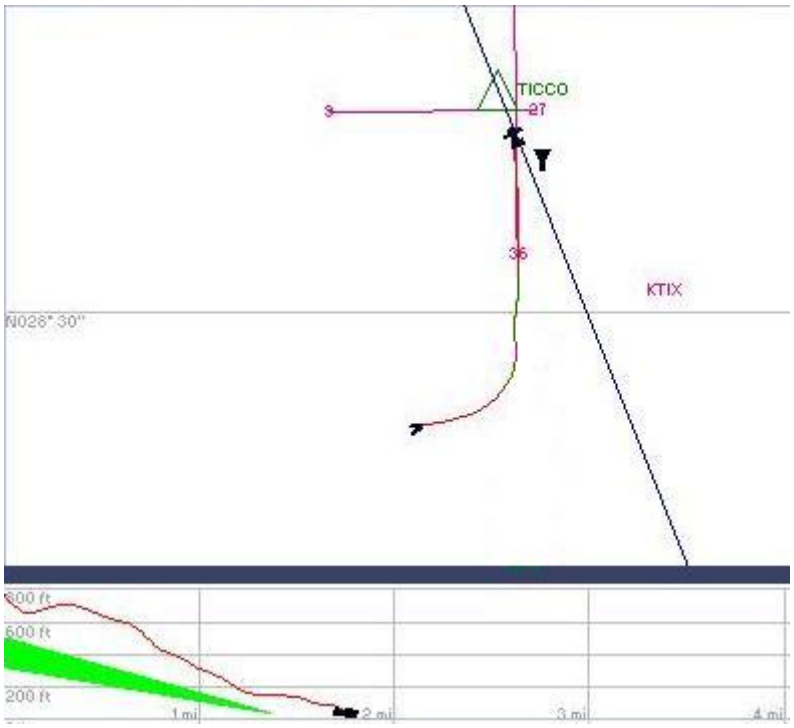

Figure 73: Pilot #6 Performance at 40% eFOV

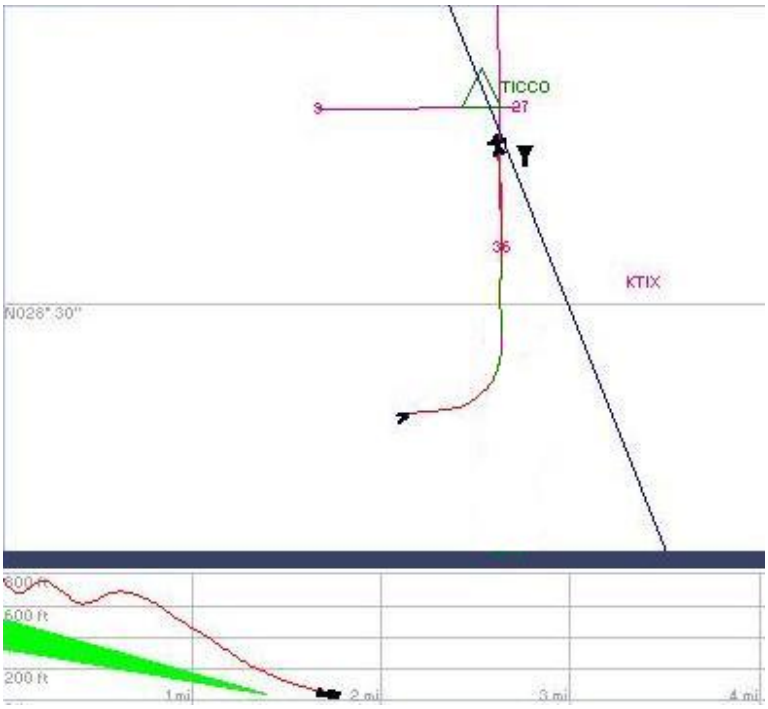

Figure 74: Pilot #6 Performance at 20% eFOV

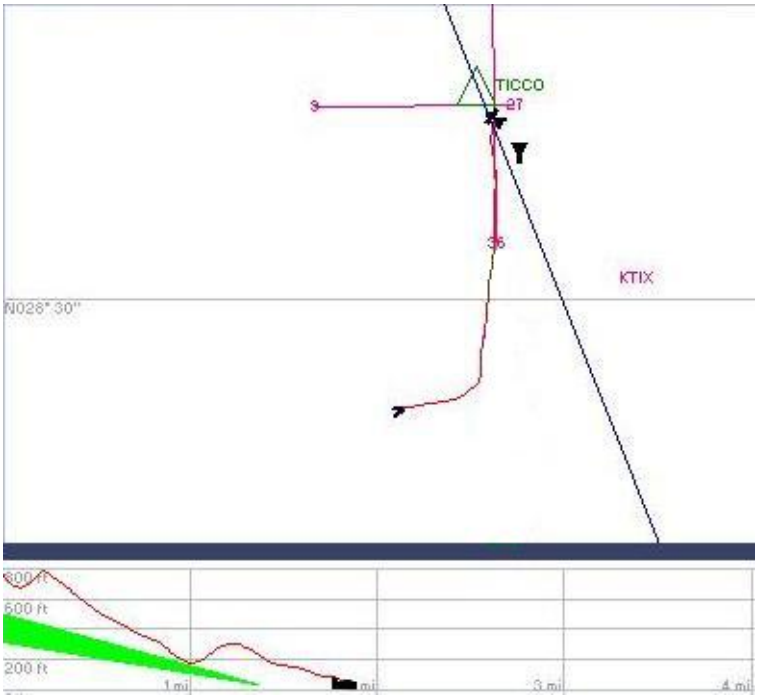

Figure 75: Pilot #6 Performance at 10% eFOV

Pilot #7

Information

Table 37: Pilot #7 DFA

effective FOV	Dwell Frequency per AOI (DFA)						
	OW-L	OW-LC	OW-RC	OW-R	IP	OW-LL	OW-LR
10%	5	20	13	0	23	0	0
20%	4	26	1	0	21	0	0
40%	3	20	4	0	15	0	0
60%	0	26	11	0	21	0	0
80%	1	9	13	0	12	0	0

Table 38: Pilot #7 MDD

effective FOV	Mean Dwell Duration (MDD)						
	OW-L	OW-LC	OW-RC	OW-R	IP	OW-LL	OW-LR
10%	1.43856	2.3976	2.589715		1.08587		
20%	0.857475	3.935804	0.5328		0.797614		
40%	0.888	3.534795	3.538125		0.87468		
60%		2.582031	0.653891		1.056086		
80%	1.2321	1.554	5.233223		1.3209		

Effort

Table 39: Pilot #7 Effort

Max eFOV	Eye Offset (rad)	
	X Gaze	Y Gaze
10%	0.6172	0.6187
20%	0.5578	0.7292
40%	0.5781	0.6396
60%	0.6313	0.6437
80%	0.7797	0.7563

Max eFOV	Head Offset (deg)		
	Pitch	Yaw	Roll
10%	56.535	19.113	28.752
20%	6.285	-4.234	14.909
40%	6.615	-13.207	17.187
60%	23.838	0	12.373
80%	12.362	-9.159	4.766

Min	Eye Offset (rad)	
eFOV	X Gaze	Y Gaze
10%	0.4234	0.4188
20%	0.2609	0.4417
40%	0.2594	0.2875
60%	0.2797	0.2937
80%	0.325	0.4271

Min	Head Offset (deg)		
eFOV	Pitch	Yaw	Roll
10%	-63.144	-42.667	3.4
20%	-36.449	-23.035	2.34
40%	-37.692	-40.641	3.063
60%	-0.194	-18.116	0
80%	-23.633	-24.776	-3.693

Range	Eye Offset (rad)	
eFOV	X Gaze	Y Gaze
10%	0.1938	0.1999
20%	0.2969	0.2875
40%	0.3187	0.3521
60%	0.3516	0.35
80%	0.4547	0.3292

Range	Head Offset (deg)		
eFOV	Pitch	Yaw	Roll
10%	119.679	61.78	25.352
20%	42.734	18.801	12.569
40%	44.307	27.434	14.124
60%	24.032	18.116	12.373
80%	35.995	15.617	8.459

Mean	Eye Offset (rad)	
eFOV	X Gaze	Y Gaze
10%	0.47625	0.474399
20%	0.362598	0.505155
40%	0.339313	0.433909
60%	0.36198	0.361516
80%	0.620488	0.584106

Mean	Head Offset (deg)		
eFOV	Pitch	Yaw	Roll
10%	-3.28287	-25.09064	9.655915
20%	-3.558053	-14.24126	7.163596
40%	-3.842217	-28.92667	9.154678
60%	8.577764	-14.99684	9.406065
80%	0.932495	-19.74642	1.550897

Variance	Eye Offset (rad)	
eFOV	X Gaze	Y Gaze
10%	0.000723	0.001676
20%	0.001066	0.001761
40%	0.001466	0.003166
60%	0.002773	0.00273
80%	0.005196	0.004368

Variance	Head Offset (deg)		
eFOV	Pitch	Yaw	Roll
10%	111.0147	53.27459	9.072112
20%	102.5834	13.16517	3.521904
40%	43.49293	28.8159	9.430641
60%	10.41772	7.845243	2.007743
80%	26.24074	9.374411	1.518903

Std Dev	Eye Offset (rad)	
eFOV	X Gaze	Y Gaze
10%	0.026896	0.040938
20%	0.032653	0.04196
40%	0.038283	0.056266
60%	0.05266	0.052245
80%	0.072082	0.066091

Std Dev	Head Offset (deg)		
eFOV	Pitch	Yaw	Roll
10%	10.53635	7.298944	3.011995
20%	10.12834	3.628384	1.876674
40%	6.594917	5.368044	3.070935
60%	3.22765	2.800936	1.416948
80%	5.122572	3.061766	1.232438

Importance

Table 40: Pilot #7 Importance

Max	Eye Vel (rad/sec)	
eFOV	dy/dt	dx/dt
10%	2.954955	2.627628
20%	2.90991	4.318318
40%	5.303303	4.816817
60%	2.204204	5.441441
80%	4.244565	3.776435

Max	Head Vel (deg/sec)		
eFOV	dy/dt	dx/dt	dz/dt
10%	355.697	123.4545	135.2727
20%	105.2537	73.83871	23.90592
40%	84.36364	60.29379	20.13483
60%	52.24812	19.52525	13.01683
80%	40.6776	26.03366	17.84781

Min	Eye Vel (rad/sec)	
eFOV	dy/dt	dx/dt
10%	-1.778443	-2
20%	-2.990881	-2.734375
40%	-5.444444	-5.069069
60%	-2.57958	-2.627628
80%	-4.185185	-4.695364

Min	Head Vel (deg/sec)		
eFOV	dy/dt	dx/dt	dz/dt
10%	-543.6364	-120.1818	-70.51256
20%	-104.7102	-54.96095	-21.8451
40%	-77.8427	-56.36364	-21.57303
60%	-27.1184	-19.41276	-18.67839
80%	-66.75031	-21.51393	-21.51393

Range	Eye Vel (rad/sec)	
eFOV	dy/dt	dx/dt
10%	4.733398	4.627628
20%	5.900791	7.052693
40%	10.74775	9.885886
60%	4.783784	8.069069
80%	8.42975	8.471799

Range	Head Vel (deg/sec)		
eFOV	dy/dt	dx/dt	dz/dt
10%	899.3333	243.6364	205.7853
20%	209.9638	128.7997	45.75102
40%	162.2063	116.6574	41.70787
60%	79.36651	38.93801	31.69522
80%	107.4279	47.54759	39.36174

Mean	Eye Vel (rad/sec)	
eFOV	dy/dt	dx/dt
10%	-0.000466	0.001059
20%	4.38E-05	0.000234
40%	0.001163	-0.001519
60%	8.44E-05	-0.000421
80%	0.000296	-0.001168

Mean	Head Vel (deg/sec)		
eFOV	dy/dt	dx/dt	dz/dt
10%	0.491705	0.093633	-0.120029
20%	0.086927	-0.080081	-0.007426
40%	0.011425	-0.030548	-0.030634
60%	0.000148	-0.059083	-0.013635
80%	-0.033525	-0.016481	0.015897

Variance	Eye Vel (rad/sec)	
eFOV	dy/dt	dx/dt
10%	0.069594	0.12485
20%	0.063098	0.104103
40%	0.221993	0.341023
60%	0.059892	0.118323
80%	0.159999	0.115952

Variance	Head Vel (deg/sec)		
eFOV	dy/dt	dx/dt	dz/dt
10%	729.8718	402.2439	54.24695
20%	127.8182	48.85288	7.541642
40%	76.84384	67.18699	9.801334
60%	10.13326	3.695971	2.041709
80%	43.06749	9.497839	6.471603

Std Dev	Eye Vel (rad/sec)	
eFOV	dy/dt	dx/dt
10%	0.263806	0.353341
20%	0.251194	0.32265
40%	0.471162	0.583972
60%	0.244729	0.343981
80%	0.399998	0.340517

Std Dev	Head Vel (deg/sec)		
eFOV	dy/dt	dx/dt	dz/dt
10%	27.01614	20.05602	7.365253
20%	11.30567	6.989484	2.746205
40%	8.766062	8.196767	3.130708
60%	3.183279	1.922491	1.428884
80%	6.562583	3.081856	2.543935

Performance

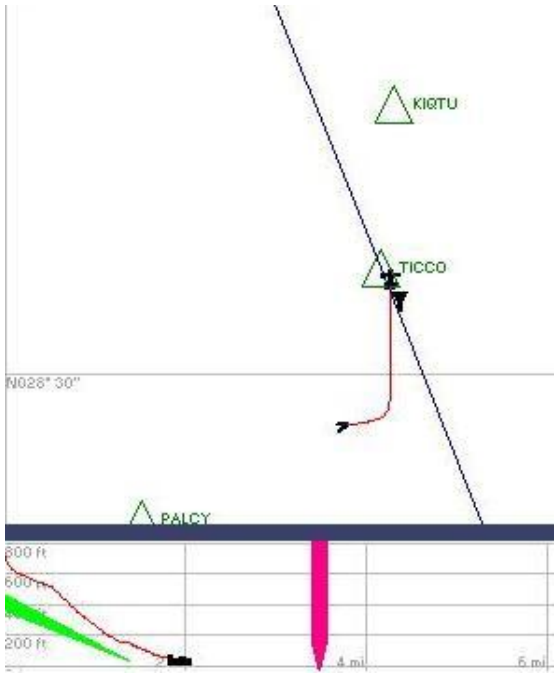

Figure 76: Pilot #7 Performance at 80% eFOV

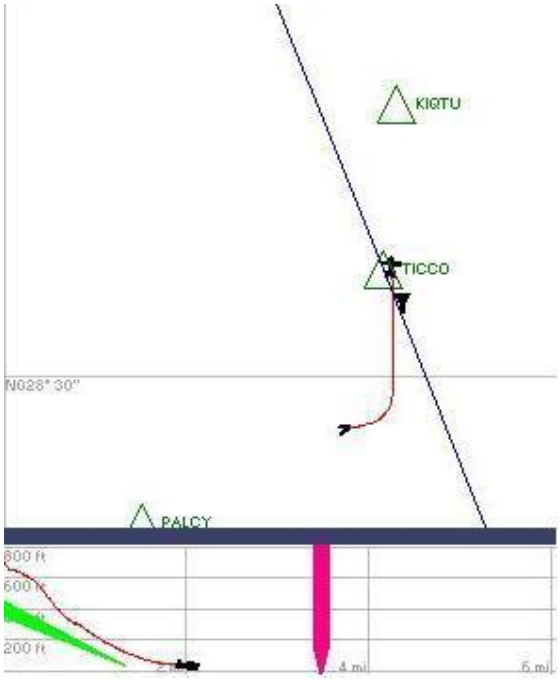

Figure 77: Pilot #7 Performance at 60% eFOV

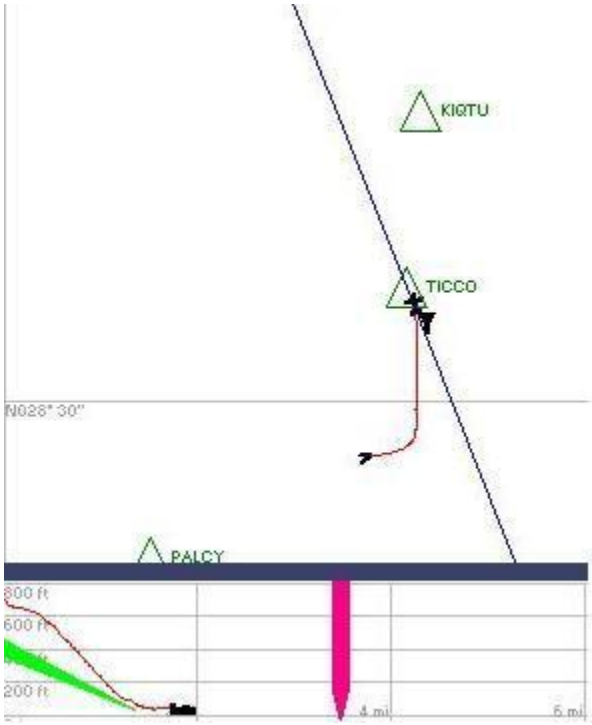

Figure 78: Pilot #7 Performance at 40% eFOV

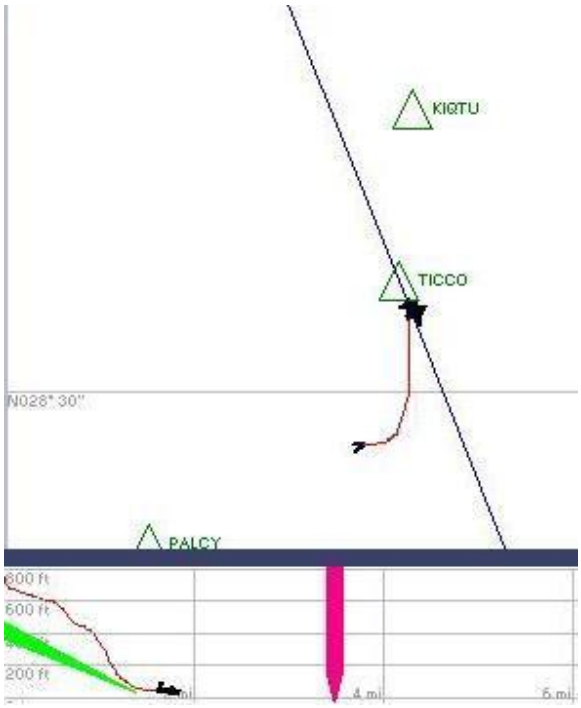

Figure 79: Pilot #7 Performance at 20% eFOV

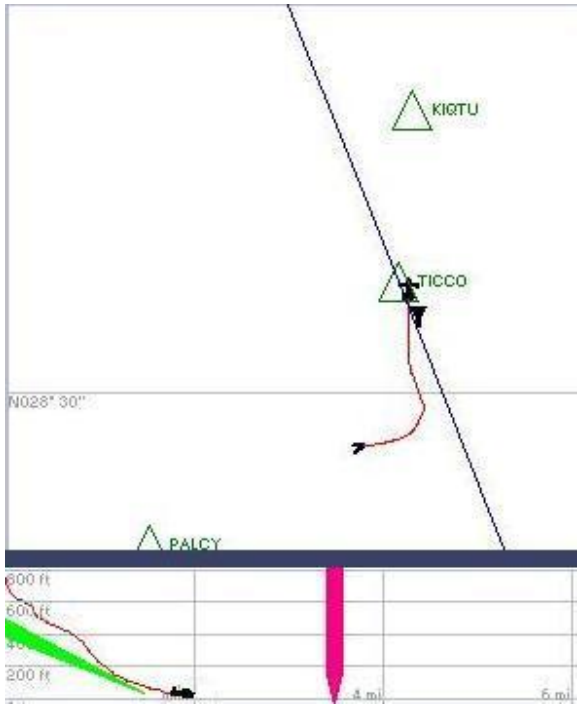

Figure 80: Pilot #7 Performance at 10% eFOV

LIST OF REFERENCES

Agrawal, B. N. (1986). *Design of Geosynchronous Spacecraft*. Prentice-Hall Inc. Engelwood Cliffs, NJ. P. 106-112.

Ames, B. (2005). Streamlined Databases Drive Military Simulation, *Military & Aerospace Electronics*, November.

Arditi, A., (1986). Binocular Vision, in K.R. Boff, L. Kaufman and J.P. Thomas (Eds.), *Handbook of Perception and Human Performance*, Wiley, New York, Ch. 23.

Arrington, K.F., Geri, G.A. (2000). Conjugate-optical retroreflector display system: Optical principles and perceptual issues, *Journal of the Society for Information Display (JSID)*, *8*(2), 123-128.

Arthur, K. (2000). *Effects of Field of View on Performance with Head-Mounted Displays*, Ph.D. Dissertation, Department of Computer Science, University of North Carolina at Chapel Hill

Azuma, R. (1997, Aug). A Survey of Augmented Reality in Presence: *Teleoperators and Virtual Environments*, *6* (4), 355-385.

Azuma, R., Baillot, Y., Behringer, R., Feiner, S., Julier, S., MacIntyre, B., (2001, Nov/Dec). Recent Advances in Augmented Reality, *IEEE Computer Graphics and Applications*, *21* (6), 34-47

Barfield, W. & Weghorst, S. (1993). The Sense of Presence Within virtual environments: a conceptual framework. In *Human Computer Interaction: Software and Hardware Interfaces*. UK:Elsevier Science Publishers.

Barfield, W., Hendrix, C., Bjorneseth, O., Kaczmarek, K. A., & Lotens, W. (1995). Comparison of Human Sensory Capabilities with Technical Specifications of Virtual Environment Equipment. *Presence*, *4*(4), 329-356.

Barfield, W., Zeltzer, D., Sheridan, T.B. and Slater, M. (1995). Presence and performance within virtual environments. In: Barfield, W. and Furness III, T.A. (eds), *Virtual Environments and Advanced Interface Design*, (pp 473-513). Oxford: Oxford University Press.

Bellenkes, A. H., Wickens, C. D., & Kramer, A. F. (1997). Visual scanning and pilot expertise: The role of attentional flexibility and mental model development. *Aviation, Space, and Environmental Medicine*, *68*(7), 569-579.

Biocca, F., & Rolland, J.P. (2004, August). US Patent No. 6,774,869. Washington, DC: U.S. Patent and Trademark Office

Biocca, F., Harms, C. & Burgoon, J.K. (2003). Towards a More Robust Theory and Measure of Social Presence: Review and Suggested Criteria. *Presence*, *12*(5), 456-480

Bristow Academy - Tuition and Fees. (2007). Retrieved November 20, 2007, from http://www.heli.com/prospective-student/2-tuition-and-fees-FAA.php#5

Boer, E.R., Rakauskas, M.E., Ward, N.J., Goodrich, M.A. (2005). Steering Entropy Revisited. *Presented at the 3rd International Symposium on Human Factors in Driver Assessment, Training, and Vehicle Design*. Rockport, Maine (June 27-30)

Bridgeman, B. (1992). Conscious vs unconscious processes: The case of vision. *Theory and Psychology*, *2*(1), 73-88.

Cakmakci, O. and Rolland, J.P. (2006). Head-worn display: A review. Invited paper. IEEE/OSA *Journal of Display Technology*, *2*(3), 199-216.

Cakmakci, O. and Rolland, J.P. (2007), Design and Fabrication of a Dual-Element Off-Axis Near-Eye Optical Magnifier, *Optics Letters, 11* (32), 1363-1365

Chan, H.S., & Courtney, A. J. (1993). Effects of cognitive foveal load ona peripheral single-target detection task. *Perceptual and Motor Skill*, 77, 515-533.

Covelli, J., Martins, R., Rolland, J.P. (2005). Using Mixed Reality for Simulator Situation-Awareness, from *I/ITSEC 2005 Proceedings*, No. 2091.

Darken, R., & Lennerton, M. (2003). A Chromakey Augmented Virtual Environment for Deployable Training, *I/ITSEC 2003 Conference Proceedings*

Department of the Army (2000) *Aircrew Training Manual* Utility Helicopter, UH-60/EH-60. (TC 1-237)

Display Systems. (2003). Retrieved December 3, 2005, from http://www.es.com/resources/displays_brochure.pdf

Dolezal, H. (1982). The Restricted Field of View: A Neglected Factor in Adaptation Research, *Living in a world transformed: Perceptual and performatory adaptation to visual distortion* (pp. 57-79). New York: Academic Press

Draper, J. V., Kaber, D. B., & Usher, J. M. (1998). Telepresence. *Human Factors*, *40*(3), 354–375.

Endsley, M. R. (1988). Design and evaluation for situation awareness enhancement. In *Proceedings of the Human Factors Society 32nd Annual Meeting* (pp. 97–101). Santa Monica, CA: Human Factors Society.

Endsley, M. R. (1990a). Predictive utility of an objective measure of situation awareness. In *Proceedings of the Human Factors Society 34th Annual Meeting* (pp. 41–45). Santa Monica, CA: Human Factors and Ergonomics Society.

Endsley, M. R. (1995). Toward a theory of situation awareness in dynamic systems. *Human Factors*, *37*, 32–64.

Endsley, M. R. (1995b). Measurement of situation awareness in dynamic systems. *Human Factors*, *37*, 65–84.

Endsley, M. R. (2000). Theoretical underpinnings of situation awareness: A critical review. In M. R. Endsley & D. J. Garland (Eds.), *Situation awareness analysis and measurement*. (pp. 10-25) Mahwah, NJ: Lawrence Erlbaum Association.

Endsley, M. R., & Bolstad, C. A. (1994). Individual differences in pilot situation awareness. *International Journal of Aviation Psychology*, *4*, 241–264.

Evans, M.E., Wei, C., Spyridakis, J.H. (2004). Using Statistical Power Analysis to Tune-Up a Research Experiment: A Case Study. From *Professional Communication Conference Proceedings*, p. 14-18.

Fidopiastis, C.M., Fuhrman, C., Meyer, C., & Rolland, J.P., Methodology for iterative evaluation of prototype head-mounted displays in virtual environments: visual metrics. *Presence: SI Immersive Projection Technology*, *14*(5), 550-562 (2005).

Fischer, R. E., (1994, July/Aug). Optics for head-mounted displays, *Information Display*, *10*, 7-8.

Fisher, R. W., (1996). Head-mounted projection display system featuring beam splitter and method of making same. US patent 5,572,229, November 5, 1996.

Flach, J. M., & Holden, J. G. (1998). The reality of experience: Gibson's way. Presence: *Teleoperators and Virtual Environments*, *7*(1), 90–95.

Flexman, R. P. & Stark, E.A. (1987). Training simulators. In G. Salvendy (Ed.), *Handbook of Human Factors* (pp 1012-1037). New York: John Wiley & Sons.

Folk, c. L., Remington, R. W., & Jonston, J. C. (1992). Involuntary covert orienting is contingent on attentional control settings. *Journal of Experimental Psychology: Human Perception and Performance*, *18*, 1030-1044.

Fowlkes, J. E., Dwyer, D. J., Oser, R. L., & Salas, E. (1998). Event-based approach to training (EBAT), *The International Journal of Aviation Psychology*, *8*, 209-221.

Fowlkes, J. E., Lane, N. E., Salas, E., Franz, T., & Oser, R. L. (1994). Improving the measurement of team performance: The TARGETs methedology, *Military Psychology*, *4*, 63-74.

Fox, J., Fadden, S., Konrad, C., Marsh, R., Merwin, D., Sochacki, J., Sohn, Y. W., Tham, M., Wickens, C. D., Lintern, G., Kramer, A., & Doane, S. (1995). Modeling pilot scanning behavior: Strategies and expertise. In R. Jensen & L. A. Rakovan (Eds.), *Proceedings of the 8th International Symposium on Aviation Psychology* (Vol. 2; pp. 845-862). Columbus, OH: Dept. of Aerospace Engineering, Applied Mechanics, and Aviation, Ohio State University.

Foyle, D.C., Kaiser, M.K., Johnson, W.W. (1992). Visual Cues in Low-level Flight: Implications for Pilotage, Training, Simulation, and Enhanced/Synthetic Vision Systems, *48th Annual Forum Proceedings of the American Helicopter*

French, M. (2003). U.S. Navy to use more Simulation Training, *Federal Computer Week*, 6 November.

Gallimore, J.J., Patterson, F.R., Brannon, N.G., Nalepka, J.P. (2000). The opto-kinetic cervical refelx during formation flight. *Aviation, Space and Environmental Medicine*. Aug 2000, *71*(8), p 812-821.

Gibson, J. J. (1979). *The ecological approach to visual perception*. Boston: Houghton Mifflin.

Girolamo, H., Rash, C., Gilroy, T., (1997). *Advanced Information Displays for the 21st-Century Warrior*, Aircrew Health and Performance Division, U.S. Army Aeromedical Research Laboratory, Fort Rucker, AL.

Guest, M., Rolland, J.P. (1999). *Search strategies when masses are missed in mammography*, Technical Report TR99-007, University of Central Florida, Orlando, FL.

Hamza-Lup, F. G., & Rolland, J. P. (2004a, March). Adaptive scene synchronization for virtual and mixed reality environments. *Proceedings of IEEE Virtual Reality* 2004 (pp. 99–106). Chicago, IL.

Hamza-Lup, F. G., & Rolland, J. P. (2004b). Scene synchronization for real-time interaction in distributed mixed reality and virtual reality environments. *Presence: Teleoperators and Virtual Environments*, *13*(3), 315–327.

Hamza-Lup, F. G., Davis, L., & Rolland, J. P. (2002, September). The ARC display: An augmented reality visualization center. *International Symposium on Mixed and Augmented Reality (ISMAR)*, Darmstadt, Germany.

Hart, S. G.,& Staveland, L. E. (1988). Development of NASA–TLX (Task Load Index): Results of empirical and theoretical research. In N. Meshkati (Ed.), *Human mental workload* (pp. 139–183). Amsterdam: North-Holland.

Harvey, J. F. et al., (1982, Sep). Pilot helmet mounted CIG display with eye coupled area of interest. US patent 4,348,186, September 7, 1982.

Hays, R. T., Jacobs, J. W., Prince, C., & Salas, E. (1992) Flight simulator training effectiveness: A meta-analysis. *Military Psychology*, *4*, 63–74.

Helmet Mounted Displays: Design Issues for Rotary-Wing Aircraft, *U.S. Army Research Lab Handbook*, Vol. 4.

Henderson, J. M., & Hollingworth, A. (1999). The role of fixation position in detecting scene changes across saccades. *Psychological Science*, *10*(5), 438-443.

Henderson, J. M., & Hollingworth, A. (2003). Global transsaccadic change blindness during scene perception. *Psychological Science*, *14*(5), 493-497.

How to determine sample size (n.d.). Retrieved February 5, 2007 from http://www.isixsigma.com/library/content/c000709a.asp

Hua, H., Ha, Y. & Rolland, J.P., (2003). Design of an ultra-light and compact projection lens, *Applied Optics 42*(1), 97-107.

Hua, H., Rolland, J., (2000). Compact lens assembly for the teleportal augmented reality system, U.S. patent 6,731,434, May 4, 2000

Hyvärinen, L. (2007). *Transdisciplinary assessment of vision*. Retrieved September 7, 2007, from http://www.lea-test.fi/en/assessme/trans/index.html

International Society for Presence Research. (2000). The Concept of Presence: Explication Statement. Retrieved September 5, 2007 from http://ispr.info/

Jain, A. K. (1989). *Fundamentals of Digital Image Processing*, Prentice Hall, ISBN 0133361659

Johansson, R., Holsanova, J., & Holqvist, K. (2005). What Do Eye Movements Reveal About Mental Imagery? Evidence From Visual And Verbal Elicitations, In Bara, B. G., Barsalou, L., Bucciarelli, M. (Eds.), *Proceedings of the 27th Annual Conference of the Cognitive Science Society*, pp. 1054-1059. Mahwah, NJ: Erlbaum

Jones, D. G., & Endsley, M. R. (2004). Use of Real-Time Probes for Measuring Situation Awareness, *International Journal of Aviation Psychology*, *14* (4), 343-367

Keller, M., Schnell, T., Lemos, K., Glaab, L., Parrish, R. (2003), Pilot Performance as a Function of Display Resolution and Field of View in Simulated Flight Using Synthetic Vision Systems, In *Proceedings of 22nd Digital Avionics Systems Conference*, Dawn of the 2nd Century / Racing to Transform the Legacy, The Crowne Plaza, Indianapolis, Indiana, 12-16 October 2003.

Kennedy, R. S., Lane, N.E., Berbaum, K.S., & Lilienthal, M. G. (1993). Simulator sickness questionnaire: An enhanced method for quantifying simulator sickness. The *International Journal of Aviation Psychology*, *3*(3), 203-220.

Kolasinski, E.M. (1995). *Simulator sickness in virtual environments (ARI Technical Report 1027)*. Alexandria, VA: U.S. Army Research Institute for the Behavioral and Social Sciences

Kosslyn, S. M. (1994). *Image and brain*. Cambridge, Mass.: The MIT Press.

Land, M. F. (1995). The functions of eye movements in animals remote from man. In J. M. Findlay & R. Walker (Eds.), *Eye movement research: Mechanisms, processes and applications. Studies in visual information processing*, 6 (pp. 63-76). New York, NY: Elsevier Science.

Leek, E. C., Reppa, I., & Tipper, S. P. (2003). Inhibition of return for objects and locations in static displays. *Perception & Psychophysics*, *65*(3), 388-395.

Levi, D. M., Klein, S. A., & Aitsebaomo, A. P. (1985). Vernier acuity, crowding and cortical magnification. *Vision Research*, *25*(7), 963-977.

Line Oriented Flight Traiing (LOFT) (2005). *Eastern Caribbean Civil Aviation Authority (ECCAA) Document*, Operations Advisory Circular (OAC-015, rev 1 dtd 11/05/05).

Lowry, R. (2007). Orthogonal Latin Square Designs with n = j2, Retrieved August 3, 2006, from http://faculty.vassar.edu/lowry/lsqtext.html.

Marshall, H., Ragusa, C., Grayson, S., Green, G. (2004). Development of a Next Generation Embedded Simulation Engine for FCS, *I/ITSEC 2004 paper No. 1525*.

Martin-Emerson, R., & Kramer, A. F. (1995). Capture of attentioon by visual onsets. In *Proceedings of the Human Factors and Ergonomics Societey 39th annual meeting* (pp. 1385-1389). Santa Monica, CA: Human Factors and Ergonomics Society.

Martins, R. & Rolland, J.P., (2003, Sep). Diffraction of Phase Conjugate Material in a New HMD Architecture, SPIE AeroSense: Helmet and Head-Mounted Displays VIII: Technologies and Applications, *SPIE Proceedings* Vol. 5186, pp. 277-283, Editors: C. E. Rash and C. E. Reese.

Martins, R., Shaoulov, V., Ha, Y. & Rolland, J.P. (2004, Sep). Projection-based head-mounted displays for wearable computers, SPIE AeroSense: Helmet- and Head-Mounted Displays IX: Technologies and Applications, *SPIE Proceedings* Vol. 5442, pp. 104-110, Editors: C. E. Rash and C. E. Reese.

Martins, R., Shaoulov, V., Ha, Y. & Rolland, J.P. (2007), A mobile head-worn projection display, *Optics Express, 15*, 14530-14538.

Matin, E. (1974). Saccadic suppression: A review and an analysis. *Psychological Bulletin*, *81*(12), 899-917.

McConkie, G. W., & Rayner, K. (1975). The span of the effective stimulus during a fixation in reading. *Perception and Psychophysics*, *17*(6), 578-586.

Meehan, M. (2000). An objective surrogate for presence: Physiological response. *3rd Int. Wkshp. on Presence*. Delft, The Netherlands.

Milgram, P. & Kishino, F., (1994). A Taxonomy of Mixed Reality Visual Displays, *IEICE Trans. Information Systems*, vol. E77-D, no. 12, pp. 1321-1329

Montgomery, D.C. (2004). *Design and Analysis of Experiments*, John Wiley & Sons, ISBN 047148735x

Nikolic, M. I., Orr, J.m M., & Sarter, N. B. (2004). Why Pilots Miss the Green Box: How display context undermines attention capture, *International Journal of Aviation Psychology*, *14* (1), 39-52

Pashler, H., Johnston, J. C., & Ruthruff, E. (2001). Attention and performance. *Annual Review of Psychology*, *52*, 629-651.

Patterson, R., Winterbottom, M. & Pierce, B.J. Perceptual Issues with the use of head-mounted displays (review paper). *Human Factors*, in press.

Pausch, R., Crea, T., & Conway, M. (1992). A literature survey for virtual environments: Military flight simulator visual systems and simulator sickness. *Presence*, *1*(3), 344-363

Poole, A., Ball, L. J., & Phillips, P. (2004). In search of salience: A response time and eye movement analysis of bookmark recognition. In S. Fincher, P. Markopolous, D. Moore, & R. Ruddle (Eds.), People and Computers XVIII-Design for Life: *Proceedings of HCI* 2004. London: Springer-Verlag Ltd.

Poulton, E. C. (1973). Unwanted range effects from using within-subject experimental designs. Psychological Bulletin, *80*, 113-121.

Prinzo, O. V. (2003). Pilot's Visual Acquisition of Traffic: Operational Communication From an In-Flight Evaluation of a Cockpit Display of Traffic Information, *International Journal of Aviation Psychology*, *13* (1), 211-231

Proctor, M. D., Panko, M., & Donovan, S. J. (2004). Considerations for Training Team Situation Awareness and Task Performace Through PC-Gamer Simulated Multiship Helicopter Operations, *International Journal of Aviation Psychology*, *14* (2), 191-205

Proctor, M., & Lipinski, M. J. (2000). Technical performance measures and distributed-simulation training systems, *Acquisition Review Quarterly*, *7*, 19-32.

Prothero, J. D., Parker, D. E., Furness III, T. A., & Wells, M. J. (1995). Towards a robust, quantitative measure for presence. In *Proceedings of the Conference on Experimental Analysis and Measurement of Situation Awareness*, 359-366.

Prothero, J. D., Parker, D. E., Furness III, T. A., & Wells, M. J. (1995). Towards a robust, quantitative measure for presence. In *Proceedings of the Conference on Experimental Analysis and Measurement of Situation Awareness*, 359-366. Available: http://www.hitl.washington.edu/publications/p-95-8.

Reber, A. (1995). *Implicit Learning and Tacit Knowledge: An Essay on the Cognitive Unconscious*. New York, Oxford University Press.

Richardson, D. C., & Kirkham, N. Z. (2004). Multi-modal events and moving locations: evidence for dynamic spatial indexing in adults and six month olds. *Journal of Experiemental Psychology*: General, in press.

Richardson, D. C., & Spivey, M. J. (2004). *Eye-Tracking: Characteristics and Methods*, In Wnek. G. & Bowlin, G. (Eds.) Encyclopedia of Biomaterials and BiomedicalEngineering. Marcel Dekker, Inc

Rinalducci, E. J., & Rose, P. N. (1986). The effects of foveal load on peripheral visual sensitivity. *Proceedings of the Human Factors Society 30th annual meeting* (pp. 608-610). Santa Monica, CA: Human Factors Society.

Rinalducci, E. J., Lassiter, D. L., MacArthur, M., Piersal, J., & Mitchell, L. K. (1989). Further experiments on the effects of foveal load on peripheral vision. *Proceedings of the Human Factors Society 33rd annual meeting* (pp. 1450-1453). Santa Monica, CA: Human Factors Society.

Rodriquez, A.M., Foglin, M., Rolland, J.P. (2003). Embedded training display technology for the Army's future combat vehicles, In *Proceedings of the Image Conference Society*, 228-233.

Rolland, J. P., Ha, Y., & Fidopiastis, C. (2004). Albertian errors in head-mounted displays: Choice of eyepoints location for a near or far field tasks visualization, *JOSA* A, *21*(6), 901–912

Rolland, J. P.; Biocca, F., Hamza-Lup, F., Ha, Y.., & Martins, R. (2005). Development of Head-Mounted Projection Displays for Distributed, Collaborative, Augmented Reality Applications, *Presence: Teleoperators & Virtual Environments*, Oct2005, *14* (5), 528-549

Rolland, J.P., Davis, L. D., & Baillot, Y., (2001). A survey of tracking technology for virtual environments, in *Fundamentals of Wearable Computers and Augmented Reality*. (Chapter 3) Ed. Barfield and Caudell (Mahwah, NJ), 67-112.

Rolland, J.P., Davis, L. D., Ha., Y., Meyer, C., Shaoulov, V., Akcay, A., Zheng, H., Banks, R., & DelVento, B. (2002), 3D visualization and imaging in distributed collaborative environments, *IEE Computer Graphics and Applications, 22*(1), 11-13.

Rolland, J.P., Martins, R. & Ha, Y., (2003). Head-mounted display by integration of phase-conjugate material, US Patent: University of Central Florida, Filed April 18, 2003

Rolland, J.P., & Hua, H. (2005), Head-mounted displays, in *Encyclopedia of Optical Engineering*, R. Barry Johnson and Ronald G. Driggers, eds. http://www.dekker.com/servlet/product/productid/E-EOE

Sadowski, W., & Stanney, K. (2002). Presence in virtual environments. In K. M. Stanney (Ed.), *Handbook of virtual environments: Design, implementation, and applications* (pp. 791-806). Mahwah, NJ: Lawrence Erlbaum Associates, Inc.

Sarter, N. B., & Woods, D. D. (1997). Team play with a powerful and independent agent: Operational experiences and automation surprises on the Airbus A-320. *Human Factors*, *39*, 553-569.

Sarter, N. B., & Woods, D. D. (2001). Teamplay with a powerful and independent agent: A full mission simulation study. *Human Factors*, *42*, 390-402.

Schloerb, D. W. (1995). A quantitative measure of telepresence. *Presence: Teleoperators and Virtual Environments*, *4*(1), 64–80.

Schnell, T., & Merchant, S. (2001). *Assessing pilot performance in flightdecks equipped with synthetic vision information systems* (Tech. Rep.). Cedar Rapids, IA: Rockwell Collins.

Schnell, T., Kwon, Y., Merchant, S., & Etherington, T. (2004). Improved Flight Technical Performance in Flight Decks Equipped With Synthetic Vision Information System Displays, *International Journal of Aviation Psychology 14* (1), 79-102

Schons, V., & Wickens, C. D. (1993). *Visual separation and information access in aricraft display layout* (Tech. Rep. No. ARL 93-7/NASA A3193-1). Savoy: University of Illinois, Aviation Research Lab.

Shappell, S. A. and Wiegmann, D. A. (2000). *The human factors analysis and classification system - HFACS*. Technical Report DOT/FAA/AM-00/7, FAA, Feb. 2000.

Singer, M.J. and Witmer, B.G. (1997). Presence; Where are we now? In M. Smith, G. Salvendy, and R. Koubek (Eds.), *Design of computing systems: Social and ergonomic considerations* (pp. 885-888). Amsterdam, Netherlands: Elsevier Science Publishers, San Francisco, CA, August 24-29.

Slater, M. (2002). Presence and the sixth sense, *Presence: Teleoperators and Virtual Environments*, August 2002 , *11* (4), 435-439.

Slater, M. (2004). How Colorful Was Your Day? Why Questionnaires Cannot Assess Presence in Virtual Environments, *Presence: Teleoperators & Virtual Environments*, Aug 2004, *13* (4), 484-493

Slater, M., & Wilbur, S. (1997). A framework for immersive virtual environments (FIVE): Speculations on the role of presence in virtual environments. *Presence: Teleoperators and Virtual Environments*, *6*(6), 603–616.

Spivey, M. J., & Geng, J. J. (2001). Oculomotor mechanisms activated by imagery and memory: Eye movements to absent objects. *Psychological Research/Psychologische Forschung*, *65*(4), 235-241.

Stanney, K.M., Salvendy, G., Deisigner, J., DiZio, P., Ellis, S., Ellison, E., Fogleman, G., Gallimore, J., Hettinger, L., Kennedy, R., Lackner, J., Lawson, B., Maida, J., Mead, A., Mon-Williams, M., Newman, D., Piantanida, T., Reeves, L., Riedel, O., Singer, M., Stoffregen, T., Wann, J., Welch, R., Wilson, J., Witmer, B. (1998). *Aftereffects and sense of presence in virtual environments: Formulation of a research and development agenda*. Report sponsored by the Life Sciences Division at NASA Headquarters. International Journal of Human-Computer Interaction, *10*(2), 135-187.

Stein, E. S. (1985). *Air traffic controller workload: An examination of a workload probe* (Tech. Rep. No. DOT/FAA/CT–TN84/24). Atlantic City, NJ: Federal Aviation Administration William J. Hughes Technical Center.

Steuer, J. (1992). Defining virtual reality: Dimensions determining telepresence. *Journal of Communication*, *42*(2), 73-93.

Stewart, J. E., Dohme, J. A., & Nullmeyer, R. T. (2002). U.S. Army Initial Entry Rotary-Wing Transfer of Training Research, *International Journal of Aviation Psychology*, *12* (4), 359-375

Thiele, A., Henning, P., Kubischik, M., & Hoffmann, K. P. (2002). Neural mechanisms of saccadic suppression. *Science*, *295*(5564), 2460-2462.

Treue, S. (2001). Neural correlates of attention in primate visual cortex. *Trends in Neurosciences*, *24*, 295-300.

Tsimhoni, O. & Liu, Y. (2003). A Queuing Network Model for Eye Movement, In *Proceedings of the Human Factors and Ergonomics Society 47thAnnual Meeting* (pp. 1875-1879). Santa Monica, CA: Human Factors and ErgonomicsSociety

Wells, J. W., & Venturino, M. (1990). Performance and head movements using a helmet-mounted display with different sized fields-of-view, *Optical Engineering 29,* 870-877

Werner, E. B. (1991). *Manual of visual fields*. New York: Churchill Livingstone.

Whitley, B. E., (1996). *Principles of research in behavioral science*. Mountain View, CA: Mayfield

Wickens, C. D., Xu, X., Hellenberg, J. R., Carbonari, R., & Marsh, R. (2000). *The Allocation of Visual Attention for Aircraft Traffic Monitoring and Avoidance: Baseline Measures and*

Implications for Freeflight, (Technical Report ARL-00-2/FAA-00-2) Savoy, IL: University of Illinois, Aviation Research Lab

Williams, L. J. (1985). Tunnel vision induced by a foveal load manipulation. *Human Factors*, *27*, 221-227.

Winterbottom, M., Patterson, R. & Pierce, B.P. Visual suppression of monocularly presented symbology against a fused background in simulation and training environment. Accepted for presentation to the meeting of the *Society for Photo-Electronic Instrumentation Engineering, Defense and Security Symposium*, Orlando, FL, April 17-21, 2006.

Witmer, B.G. & Singer, M.J. (1998). Measuring presence in virtual environments: A Presence Questionnaire. *Presence: Teleoperators and Virtual Environments*, *7*, 225-240.

Yarbus, A. L. (1967). Eye movements during perception of complex objects, in L. A. Riggs, ed., *Eye Movements and Vision*, Plenum Press, New York, chapter VII, pp. 171-196.

Zahoric, P., & Jenison, R. L. (1998). Presence and being-in-the-world. *Presence: Teleoperators and Virtual Environments*, *7*(1), 78–89